1-1-2020

Biological Evaluation Of Maasia Glauca (Hassk.) Mols, Kessler & Rogstad

Thanh-Thanh Claire Tran

BIOLOGICAL EVALUATION OF *MAASIA GLAUCA* (HASSK.) MOLS, KESSLER & ROGSTAD

A Dissertation presented in partial fulfilment of requirements
for the degree Doctor of Philosophy
in the Department of Department of BioMolecular Sciences
Division of Pharmacognosy
School of Pharmacy
The University of Mississippi

By
Thanh-Thanh (Claire) V. Tran
May 2020

Abstract

Natural products-based drug discovery has gained a renewal of interest due to the decline of newly approved drugs based on the screening of synthetic compound libraries. Within natural sources, plants have provided 47% of new molecular entities, and only a small percentage of plant species (6%) have been pharmacologically studied. Plant species belonging to the diverse Annonaceae family have been used traditionally for a variety of ailments, including but not limited to dysentery, fever, and cancers. Among all the cancers, colorectal cancer (CRC) is the third most commonly diagnosed cancer worldwide. The lack of effectiveness of chemotherapeutic drugs due to drug resistance renders poor treatment outcomes. Colorectal cancer progression is associated with aberrant Wnt/β-catenin signaling pathway. Constitutive activation of this pathway drives the expression of Wnt target genes that lead to cell proliferation and growth. The expression of Wnt target genes is controlled by the T-cell factor (TCF)/β-catenin complex. Therefore, inhibition of TCF/β-catenin interaction is a promising therapeutic target for CRC. The goal of this investigation is to discover new natural products that would be effective against the proliferation of colorectal cancer cells through interference with the Wnt/β-catenin signaling pathway. A collection of plant extracts belonging to the Annonaceae plant family was selected to screen for anti-proliferative activity against colorectal cancer cells. With high activity against colorectal cancer cells, low toxicity on normal cells, and the lack of pharmacological/phytochemical studies, *Maasia glauca* was selected for further bioactive-guided fractionation and mechanism of action studies. The results of this study indicated that the new seconlignans present in the extract could contribute to the overall activity of *M.glauca* crude

extract in inhibiting proliferation of the colorectal cancer cells. It was also observed that the scalemic mixture and the two secolignans exhibit stronger effects as compared to the crude extract. Further analyses suggest that the two new secolignans inhibit the proliferation of HCT116 colorectal cancer cells by causing the cell cycle arrest at G2/M phase and promoting apoptosis. Our data also demonstrate that crude extract, the scalemic mixture, and the two enantiomers suppress the Wnt signaling pathway. Consequently, real-time PCR analysis revealed down-regulated expression levels of the Wnt target genes. Our results suggest that the compounds suppress the Wnt pathway, lead to the growth inhibitory effects, and apoptosis via arresting cells at the G2/M phase. Together, our findings demonstrate the potential for therapeutic use of these compounds. Further studies are warranted.

DEDICATION

This dissertation is dedicated to my beautiful mother and beloved father.
To my nieces and nephews

LIST OF ABBREVIATIONS

APC: Adenomatous Polypopsis Coli

C: Celsius

$CHCl_3$: Chroloform

CI: Combination Index

CRC: Colorectal Cancer

DMEM/F12: Dulbecco's Modified Eagle Medium/ Ham's F-12

DMSO: Dimethyl Sulfoxide

ESI: Electrospray Ionization

EtOH: Ethanol

FDA: Food and Drug Administration

FITC: Fluorescein-5-isothiocyanate

GI_{50}: Concentration for half-maximal (50%) inhibition of cell proliferation

HMBC: Heteronuclear Multiple Bond Correlation

HPLC: High Performance Liquid Chromatography

hr: hour

LC: Liquid chromatography

MeOH: Methanol

MS: Mass Spectrometry

NCI: National Cancer Institute

NMR: Nuclear Magnetic Resonance

PCR: Polymerase Chain Reaction

PI: Propidium Iodide

qRT-PCR: Real-Time Quantitative Reverse Transcription Polymerase Chain Reaction

QToF: Quadruple Time-of-Flight

rpm: rotation per minute

RT: Retention Time

TCF: T-Cell Factor

TLC: Thin Layer Chromatography

UHPLC: Ultra High Performance Liquid Chromatography

UV: Ultraviolet

VLC: Vacuum Liquid Chromatography

Wnt: Wingless-Related Integration Site

Acknowledgments

During the last five years, I have had the opportunity to study and train under the guidance of excellent professors. I would like to thank all the people who have supported and guided me through this process of learning.

I am grateful to my advisor, Dr. Ikhlas Khan, who provided useful advice and feedback to guide me through this 5-year journey. Without his on-going support, I would not be able to accomplish this work.

I would like to express my gratitude towards Dr. Shabana Khan, my co-advisor. She not only provided me a chance to grow as an independent scientist, but also gave valuable advice, criticism, and teaching. Without her tremendous support, I would not be able to learn how to be an independent scientist.

I also would like to extend my thanks to my committee members, Dr. Dale Nagle and Dr. David Colby for their thoughtful inspiration, guidance, and discussion.

I would like to give special thanks to my laboratory members for their tremendous support, guidance, continuous feedbacks, and their presence: Mr. John Trott, Mrs. Katherine Martin, Mrs. Olivia Dale, Dr. Mona Haron, and Dr. Islam Husain.

I would like to express my gratitude to Dr. John Rimoldi for his unwavering support and encouragement.

In addition, I would like to express my greatest gratitude to all the professors who have provided me with excellent educational experience: Dr. Daneel Ferreira, Dr. Marc Slattery, Dr.

Dale Nagle, Dr. Jordan Zjawiony, Dr. John Rimoldi, Dr. Joshua Sharp, Dr. Tracy Brooks, and Dr. Yu-Dong Zhou.

I am very thankful for Dr. Amar Chittiboyina, Dr. Zulfiqar Ali, Dr. Bharathi Avula, Dr. Mohamed Albadry and all members of Dr. Khan's group for their assistance and care.

I would like to thank Ms. Jennifer Taylor, Ms. Sherrie Gussow, Ms. Danielle Noonan, Ms. Candace Lowstutter, and Mrs. Karin Ballering for their full support and encouragement. Furthermore, to all my graduate fellows who add to my experience, with special note to Yusheng Li for his assistance, I send many thank you.

In addition, I would like to thank the Graduate School for the "Graduate Student Dissertation Fellowship". I would like to thank the Department of BioMolecular Sciences for all the care, the guidance, the teaching, and the constructive criticisms so that my stay here was fulfilling and beneficial. I am very grateful and thankful for all the assistance and care I have received for the last 5 years here at the University of Mississippi. Truly, this journey has been a unique and unforgettable experience I have had.

Last but not least, this journey would not made this far without the presence of my loving family who supported me unconditionally. Their presence and undeniable love is the source of my drive. Truly, without them, I would not progress this far.

Table of Contents **Page**

Chapter 1: Introduction 1
1.1 Colorectal cancer statistics 1
1.2 Risk factors 2
1.3 Pathogenesis 4
1.4 The canonical Wnt pathway 4
1.5 Treatments and resistance 6
1.6 Nature as a source for drug discovery 7
1.7 Overall goals and specific aims 8
Chapter 2: Establish optimal biological assays to screen natural products (plant extracts) for anti-proliferative activity in colorectal cancer cells 11
2.1 Materials and method 15
2.2 Results 16
2.3 Discussion 20
Chapter 3: Perform bioactivity-guided fractionation, isolation, and characterization of active metabolites from the most promising plant extract (*M. glauca)*. 22
3.1 Materials and method 22
3.2 Results 25
3.3 Discussion 35
Chapter 4: Determine the mechanism of action of the anticancer effect. 37
4.1 Materials and methods 37
4.2 Results 39
4.3 Discussion 42
Chapter 5: Evaluate drug combination *in-vitro*. 54
5.1 Materials and method 54
5.2 Results and discussion 54
In Summary 60
Bibliography 62
Appendices 72

Vita.....105

LIST OF TABLES

TABLE **PAGE**

Table 2.1. Annonaceae plant species used in the initial screening……. .12-14

Table 2.3.1. GI_{50} values of the individual sample …… . .17-19

Table 2.3.2. GI_{50} values of the most potent extracts……. 20

Table 2.1.4. Half-maximal cell growth inhibitory effects of 95% ethanolic extract *M. glauca* against a panel of cancer cells (μg/mL) ……21

Table 3.1. ^{1}H and ^{13}C NMR data for **1** and **2** ($CDCl_3$, 400 MHz) …… 31

Table 3.2. Half-maximal cell growth inhibitory effects of 95% ethanolic crude extract, six fractions, and **1** and **2** against HCT116 and HT29 cells (GI_{50} in μg/mL) …… 32

Table 3.3. Tentative compound identification in *M. glauca* crude extract ……. 35

Table 4.1. Primers of the Wnt target genes. ……. 39

Table 5.1. Combination indices of all combinations ……60

LIST OF FIGURES

FIGURE **PAGE**

Figure 1.1. Worldwide incidence rate. Adopted and modified from The Global Cancer Observatory, 2019 …… . ..10

Figure 1.2. The canonical Wnt signaling pathway. Adopted and modified from Zhan et al., 2017 …… 10

Figure 2.3. Summary of the initial screening…….16

Figure 3.1. Fractionation scheme …… 28

Figure 3.2. Concentration-response curve of fractions of *M. glauca* on HCT-116 cells …… 28

Figure 3.3. Concentration-response curve of fractions of *M. glauca* on HT-29 cells ……..28

Figure 3.4. Fraction 2 and crude extract exhibited concentration and time-dependent anti-proliferative activity in HCT116 cells ……...29

Figure 3.5. Fraction 2 and crude extract exhibited concentration and time-dependent anti-proliferative activity in HT29 cells. ……...30

Figure 3.6. ^{13}C NMR spectrum of daughter fraction 2 which is a scalemic mixture, comprised of **1** and **2** …… ……..75

Figure 3.7. ^{1}H NMR spectrum of the daughter fraction 2 ……76

Figure 3.8. HMBC NMR spectrum of the daughter fraction 2…… 77

Figure 3.9. MS and MS/MS spectra for the daughter fraction 2(comprised of **1** and **2)** …. ……79

Figure 3.10. Crystal structure of the scalemic mixture.……..33

Figure 3.11. HPLC chromatogram of the scalemic mixture, daughter fraction 2…… 34

Figure 3.12. UHPLC Chromatogram of *M. glauca* crude extract …… 34

Figure 3.13. MS and MS/MS spectra for malic acid …… ..80

Figure 3.14. MS/MS spectrum for quinic acid ……... 80

Figure 3.15. MS and MS/MS spectra for magnoflorine …… . …81

Figure 3.16. MS and MS/MS spectra for the unknown compound with molecular Formula ……82

Figure 3. 17. MS and MS/MS spectra for dihydroberberine ……83

Figure 3.18. MS and MS/MS spectra for anonaine ……..84

Figure 3.19. Calibration curve for relative quantification for the daughter fraction 2 (comprised of **1** and **2**) …… 85

Figure 4.1. Cell apoptosis analyzed by flow cytometry with *M. glauca* treatment. …… 44

Figure 4.2. Cell apoptosis analyzed by flow cytometry with the daughter fraction 2 Treatment …… 45

Figure 4.3. Cell apoptosis analyzed by flow cytometry with **1** treatment ……46

Figure 4.4. Cell apoptosis analyzed by flow cytometry with **2** treatment …… . .47

Figure 4.5. Cell cycle analysis of **1** and **2**. ……48

Figure 4.6. B-catenin/TCF transcriptional activity in HCT116 cells treated with *M. glauca*, fraction 2, **1,** or **2.** …… . . 49

Figure 4.7. Expression levels of Wnt target genes measured by qRT-PCR in HCT116 cells that were treated with *M. glauca*. …… 50

Figure 4.8. Expression levels of Wnt target genes measured by qRT-PCR in HCT116 cells that were treated with fraction 2. …… 51

Figure 4.9. Expression levels of Wnt target genes measured by qRT-PCR in HCT116 cells that were treated with **1.** …… . . .52

Figure 4.10. Expression levels of Wnt target genes measured by qRT-PCR in HCT116 cells that were treated with **2** ……53

Figure 5.1. Concentration-response curve of irinotecan in combinationa with **1** in HCT116 cells ……... 56

Figure 5.2. Isobologrram representation of irinotecan in combination with **1** in HCT116 cells ……56

Figure 5.3. Concentration-response curve of irinotecan in combination with **2** in HCT116 cells ……57

Figure 5.4. Isobologrram representation of irinotecan in combination with **2** in HCT116 cells ……57

Figure 5.5. Concentration-response curves of irinotecan in combinations with **1** in HT29 cells ……..58

Figure 5.6. Isobologrram representation of irinotecan in combinations with **1** in HT29 cells ……..58

Figure 5.7. Concentration-response curve for irinotecan in combinations with **2** in HT29 cells ……..59

Figure 5.8. Isobologrram representation of irinotecan in combinations with **2** in HT29 cells ……..59

Chapter 1: Introduction

1.1 Colorectal cancer statistics

Colorectal cancer (CRC) is a major common public health issue and is one of the cancers that cause the most cancer deaths worldwide. This cancer is the cancer of the colon or rectum and usually begins with the development of noncancerous polyps that can take a course of ten to twenty years to grow, accumulating mutations as the polyps evolve. Adenomatous polyps, which derived from the glandular cells, account for 96% of all CRC (Stewart, S.L. et al, 2006). Colorectal cancer is the third leading cause of cancer deaths, the second most common cancer in females, and the third in males. The incidence of this cancer is rising globally, with the highest incidence cases in countries with increasing advanced human development (Figure 1). Incidence rate in the developed countries is stabilized or even decreasing but still remains the highest in the world (Ferlay J, Colombet M, and Bray F, 2018). With this regard, CRC is sometimes seen as a marker for industrializing countries that are undergoing the transition to higher economic and social development (Arnold et al., 2017). With a high incidence and mortality rate, CRC is a global health burden that needs to be tackled.

In the United States, CRC incidence and mortality rates are decreasing but it still remains one of the top countries with high rates. There is also a wide disparity in mortality rates among ethnicities within the United States. Non-Hispanic Blacks have the highest incidence and mortality rate, whereas Asian/Pacific Islanders have the lowest rates (Robbins et al., 2012; Edwards et al., 2010). Among the Asian/Pacific Islanders subgroups, Japanese have the highest rates and Asian Indian/Pakistani have the lowest (Torre et al., 2016). The disease disparity

among ethnic groups may reflect socioeconomic levels, which lead to the lack of early detection, newer treatments, and risk factors exposure. In addition, CRC is often associated with older age groups, usually older than 50 years of age. However, the incidence of this cancer in the older age group is declining whereas the incidence in the younger age group is increasing. The incidence rate increased from 6% in 1990 to 12% in 2013 in younger age group (NCI, 2016). Colorectal cancer remains a public concern where it now not only affects the elderly but also the young.

1.2 Risk factors

Importantly, the etiology of CRC needs to be addressed in order to reduce the burden of this disease. However, the root causes of this disease are not well understood; nonetheless, there are several risk factors associated with CRC that can be addressed.

Two of the risk factors are certain diet and lifestyle. Epidemiological evidence reflects a strong correlation between red or processed meat consumption and the progression of this disease with high incidence in countries with high intake of red/processed meat (Cross et al., 2010; Martinez et al., 2007; Stewart, B.W. and Wild, C.P, 2014). Further, research in mice have shown that consumption of dietary fat can indirectly alter the microbiota leading to inflammatory bowel disease, a chronic inflammatory condition that increases the risk of developing CRC (Devkota et al., 2012). Apart from dietary choices, certain lifestyle choices show strong correlation with the progression of CRC. For instance, data from meta-analysis show that lack of physical activity is directly correlated with CRC, and there was a significant reduced risk of CRC in individuals who are physically active (Wolin et al., 2009; Wolin et al., 2011). Another lifestyle risk is tobacco usage. Studies showed that tobacco use could increase the risk of developing the carcinoma in Europeans (Leufkens et al., 2011); a similar study in the United States also indicated the increased risks of getting CRC with the use of tobacco (Hannan et al., 2009). Along

with tobacco, consumption of alcohol is another important risk factor that can increase the chance of developing CRC. Research indicates that moderate drinking (2-3 drinks/day) and heavy drinking (more than 3 drinks/day) show increased risks of developing CRC whereas light drinking (up to one drink/day) does not show significant association with CRC (Bagnardi et al., 2013, Bagnardi et al., 2015). There is also evidence that link obesity and CRC development. General obesity (indicated by body mass index) and abdominal obesity (indicated by waist circumference) are positively associated with CRC. Obese individuals (>30 kg/m^2) are 30% more likely to develop CRC compared to individuals who have normal BMI (Ma et al. 2013). In addition, those individuals can have a reduced CRC survival rate (Wang et al., 2017). Clearly, behavioral habits and dietary choices are modifiable risk factors that contribute to the progression of CRC. Because of such a strong correlation of certain dietary choices and behavioral habits, CRC is often regarded as a "lifestyle" disease. Therefore, it is essential to evaluate dietary and lifestyle habits to minimize the risks of developing CRC.

In contrast to modifiable risk factors, there are non-modifiable risk factors that can also increase the risks of developing CRC. People with a family history of CRC have two to four times higher risk of having this disease compared to people without a family history of CRC (Butterworth et al., 2006). Of all CRC cases, there are about 5% of hereditary syndromes due to some genetic mutations. Of the 5%, Lynch accounts for up to 4%, making it the most common predisposing genetic syndrome that increases the risk of developing CRC. Familial adenomatous polyposis is the second most common inherited disorder (Patel et al., 2012). Apart from hereditary syndromes, personal medical history such as inflammatory bowel disease (IBD) and type-2 diabetes mellitus can also raise CRC risk. Chronic inflammation of the digestive tracts such as Crohn's disease and colitis are examples of IBD that have a positive correlation with

developing CRC; the risk is higher with more severe and longer duration of inflammation (Lutgens et al., 2013). There is evidence from meta-analysis showing type-2 diabetes mellitus has a positive correlation with CRC risk (Tsilidis et al., 2015).

1.3. Pathogenesis

There are three pathways in the development of CRC. Chromosomal instability pathway accounts for 85% of all sporadic CRC, and it is the most common pathway in CRC pathogenesis. The second most common one is the microsatellite instability pathway, followed by the CpG methylator pathway. In the chromosomal instability pathway, there are several genetic signaling alterations, including deregulated Wnt signaling pathway, mutated *TP*53, and mutated *KRAS*. Of these genetic alterations, Wnt signaling pathway is the most notable, which accounts for about 93% of all CRC (Muzny et al., 2012). In the chromosomal instability pathway, the sequence of CRC is most likely initiated by a series of mutations in the *APC* gene, which belongs to the Wnt signaling pathway, causing the normal crypt to become aberrant. Subsequent mutations in the telomerase and *TP*53 gene lead to high-grade adenoma and carcinoma (Fearon et al., 1990; Stewart and Wild, 2014). This process is called adenoma-carcinoma sequence.

Microsatellite instability accounts for about 15% of all CRC. The instability is due to mutations in the DNA mismatch repair system and the development of CRC in this pathway also follows the adenoma-carcinoma sequence. The least common pathway is the CpG methylator pathway. This pathway is characterized by the methylation of various promoter genes and is often overlapped with the chromosomal and the microsatellite instability pathway (Stewart and Wild, 2014). Overall, chromosomal instability is the main pathway in the disease pathogenesis, while the Wnt signaling pathway is the driver in tumor initiation (Kinzler et al., 1996).

1.4. Canonical Wnt signaling pathway

Given the importance of the Wnt signaling pathway in CRC, it is essential to explore its signal transduction pathway. In the canonical Wnt pathway or the Wnt/β-catenin pathway, the absence of the Wnt ligands leads to the destruction of β-catenin by the destruction complex, which made up of Axin, APC, CK1, and GSK3β. With β-catenin tagged for destruction, it cannot translocate into the nucleus, therefore, Wnt/ β-catenin target genes could not be expressed. In active Wnt signaling, the presence of Wnt ligand triggers a signaling cascade. Briefly, a Wnt ligand binds to a Fzd receptor and co-receptor, recruits Dvl, which in turn recruits and inactivates the destruction complex; as a result, β-catenin can translocate into the nucleus, binds to TCF/LEF and induce expression of the target genes such as *CMYC* and *CCND1* which are responsible for cell proliferation (Figure 2, Zhan et al., 2017).

Wnt signaling pathway is a promising therapeutic target for CRC. As mentioned above in addition to the loss of APC leading to tumor initiation, aberrant Wnt signaling is also essential for the maintenance and progression of the tumor. Wnt signaling target proteins such as L1-CAM and ADAM10 were reported to express in invasive colon cancer tissue (Gavert et al., 2005). In a mouse model, expression of L1-CAM was found to drive cancer cells to metastasize to the liver (Gavert et al., 2007). These studies indicated that the aberrant Wnt signaling pathway also plays a role in tumor invasion and metastasis. In addition, restoration of APC expression can induce disease regression even in the presence of *KRAS* and *TP*53 mutations (Lukas et al. 2015). Therefore, it is important to explore or discover inhibitors of the Wnt pathway.

There are several inhibitors of Wnt pathway in pre-clinical trials and clinical trials, but to date, there are no FDA-approved drugs targeting this pathway for CRC (Krishnamurthy & Kurzrock, 2018). There are multiple points of actions for targeting the Wnt signaling pathway. For upstream inhibition, monoclonal antibody OMP-18R5 acts upon the Fzd receptor and small

molecule LGK974 acts on Porc, a crucial step in processing Wnt ligands (Liu et al., 2013; Smith et al., 2013). For downstream targets, β-catenin/TCF complex is the point of action. Small molecules iCRT3, iCRT5, and iCRT14 were shown to cause an inhibitory effect at the β-catenin/TCF complex level using luciferase reporter gene assay (Gonsalves et al., 2011). With a higher mutation rate in the downstream level such as in β-catenin than that in the upstream level, targeting downstream targets would be more beneficial (Zhan et al., 2017).

1.5. Treatments and resistance

Currently, the treatment for CRC depends on the stages or the severity of the disease. With early or localized CRC, surgery is the golden standard. Often times, a small part of the nearby colon and lymph nodes will be resected together with the tumors. For regional CRC, where the cancer cells have spread through the colon's wall or to nearby lymph nodes, surgical resection is usually the first treatment followed by adjuvant chemotherapy or radiation for better outcomes. Fluorouracil or oxaliplatin could be used as chemotherapy for this stage (Sargent et al., 2009; Shah et al., 2016). For the distant stage where cancer has spread to nearby organs, surgery can be used to prevent further complications. At this later stage, the overall goal is to alleviate and improve the symptoms for the patients. For these reasons, chemotherapy or targeted therapy can be used to prolong survival. The 5-year survival rate for this late stage is about 14% (American Cancer Society, 2019).

Research indicates new roles of the Wnt signaling pathway in drug resistance. Increased Fzd or APC mutations increase ABCB1 and CD44 expression, which are involved in multi-drug resistance (Martin-Oronzco et al., 2019). Further, data suggest that Wnt/ β-catenin influences cancer cells' response to chemo-radiation. Data show that overexpression of mutated β-catenin induces treatment resistance, and silencing β-catenin increases the sensitivity of cancer cells to

chemo-radiation (Emons et al., 2017). Consequently, Wnt signaling pathway is a promising therapeutic target for CRC.

1.6. Nature as a source for drug discovery

The decline in newly approved drugs based on high-throughput screening of synthetic compound libraries leads to a renewal of interest in natural products-based drug discovery (Scannell et al., 2012; Atanasov et al., 2015). Within natural sources, plants have been the rich supply for new molecular entities (NMEs); indeed, the plant kingdom can provide diverse classes of bioactive compounds that contribute to 47% of NMEs (Patridge et al., 2016). Plants provide a diverse class of compounds, and there is only a small portion of existing plant species (6%) that have been studied for pharmacological activities up to date (Verpoorte, R., 2000).

Plant-based drug discovery combined with ethnopharmacological knowledge, can increase the probability of discovering new bioactive compounds. This dissertation will focus on the Annonaceae plant family or custard apple family, which is the largest family in the Order of Magnoliales. This diverse plant family contains 130 genera and 2300 species. Many species within this family have been used traditionally for treating various ailments, including but not limited to scurvy, dysentery, gonorrhea, and cancers (Watt et al., 1962). For instance, the seed of *Xylopia aethiopica* (common name: Eru), the bark of *Uvaria chamae* (common name: Eruju), and the root of *Uvaria afzelii* (common name: Gbogbonse) are used in Nigeria for the management of various cancers (Soladoye et al., 2010). The whole plant of *Annona glabra* (common name: pond apple) is used for anticancer effects in China (Cochrane et al., 2008). Given the valuable traditional uses of this family, there have been some extensive phytochemical studies on the Annonaceae family resulting in the characterization of structurally diverse

secondary metabolites such as alkaloids (Malebo et al., 2013), flavonoids (Chokchaisiri et al., 2015), terpenoids (Anna et al., 2013), and lignans (Rayanil et al., 2016).

1.7. Overall goals and specific aims

From 1981 to 2014, there were 174 FDA-approved anticancer drugs. Of those anticancer drugs, more than half belongs to unmodified natural products, synthetic compounds with natural product pharmacophores, botanical drug, or semi-synthetic drugs derived from natural products (Newman & Cragg, 2014). The goal of this investigation is to discover bioactive compounds with anti-proliferative activities in colorectal cancer cells. To achieve the goal, *in-vitro* phenotypic cell-based assays were chosen. Due to their efficiency in discovering drug hits as well as their utility in addressing the underlying mechanism of action (Atanasov et al., 2015), cell-based assays coupled with bioactivity-guided fractionation can be a promising approach for identifying potential new anti-colorectal cancer agents.

The objectives of this dissertation are to screen plant extracts for anti-proliferative activity against colon cancer cells and use bioactivity-guided fractionation to isolate the bioactive secondary metabolites from the most promising plant extract that are effective against colorectal cancer cells as well as to determine the mechanism of action of anti-colon cancer effect.

In the majority of colorectal cancers, the Wnt/β-catenin signaling pathway is over-activated where β-catenin can complex with the transcription factor, TCF, leading to the expression of Wnt downstream target genes, which regulate cancer progression. Targeting the interaction between β-catenin and TCF is one of the most effective strategies for blocking Wnt signaling (Cheng et al., 2019). Discovering inhibitors that can interfere with this pathway at this downstream level can be a promising approach towards colorectal cancer therapy.

The overall goal of this dissertation is **to discover natural products that would be effective against the proliferation of colorectal cancer cells through interference with the Wnt/β-catenin signaling pathway.** The overall goal will be achieved using the following specific aims.

Specific Aim 1: Establish optimal biological assays to screen natural products (plant extracts) for anti-proliferative activity in colorectal cancer cells.

To develop a method for screening crude extracts available in the NCNPR against colorectal cancer cell lines: HCT-116 and HT-29.

Specific Aim 2: Perform bioactivity-guided fractionation, isolation, and characterization of active metabolites from the most promising plant extract (*M. glauca)*.

To isolate secondary metabolites based on bioactivity-guided fractionation and to characterize and identify the structure of bioactive secondary metabolites using spectroscopic techniques.

Specific Aim 3: Determine the mechanism of action of anticancer effect.

To determine the effects of the plant extract and active metabolite/s on apoptosis, cell cycle arrest, and the Wnt/β-catenin signalling pathway in HCT-116 cells.

Specific Aim 4: Evaluate the effects of isolated compounds in combination with the drug irinotecan *in-vitro*.

To evaluate the effects of the active secondary metabolite/s in combination with irinotecan, an FDA-approved cancer drug used for metastasized CRC.

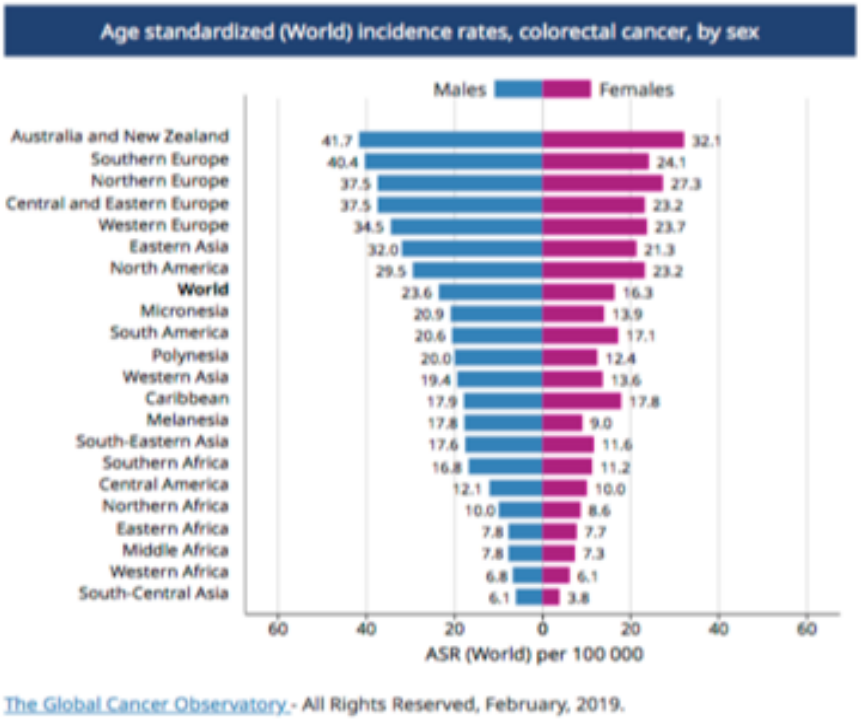

Figure 1.1. Worldwide incidence rate. Adopted and modified from The Global Cancer Observatory, 2019.

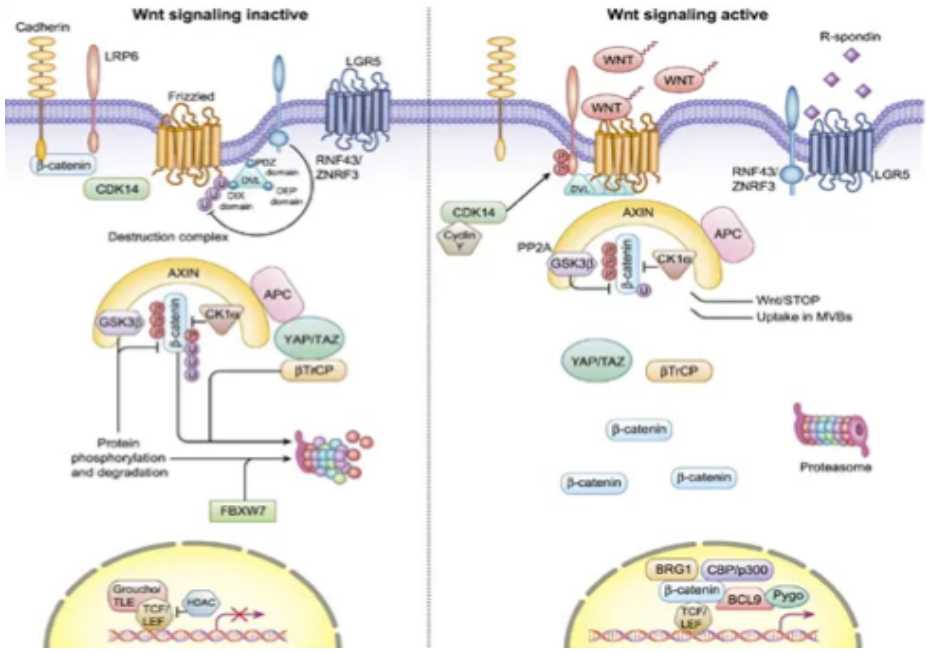

Figure 1.2. The canonical Wnt signaling pathway. Adopted and modified from Zhan et al., 2017.

Chapter 2: Establish optimal biological assays to screen natural products (plant extracts) for anti-proliferative activity in colorectal cancer cells

2.1 Selection of plants

A collection of the Annonaceae plant family was selected from the National Center for Natural Products Research (NCNPR) repository, University of Mississippi. Plants were collected from Loreto, Mexico and New Guinea where there is a high biodiversity. The taxonomic identity of these species was confirmed by Dr. Charles Burandt, a former research botanist in the NCNPR, University of Mississippi. Samples of these species were deposited at the NCNPR. A collection comprised of 85 plant samples belonging to 17 genera with a total of 31 species was used for anti-proliferative screening. Different plant parts of the same species were included in the screening. The descriptions of the 85 plant samples are listed in Table 2.1.

Table 2.1. Annonaceae plant species used in the initial screening

Plant Species	Vernacular Names	Use For	Plant Part
Anaxagorea brachycarpa			Root
Anaxagorea brachycarpa			WS-SB
Annona aff. muricata	Graviola	Diabetes [1]	WS-SB
Annona aff. muricata	Graviola	Anti-inflammation [1]	Root
Annona aff. muricata	Graviola	Headach, Insomnia Diabetes, Cystitis [1]	Leaves, Twigs
Annona ambotay		Fever [2]	Leaves, Twigs
Annona ambotay			ST
Annona deminuta			Root
Annona deminuta			Leaves, Twigs
Annona deminuta			WS-SB
Annona montana *	mountain soursop	Fever, Headache [2]	Leaves, Twigs
Annona montana *	mountain soursop		ST
Asimina triloba	Papaw	Ashma, Fever, Antibacterial activity [3]	Leaves
Cananga odorata	Ylang Ylang,Cananga	Itchness, Dandruff [2]	Bark
Cymbopetalum aff. alkekengi			Root
Cymbopetalum aff. alkekengi			WS-SB
Cymbopetalum aff. alkekengi			Leaves, Twigs
Cymbopetalum alkekengi			Root
Cymbopetalum alkekengi			Leaves, Twigs
Cymbopetalum alkekengi			WS-SB
Duguetia spixiana *			Root
Duguetia spixiana *			WS-SB
Duguetia spixiana *			WS-SB

Table 2.1. Annonaceae plant species used in the initial screening

Plant Species	Vernacular Names	Use For	Plant Part
Froesiodendron amazonicum			Root
Froesiodendron amazonicum			Root
Froesiodendron amazonicum			Leaves, Twigs
Froesiodendron amazonicum			Leaves, Twigs
Froesiodendron amazonicum			ST-BK
Froesiodendron amazonicum			WS-SB
Guatteria acutissima			WS-SB
Guatteria acutissima			Leaves, Twigs
Guatteria inundata **			WS-SB
Guatteria inundata **			Leaves, Twigs
Guatteria inundata **			Root
Guatteria juruensis			ST-BK
Guatteria juruensis			Root
Guatteria juruensis			Leaves, Twigs
Guatteria megalophylla			Root
Guatteria megalophylla			WS-SB
Guatteria megalophylla			Leaves, Twigs
Guatteria multivenia			WS-SB
Guatteria multivenia			WS-SB
Guatteria multivenia			WS-SB
Guatteria multivenia			WS-SB
Guatteria multivenia			Root
Guatteria multivenia			Root
Guatteria multivenia			Leaves, Twigs
Guatteria multivenia			Leaves, Twigs
Guatteria multivenia			Leaves, Twigs
Guatteria sp.	guatteria		WS-SB
Guatteria sp.	guatteria		Leaves, Twigs
Guatteria sp.	guatteria		Root
Haplostichanthus longifolia			Leaves
Miliusa koolsii			Leaves
Polyalthia forbesii			Leaves
Polyalthia forbesii			Bark
Polyalthia glauca/Maasia glauca		Women's post-natal health [4]	Bark
Polyalthia michaelii			Bark
Polyalthia michaelii			Leaves
Polyalthia oblongifolia			Bark
Polyalthia oblongifolia			Leaves
Polyalthia rumpii		Fever, Hypertension, Cancers [5]	Bark
Popowia beccarii			Leaves
Popowia beccarii			Root
Pseudoxandra polyphleba			WS-SB
Pseudoxandra polyphleba			Leaves, Twigs

Table 2.1. Annonaceae plant species used in the initial screening

Plant Species	Vernacular Names	Use For	Plant Part
Rollinia cuspidata			Root
Rollinia cuspidata			WS-SB
Rollinia cuspidata			Leaves, Twigs
Unonopsis elegantissima			Root
Unonopsis elegantissima			ST
Unonopsis elegantissima			LF-ST
Unonopsis floribunda		arthritis rheumatism and diarrhea	WS-SB
Unonopsis floribunda			Root
Unonopsis floribunda			Leaves, Twigs
Unonopsis peruviana	Chuchuhuasi		WS-SB
Unonopsis peruviana	Chuchuhuasi		Leaves, Twigs
Unonopsis stipitata			LF-RT-SB-TW-WS
Uvaria grandis			Bark
Uvaria purpurea	kalak (Indonesia), akar larak (Malaysia)	abdominal pains skin diseases	Leaves
Xylopia aromatica	Ethiopian pepper		Leaves
Xylopia aromatica	Ethiopian pepper	Herbal tonic [2]	ST
Xylopia aromatica	Ethiopian pepper	Herbal tonic [2]	Bark
Xylopia cuspidata			Leaves, Twigs
Xylopia cuspidata			WS-SB

*Edible fruits **Used for wood
WS: whole stem; SB: stem bark; ST: stem; LF: leaves; TW: twig; BK: bark.

1. Moghadamtousi, S., et al.,(2015). Annona muricata (Annonaceae): A Review of Its Traditional Uses, Isolated Acetogenins and Biological Activities. *International Journal of Molecular Sciences, 16*(7), 15625–15658.
2. Tropical Plants Database, Ken Fern. tropical.theferns.info.
3. Duke, James A. and Foster, Steven. *Field Guide to Medicinal Plants and Herbs of Eastern and Central North America.* Peterson, 2014. Print.
4. Chuakul, W., Soonthornchareonnon, et al. (2004). Survey on Medicinal Plants in Southern Thailand. *Thai J. Phytopharm.*, 11(2), 29–52.
5. Wang et al., (2018). *Revista Brasileira de Farmacognosia.,* 28, 253–238 .

2.2. Materials and methods

2.2.1 Cell culture and chemicals

All cell lines were obtained from the American Type Culture Collection. The two colon cancer cell lines (HCT116 and HT29) and human embryonic kidney cell line were maintained in Dulbecco's Modified Eagle Medium:Ham's F12 (DMEM/F12) (ThermoFisher, cat# 12500062), supplemented with 10% (v/v) fetal bovine serum-premium select (R&D Systems', cat# S11550), 1% (v/v) penicillin streptomycin (ThermoFisher cat # 15070063).

2.2.2 Preparation of crude extracts of the plant material

The dried powder of each plant material (20 g) was extracted with 95% ethanol: 5% H_2O using Dionex ASE 350 extractor at 1500 psi. Briefly, the sample was heated for ten minutes at 40º C during extraction. The extract was then flushed with 95% ethanol. The sample was extracted three times at ten minutes/extraction. The extract was dried using vacuum centrifugation. Dried ethanolic extract was dissolved in DMSO to have a concentration of 20 mg/mL (stock concentration). This stock solution was further diluted as needed in biological assays.

2.2.3 Screening of crude extracts

Each crude extract was initially screened at three concentrations: 100 µg/mL, 10 µg/mL, and 1 µg/mL for antiproliferative activity against HCT-116 and HT-29 cells. This wide range of concentration was chosen to estimate the growth inhibition of 50% (GI_{50}) by each extract. Both cell lines were grown with standard culturing conditions (37ºC, 5% CO_2). The extracts that showed low GI_{50} values on both HCT116 and HT29 cells were selected for evaluating on HEK293, to determine the anti-proliferative activity on non-cancerous cells for comparison. The most potent extract was chosen based on its potency, availability, and lack of previous reports of

pharmacological and phytochemical investigation. Cell proliferation was measured by water-soluble tetrazolium salt (WST-8) assay (Boyd & Paull, 1995). Briefly, cells ($5x10^3$ cells/well) were seeded in 96-well plates; after 24 hours of attachment, cells were treated with various concentrations of test extracts for 48 hr. After treatment, old media was replaced with fresh media, WST-8 dye was added, and the cells were incubated for 3 hours (37ºC, 5% CO_2). Absorbance was measured at 450 nm, and cell proliferation was determined. GI_{50} values were estimated based on the percent growth using the below equation. Experiments were done at least in duplicates with DMSO as negative control and doxorubicin as positive control.

$$\% \text{ Growth} = \frac{Sample\ OD - Blank\ OD}{Vehicle\ OD - Blank\ OD} x100 \quad (Equation\ 1)$$

2.3. Results

2.3.1 Screening of crude extracts: Initial screening of 85 plant extracts yielded 23 extracts with the GI_{50} values of less than 50 µg/mL, seven extracts with the GI_{50} values of less than 20 µg/mL, and five extracts with the GI_{50} values of less than 10 µg/mL (Figure 2.3). GI_{50} values for individual plant sample are listed in Table 2.3.1

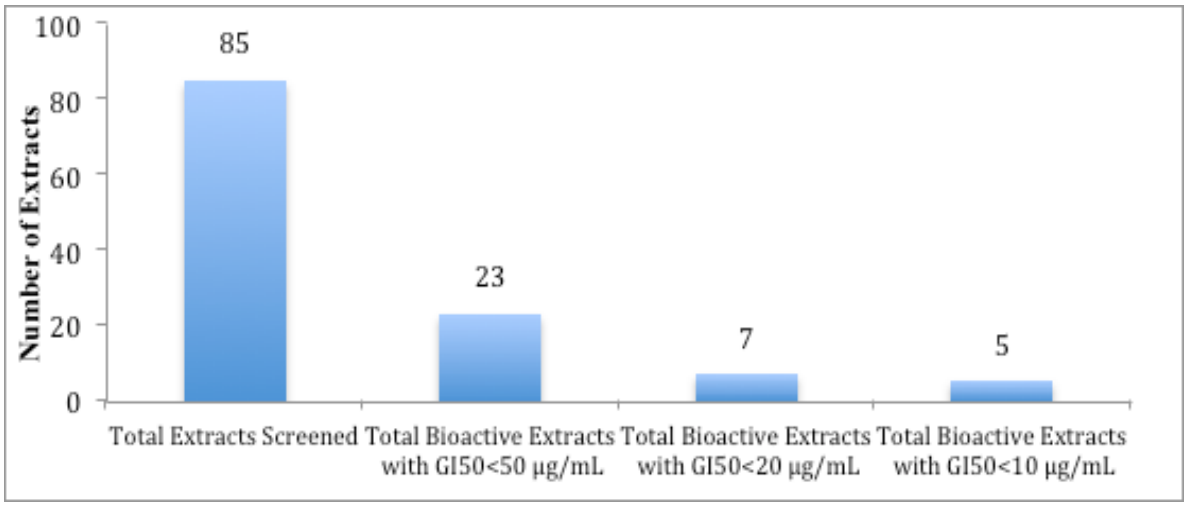

Figure 2.3. Summary of initial screening

Table 2.3.1. GI_{50} values of individual sample

		Anti-proliferative activity (GI_{50}, µg/mL)	
Plant Species	**Plant Part**	**HCT-116 cells**	**HT-29 cells**
Anaxagorea brachycarpa	Root	NA	NA
Anaxagorea brachycarpa	WS-SB	28	79
Annona aff. muricata	WS-SB	NA	NA
Annona aff. muricata	Root	NA	95
Annona aff. muricata	Leaves, Twigs	NA	NA
Annona ambotay	Leaves, Twigs	45	85
Annona ambotay	ST	90	NA
Annona deminuta	Root	NA	NA
Annona deminuta	Leaves, Twigs	70	NA
Annona deminuta	WS-SB	60	50
Annona montana *	Leaves, Twigs	39	50
Annona montana *	ST	NA	NA
Asimina triloba	Leaves	NA	NA
Cananga odorata	Bark	95	NA
Cymbopetalum aff. alkek	Root	45	90
Cymbopetalum aff. alkek	WS-SB	78	NA
Cymbopetalum aff. alkek	Leaves, Twigs	NA	NA
Cymbopetalum alkekengi	Root	NA	NA
Cymbopetalum alkekengi	Leaves, Twigs	80	NA
Cymbopetalum alkekengi	WS-SB	38	NA
Duguetia spixiana *	Root	20	80
Duguetia spixiana *	WS-SB	NA	NA
Duguetia spixiana *	WS-SB	35	65

Table 2.3.1. GI_{50} values of individual sample

		Anti-proliferative activity (GI_{50}, μg/mL)	
Plant Species	**Plant Part**	**HCT-116 cells**	**HT-29 cells**
Froesiodendron amazonicum	Root	NA	NA
Froesiodendron amazonicum	Root	NA	NA
Froesiodendron amazonicum	Leaves, Twigs	NA	NA
Froesiodendron amazonicum	Leaves, Twigs	NA	NA
Froesiodendron amazonicum	ST-BK	NA	NA
Froesiodendron amazonicum	WS-SB	NA	NA
Guatteria acutissima	WS-SB	3.5	40
Guatteria acutissima	Leaves, Twigs	13	43
Guatteria inundata **	WS-SB	5.5	50
Guatteria inundata **	Leaves, Twigs	25	NA
Guatteria inundata **	Root	6.5	60
Guatteria juruensis	ST-BK	90	NA
Guatteria juruensis	Root	15	68
Guatteria juruensis	Leaves, Twigs	42	NA
Guatteria megalophylla	Root	75	75
Guatteria megalophylla	WS-SB	NA	NA
Guatteria megalophylla	Leaves, Twigs	NA	NA
Guatteria multivenia	WS-SB	NA	NA
Guatteria multivenia	WS-SB	NA	NA
Guatteria multivenia	WS-SB	NA	NA
Guatteria multivenia	WS-SB	65	NA
Guatteria multivenia	Root	NA	NA
Guatteria multivenia	Root	100	NA
Guatteria multivenia	Leaves, Twigs	35	NA
Guatteria multivenia	Leaves, Twigs	NA	NA
Guatteria multivenia	Leaves, Twigs	NA	NA
Guatteria sp.	WS-SB	NA	NA
Guatteria sp.	Leaves, Twigs	NA	NA
Guatteria sp.	Root	NA	NA
Haplostichanthus longifolia	Leaves	NA	NA
Miliusa koolsii	Leaves	80	50
Polyalthia forbesii	Leaves	NA	NA
Polyalthia forbesii	Bark	NA	NA
Polyalthia glauca	Bark	8	18
Polyalthia michaelii	Bark	45	70
Polyalthia michaelii	Leaves	50	NA
Polyalthia oblongifolia	Bark	NA	NA
Polyalthia oblongifolia	Leaves	NA	NA
Polyalthia rumpii	Bark	NA	NA
Popowia beccarii	Leaves	NA	NA
Popowia beccarii	Root	NA	NA

Table 2.3.1. GI_{50} values of individual sample

		Anti-proliferative activity (GI_{50}, µg/mL)	
Plant Species	**Plant Part**	**HCT-116 cells**	**HT-29 cells**
Polyalthia rumpii	Bark	NA	NA
Popowia beccarii	Leaves	NA	NA
Popowia beccarii	Root	NA	NA
Pseudoxandra polyphleb	WS-SB	NA	NA
Pseudoxandra polyphleb	Leaves, Twigs	NA	NA
Rollinia cuspidata	Root	7	25
Rollinia cuspidata	WS-SB	29	65
Rollinia cuspidata	Leaves, Twigs	NA	NA
Unonopsis elegantissima	Root	NA	60
Unonopsis elegantissima	ST	NA	90
Unonopsis elegantissima	LF-ST	NA	NA
Unonopsis floribunda	WS-SB	50	NA
Unonopsis floribunda	Root	33	46
Unonopsis floribunda	Leaves, Twigs	NA	NA
Unonopsis peruviana	WS-SB	42	85
Unonopsis peruviana	Leaves, Twigs	45	100
Unonopsis stipitata	LF-RT-SB-TW-WS	40	60
Uvaria grandis	Bark	NA	NA
Uvaria purpurea	Leaves	NA	NA
Xylopia aromatica	Leaves	50	NA
Xylopia aromatica	ST	60	NA
Xylopia aromatica	Bark	95	90
Xylopia cuspidata	Leaves, Twigs	NA	NA
Xylopia cuspidata	WS-SB	NA	NA

GI_{50} values of the five promising extracts were compared (Table 2.3.2). *M. glauca* and *R. cuspidata* were selected based on their potency on both cancer cell lines to test for toxicity assessment on normal cells HEK293. With the GI_{50} of 96.41 µg/mL, *M. glauca* extract does not show strong cytotoxic activity against HEK293 in comparison to cancer cells. With the GI_{50} of 28.73 µg/mL, *R. cuspidate* extract showed anti-proliferation against HEK293 cells. With its low

toxicity on normal cells, high potency against colorectal cancer cells, and the lack of pharmacological/phytochemical studies in the literature, *M. glauca* was selected for further fractionation.

Table 2.3.2. GI_{50} values of the most potent extracts

Cell Lines / Plant Species	HCT-116 (3-concentration screen)	HT-29 (3-concentration screen)	HEK293	Part used
M. glauca	8 µg/mL	18 µg/mL	96.41 µg/mL	Bark
R. cuspidata	7 µg/mL	25 µg/mL	28.73 µg/mL	Root
G. inundata	6.5 µg/mL	60 µg/mL	Not tested	Root
G. inundata	5.5 µg/mL	50 µg/mL	Not tested	Whole stem, stem bark
G. acutissima	3.5 µg/mL	40 µg/mL	Not tested	Whole stem, stem bark

2.4. Discussion

There is minimal phytochemical information on *M. glauca*. This plant species is distributed across Southeast Asia and Oceania. Ethnic groups in Asia have been using this species for medicinal purposes. In Thailand, *M. glauca* (common name: Tara) is used as a blood tonic and carminative agent (Chuakul et al., 2004). In Malaysia, *M. glauca* is used for women's post-partum health (Eswani et al., 2010). To date, there are only a few pharmacological studies reported for this species; the chloroform extracts of *M. glauca* showed cytotoxic activities against HeLa cells by inducing p53 and pRb expression (Etikawati et al., 2015 & 2016). Furthermore, there is not much known about the chemical constituents of this species besides a polyphenolic compound that was isolated from *M. glauca* showing protective effects on beta-amyloid peptide-induced neurotoxicity (Thangnipon et al., 2013). Before this species was reassigned into a new genus Maasia, *M. glauca* was originally classified under the genus Polyalthia (Mols et al., 2008). Polyalthia genus contains mainly diterpenoids, alkaloids, and lignans (Paarakh et al., 2009; Wang et al., 2019). Because of the lack of phytochemical and

pharmacological information on this species, exploring this species would yield a higher probability of discovering new bioactive compounds or already known compounds with novel activities. In this screening study, we demonstrated that *M. glauca* has growth inhibitory effect against colorectal cancer cells HCT116 and HT29. Furthermore, *M. glauca* does not exhibit any toxicity against normal cells HEK293, indicating that it selectively exhibited anti-proliferative activity on colorectal cells. To demonstrate the selectivity of this species on colorectal cancer cells, its effect was evaluated further on four other cancer cell lines (skin melanoma:SK-MEL, carcinoma, papilloma: KB, breast carcinoma: BT-549, and ovarian carcinomaSK-OV-3) at least in duplicates with DMSO as the negative control and doxorubicin as the positive control. The results, as shown in Table 2.4.1, suggest that *M. glauca* extract does not show anti-proliferative effects on KB, BT-549, and SK-OV-3 cells. In SK-MEL cells, *M. glauca* showed slight activity with the GI_{50} values of 51 ± 12.73 (Table 2.4.1). *M. glauca* exhibited a higher potency on colorectal cancer HCT116 and HT29 cells with lower GI_{50} values in comparison to other cancerous cell lines (Table 2.3.2).

In conclusion, a collection of 85 extracts were successfully screened to refine down to one or two candidates that show growth inhibitory effects on colorectal cancer cells. Results from HEK293 cells further narrow down to one extract, *M. glauca*. In addition, further evaluation of this species on a panel of other cancer cells indicates its selectivity on colorectal cancer cells. Consequently, this study successfully identifies the promising extract for further investigation of its therapeutic potential for CRC.

Table 2.1.4. Half-maximal cell growth inhibitory effects of 95% ethanolic extract *M. glauca* against a panel of cancer cells (µg/mL)

	GI50 µg/mL	GI50 µg/mL	GI50 µg/mL	GI50 µg/mL
	SK-MEL	**KB**	**BT-549**	**SK-OV-3**
M. glauca extract	51± 12.73	NA	NA	NA
Doxorubicin	0.37 ± 0.007	0.50 ± 0.021	0.48 ± 0.1	1.02 ± 0.69

Chapter 3: Perform bioactivity-guided fractionation, isolation, and characterization of active metabolites from the most promising plant extract (*M. glauca)*

3.1 Materials and Methods

3.1.1. General experimental procedures

Agilent Technologies 6200 series mass spectrometer was employed for Mass data. NMR spectra were recorded on Bruker DRX-400 spectrometer using $CDCl_3$ as solvent; chemical shifts are given in parts per millions with respect to residual $CDCl_3$ signals. Optical rotation was determined using AUTOPOL IV Automatic Polarimeter (Rudolph, Hackettstown, NJ, USA). X-ray crystallography was performed by using Bruker XPEX3. Resolution of enantiomers by HPLC was performed on Alliance Water with a ChiralPak IP N-5, 4.6 × 250 mm, 5-micron column with PDA detector. UHPLC-DAD was performed on Agilent UHPLC 1290 Series (Agilent Technologies, Palo Alto, CA, USA). QToF-MS was performed on Agilent QToF-MS 6530 series (Agilent Technologies, Palo Alto, CA, USA).

3.1.2 Bioactivity-guided fractionation of active component from *M. glauca* based on its anti-proliferative activity

The ethanolic crude extract (1.237 g) was dissolved in 1.2 mL MeOH and sonicated for 15 min. Small amount of silica gel was added to absorb the sample and the mixture was left to dry under the hood. After overnight drying of the sample, it was loaded onto a column (8 cm long, 2 cm diameter, volume: 25.12 cm^3). The sample was fractionated using vacuum liquid chromatography (VLC) with increasing polarity of hexanes-chloroform and chloroform-methanol mixtures over silica gel. Normal-phase TLC was performed on pre-coated silica G

TLC plates with UV254 (Sorbtech) with four solvent systems: $CHCl_3$ (100%), $CHCl_3$:MeOH (9:1), $CHCl_3$:MeOH (8:2), and EtOH:$CHCl_3$:MeOH:H_2O (6:4:4:1). TLC plates were stained with vanillin. Based on the TLC profiles, the initial fractions were combined to yield daughter fractions. Each daughter fraction was concentrated under reduced pressure and speed vacuum.

Each daughter fraction was evaluated for anti-proliferative activities on HCT116 and HT29 at 6-concentrations (100 µg/mL, 50 µg/mL, 25 µg/mL, 12.5 µg/mL, 6.25 µg/mL, and 3.125 µg/mL). Cells ($5x10^3$ cells/well) were seeded in 96-well plates; after 24 hours of attachment, cells were incubated with WST-8 dye for 3 hours (for time zero control) or treated with each daughter fraction. After 48 hr of treatment, old media was replaced with fresh media, WST-8 dye was added and the cells were incubated for 3 hours (37ºC, 5% CO_2). Absorbance was measured at 450 nm, and cell proliferation was determined. GI_{50} value (the concentration that causes growth inhibition of 50%) was calculated by non-linear regression analysis using GraphPad Prism. Experiments were performed in at least triplicates with DMSO as negative control and doxorubicin as positive control. Equations 2 and 3 were used to calculated percent growth and percent death using time zero control.

$$\% \text{ Growth} = \left[\frac{\text{Drug} - \text{Time zero}}{\text{Vehicle} - \text{Time zero}}\right] \times 100 \qquad \% \text{ Death} = \left[100 - \left[\frac{\text{Drug}}{\text{Time zero}} \times 100\right]\right] \times -1$$

3.1.3 Evaluation of time-dependent anti-proliferative activities

The *M. glauca* crude extract and the fractions that show anti-proliferative activity on HCT116 and HT29 cells was selected to evaluate whether they exhibit anti-cell proliferative effect in a time-dependent manner. The assay was performed as described above. The endpoint times were 24 hr, 48 hr, and 72 hr.

3.1.4. Characterization of fraction CT.2.19.2.PG and resolution of enantiomers

Based on the activity, daughter fraction CT.2.19.2.PG was subjected to further isolation and characterization. This fraction contained a major compound based on TLC. Characterization of CT.2.19.2.PG was performed using spectroscopy and X-ray crystallography. Crystals were grown using vapor diffusion techniques (water: MeOH). Data show that this fraction is comprised of one pure compound with both *R* and *S* enantiomers. Therefore, resolution of the two enantiomers was performed using high-performance liquid chromatography (HPLC) with chiral column. In short, ChiralPAK IB N-5, 4.6x250 mm, 5-micron column was used. Twenty-five microliter of 10 mg/mL sample was injected into the column with the mobile phase, hexane: isopropanol (50:50). The flow rate was 1.5 ml/min. The total run time was 18 min, the detection wavelength was 220 nm, and the temperature was ambient.

3.1.5. Analysis of *M. glauca* sample using LC-QToF-MS

Analysis of the crude extract was performed to determine the chemical composition, tentatively identify other compounds, and to relatively quantify the active compound. 10 mg of the crude extract was sonicated in 1.0 mL of MeOH for 10 minutes, vortexed followed by centrifugation for 15 min at 5000 rpm. Prior to injection, the solution was passed through a 0.45 µm PTFE filter. For relative quantification, individual stock solution of the fraction was prepared at a concentration of 1.0 mg/mL in methanol. The calibration curve was prepared at six concentration levels. The range of the calibration curves was 10-1000 µg/mL.

For this analysis, UHPLC-DAD coupled with QToF-MS was used. For UHPLC-DAD, Agilent Poroshell 120 EC-C18 2.1x150 mm (2.7 µ) column was used. The sample was eluted with **A**—H_20 (0.1% formic acid): **B**—Acetonitrile (0.1% formic acid), with 99% **A** for 3 min, 55% **A** in the next 27 min, 100% **A** in the final 20 min, and 100% **B** wash for 5 min. The injection volume was 2 µL with flow rate of 0.2 mL/min; the temperature was kept at 35 °C. The

UV range used was from 200 to 600 nm. For QToF-MS, ESI^+/ESI^- ionization modes were used. Gas temperature was 325 °C with the flow of 11 L/min. Sheath gas temperature was 300°C with 11 L/min flow rate. Nebulizer used 30 psig. 3.5 kV was used for capillary voltage. Fragmentor used 150V. Mass range (m/z) was selected from 100-2000.

3.2. Results

Fractionation of 1.237 g *M. glauca* ethanolic crude extract yielded 55 parent fractions. Pooling parents fractions based on TLC gave a total of six daughter fractions. First daughter fraction yielded 15.1 mg, second yielded 406.9 mg, third yielded 31.3 mg, 4^{th} daughter fraction yielded 66.9 mg, 5^{th} daughter fraction yielded 341.6 mg, and 6^{th} daughter fraction yielded 10.5 mg (Figure 3.1). The percent yields of six daughter fractions were 1.22%, 32.89%, 2.53%, 5.41%, 27.61%, and 0.85%, respectively. Each daughter fraction was evaluated for anti-proliferative activity on HCT116 and HT29 cells. Only fraction 2 showed anti-proliferative effect on both HCT116 and HT29 cells. The other five fractions did not exhibit any effect on HCT116 or HT29 cell proliferation (Figure 3.2 and Figure 3.3).

Fraction 2 and *M. glauca* crude extract both showed concentration-dependent and time-dependent anti-proliferative activity in HCT116 cells. There was a significant difference in the GI_{50} values of the fraction 2 between 24 and 48 hr time-point. The GI_{50} values of the crude extract were significantly reduced between 24 and 48 hr time-point. There was no significant difference in the GI_{50} values between 48 and 72 hr for both fraction 2 and crude extract (Figure 3.4). For HT29 cells, fraction 2 and *M. glauca* crude extract exhibited concentration-dependent anti-proliferation. GI_{50} values of fraction 2 were lower than that of the crude extract in all three time-points and in both cancer cell lines. Fraction 2 inhibited proliferation of HCT116 cells with a GI_{50} value of 5.43 ± 1.36 μg/mL, while the crude fraction inhibited cell proliferation with a

GI_{50} of 12.44 ± 0.62 µg/mL at 48 hr time-point. There were no significant differences in the GI_{50} values among the three time-points for both fraction 2 and the crude extract in HT29 (Figure 3.5).

Daughter fraction 2 appeared as pale yellow-white solid and further qualitative ^{1}H and ^{13}C NMR suggested possible presence of one major compound (Appendix I, Figure 3.6 and Figure 3.7). The NMR data of fraction 2 showed resonances for six aromatic methines attributed to two 1,3,4-trisubstituted phenyl rings, an exocyclic olefinic methylene, an oxygenated methylene, two aliphatic methines, four methoxy groups, in addition to seven non-protonated sp2 hybrid carbons (Table 3.1). The individual appearance of resonances in the ^{1}H and ^{13}C NMR spectra for two symmetric phenyl rings indicated free rotation restriction of C-3–C-5 bond, which could be due to the bulkiness of the groups attached to this bond. The methoxy groups in phenyl rings, the presence of lactone ring containing exocyclic double bond, and locations of both phenyl rings at C-5 were confirmed by HMBC correlations, as shown in Appendix I, Figure 3.8. The above mentioned NMR data resulted in characterization of the planar structure of the compound as 4-(bis(3,4-dimethoxyphenyl)methyl)-3-methylenedihydrofuran-2(3*H*)-one. Mass spectrometry was used to confirm the structure with an $[M+H]^{+}$ molecular ion peak at m/z 385.1625 (calcd *m/z* 385.1678) (Appendix-II, Figure 3.9) which corresponded to the molecular formula of $C_{22}H_{24}O_6$ plus a proton. This compound belongs to a group known as secolignan.

The X-ray experiments were performed on crystals derived from daughter fraction 2/secolignan to determine the absolute configuration (Appendix III). The X-ray data indicated that the secolignan was a scalemic mixture (Figure 3.10). Therefore, resolution of the enantiomers was performed. The resolution of the enantiomers from a 20 mg/mL of the secolignan using chiral column attached to HPLC yielded **1** (5.5 mg) and **2** (5.1 mg). Compound

1 eluted at 9 min and **2** eluted at 13 min (Figure 3.11). The NMR data of both purified enantiomers were identical to those of fraction 2. The calculated specific rotation measurements were $[\alpha]^{25}_{D}$ -140.0 (*c* 0.1, $CHCl_3$) for **1** and $[\alpha]^{25}_{D}$ +140.0 (*c* 0.1, $CHCl_3$) for **2**. The absolute configurations of enantiomer **1** and **2** were established as *R* and *S*, respectively (Figure 3.6), on comparison of the optical rotation with similar known core structure, (3*S*)-2-methylene-3-[(5'-methoxy-3'-4'-methylenedioxyphenyl) (4"-hydroxy-3",5"-dimethoxyphenyl)methyl]butyrolactone (Wu el al., 2006). Ultimately, **1** and **2** were elucidated as (*R*)-4-(bis(3,4-dimethoxyphenyl)methyl)-3-methylenedihydrofuran-2(3*H*)-one and (*S*)-4-(bis(3,4-dimethoxyphenyl)methyl)-3-methylenedihydrofuran-2(3*H*)-one, respectively. Compound 1 exhibited anti-proliferative effect in both HCT116 and HT29 cells with the GI_{50} values of 7.18 ± 0.29 and 6.22 ± 1.40 μg/mL, respectively. Compound 2 showed growth inhibitory effect against both HCT116 and HT29 cells with the GI_{50} values of 6.83 ± 0.30 μg/mL and 4.81 ± 0.72 μg/mL, respectively (Table 3.2).

Analysis of the crude extract tentatively identifies other components present in the extract apart from the secolignan (Appendix II). The chromatogram showed that there are small percentage of alkaloids and acids present in the extract (Figure 3.12). However, fraction 2/secolignan is the major component. The chromatogram showed that the acids eluted out first, then the alkaloids, then the isolated secolignan. Table 3.3. showed tentative compound identification present in the crude extract. Mass spectra and MS/MS spectra for individual compound are in Appendix II, Figure 3.13-3.18. The calibration curve estimated that there is 2.58 mg of the daughter fraction 2 per 10 mg of crude extract (Appendix II, Figure 3.19.)

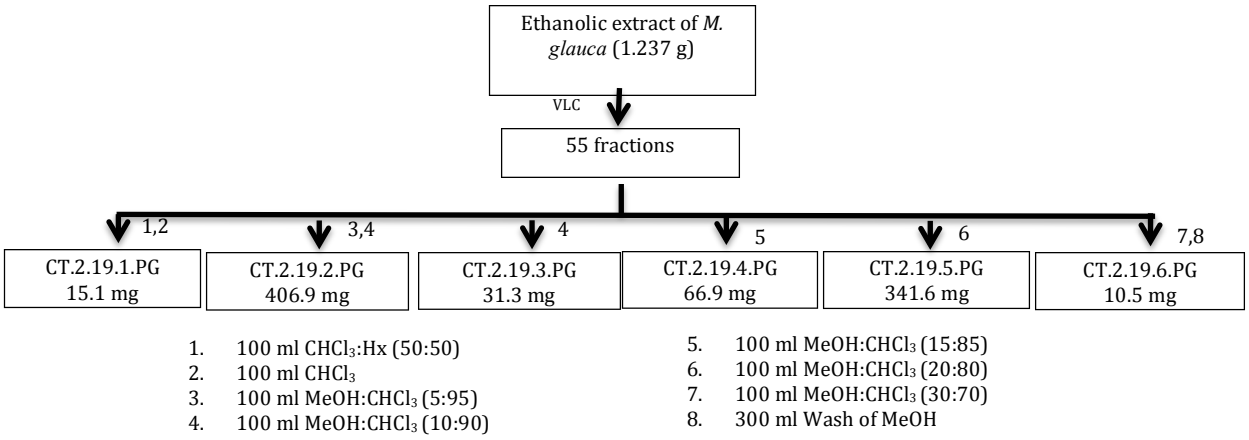

Figure 3.1. Fractionation Scheme

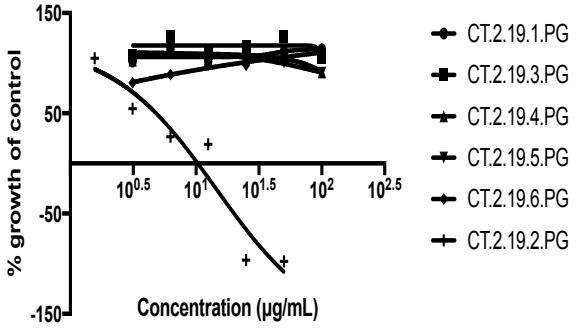

Figure 3.2. Concentration-response curve of fractions of *M. glauca* on HCT-116 cells

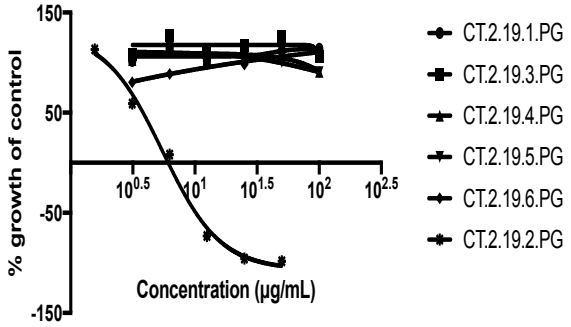

Figure 3.3. Concentration-response curve of fractions of *M. glauca* on HT-29 cells

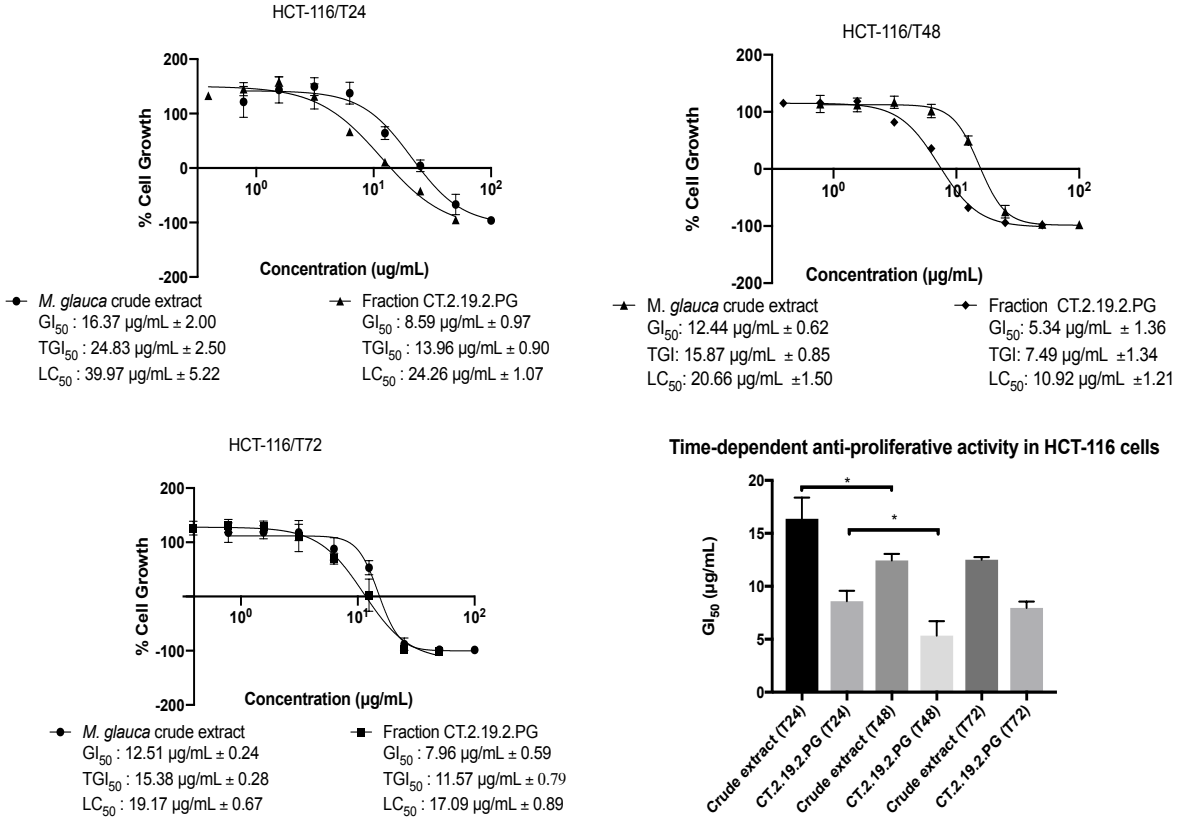

Figure 3.4. Fraction 2 and crude extract exhibited concentration and time-dependent anti-proliferative activity in HCT116 cells.

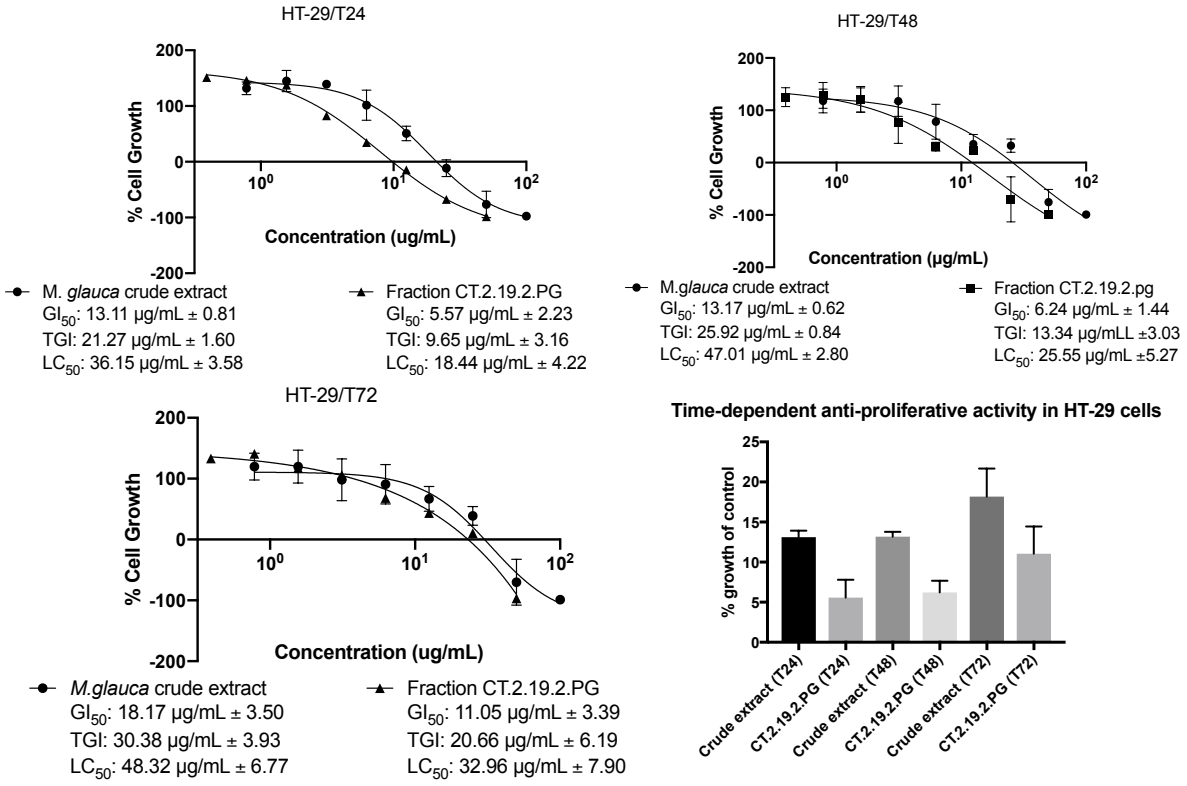

Figure 3.5. Fraction 2 and crude extract exhibited concentration and time-dependent anti-proliferative activity in HT29 cells.

Table 3.1. ^{1}H and ^{13}C NMR data for **1** and **2** ($CDCl_3$, 400 MHz)

Position	δ_H, mult. (*J* in Hz)	δ_C
1		170.90
2		136.17
3	3.86, overlapped	42.72
4	4.04, dd. (9.5) 4.34, dd. (9.5)	69.87
5	3.79, d. (11.4)	54.67
6	4.84, d. (2.1) 6.13, d. (2.1)	124.71
1′/1″		134.28/134.40
2′/2″	6.75, overlapped	111.27/111.47
3′/3″		148.10/148.19
4′/4″		149.03/149.33
5′/5″	6.84, overlapped	111.56/111.67
6′/6″	6.84, overlapped	119.16/120.14
3′/4′/3″/4″-OCH_3	3.85/3.86/3.87	55.88/55.91/55.97

Table 3.2. Half-maximal cell growth inhibitory effects of 95% ethanolic crude extract, six fractions, and **1** and **2** against HCT116 and HT29 cells (GI_{50} in µg/mL) [a]

	HCT116	HT29
95 % crude extract	12.44 ± 0.62	13.17 ± 0.62
Fraction 1	NE[b]	NE
Fraction 2	5.34 ± 1.36	6.23 ± 1.44
Fraction 3	NE	NE
Fraction 4	NE	NE
Fraction 5	NE	NE
Fraction 6	NE	NE
1	7.18 ± 0.29	6.22 ± 1.40
2	6.83 ± 0.30	4.81 ± 0.72
Doxorubicin	1.04 ± 0.04	0.38 ± 0.09

[a] GI_{50} was defined as the concentration causing 50% growth inhibition. Experiments were performed at least in triplicates with DMSO as negative control and doxorubicin as positive control.
[b] No effect up to 100 µg/mL

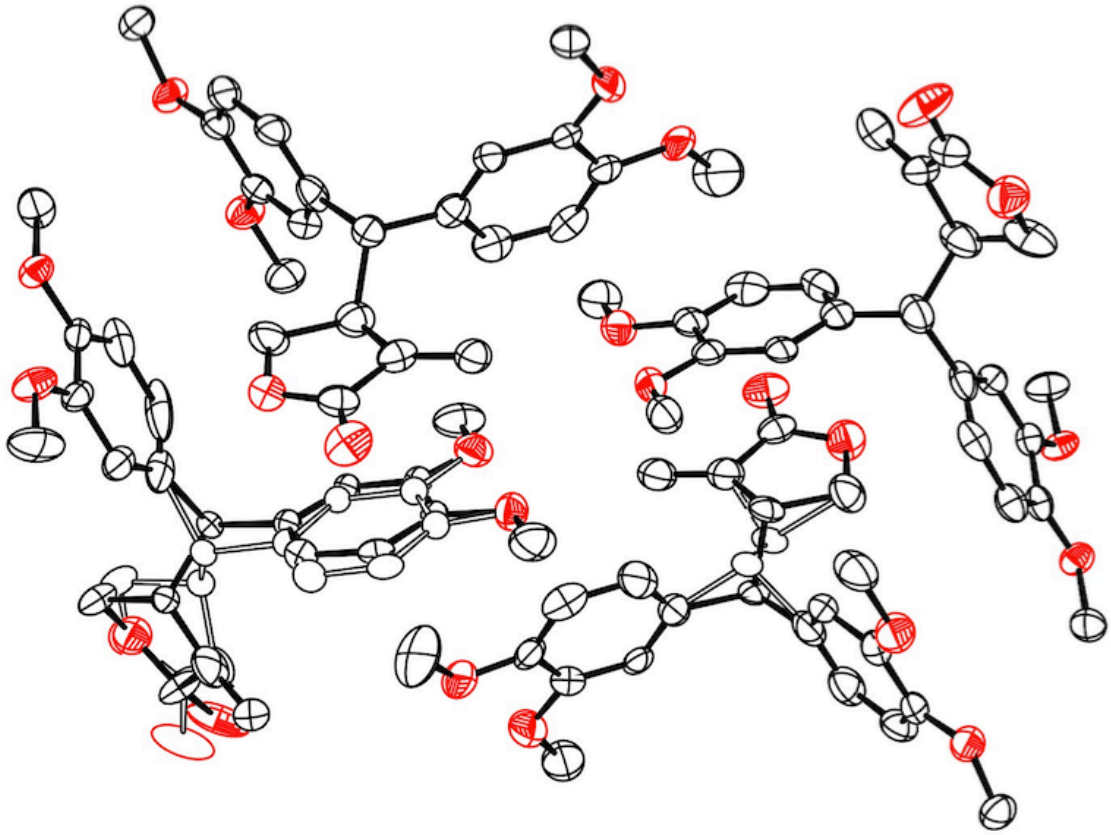

Figure 3.10. Crystal structure of the scalemic mixture.
Two of the four independent molecules are disordered, containing both enantiomers.

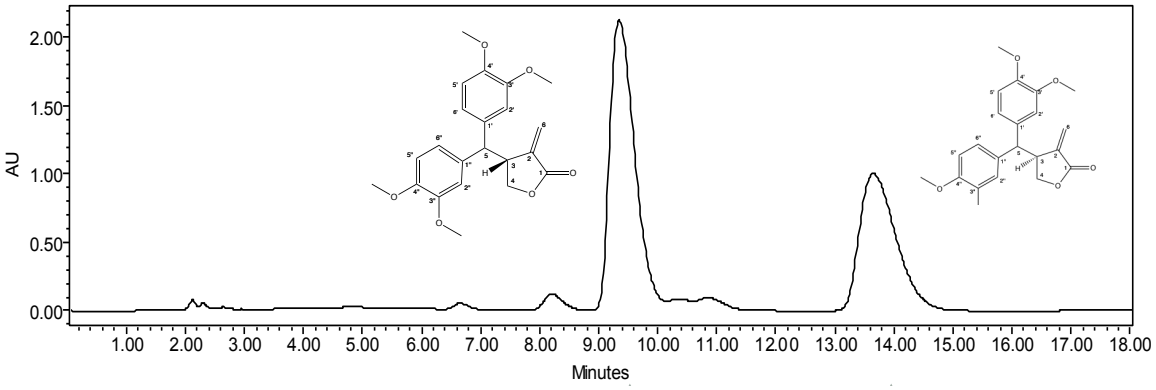

Figure 3.11. HPLC chromatogram of the scalemic mixture, daughter fraction 2

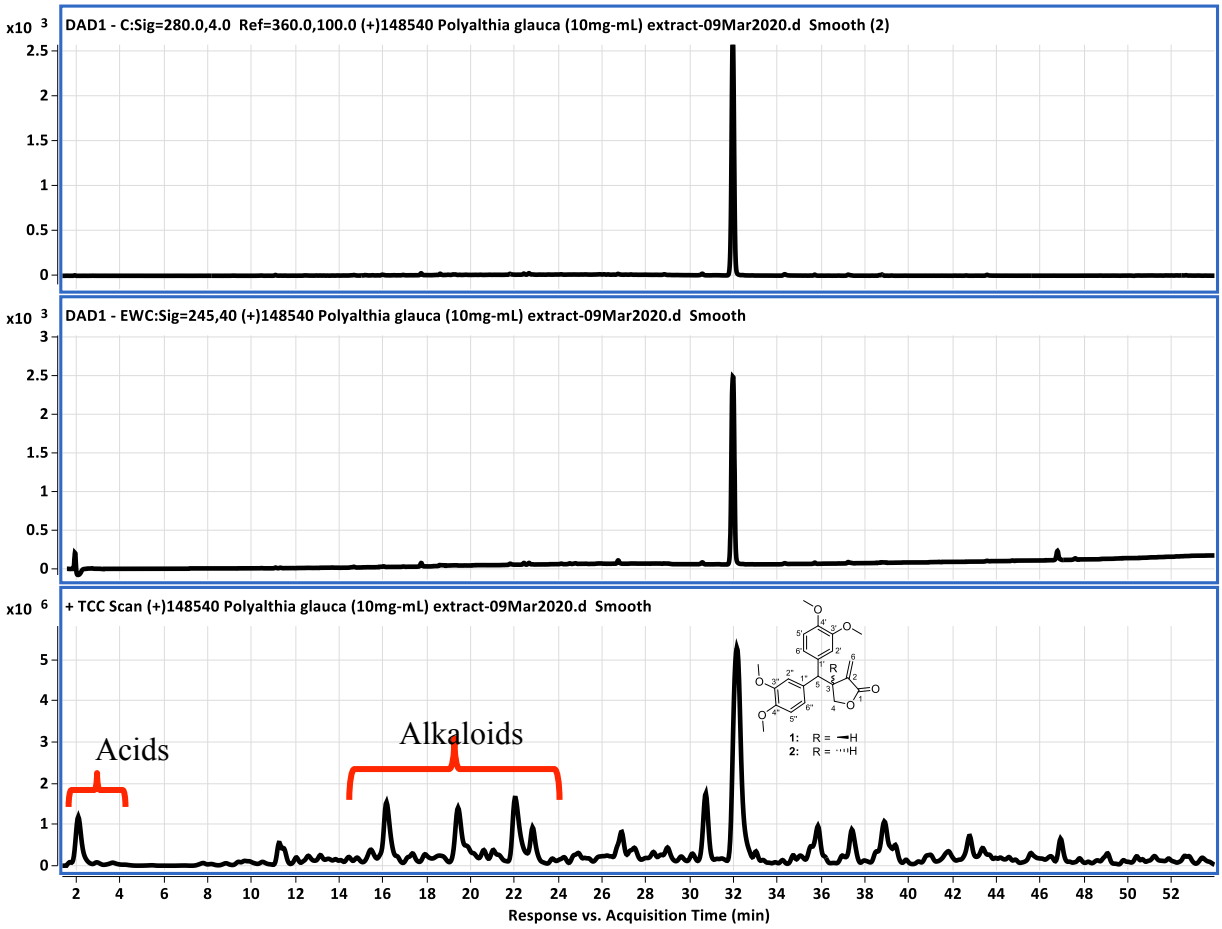

Figure 3.12. UHPLC Chromatogram of *M. glauca* crude extract

Table 3.3. Tentative compound identification in *M. glauca* crude extract

#	RT (min)	Tentative Identification	Molecular Formula	$[M+H]^+/[M-H]^-$
1	2.1	Malic acid	$C_4H_6O_5$	133.0142 $[M-H]^-$
2	2.2	Quinic acid	$C_7H_{12}O_6$	191.0561 $[M-H]^-$
3	16.1	Magnoflorine (quaternary benzylisoquinoline alkaloid)	$C_{20}H_{24}NO_4^+$	342.1778 $[M]^+$
4	19.5	Unknown	$C_{19}H_{17}NO_4$	324.123 $[M+H]^+$
5	21.9	Dihydroberberine	$C_{20}H_{19}NO_4$	338.1387 $[M+H]^+$
6	22.8	Anonaine	$C_{17}H_{15}NO_2$	266.1176 $[M+H]^+$
7	32.2	Isolated secolignan	$C_{22}H_{24}O_6$	385.1646 $[M+H]^+$

3.3 Discussion

Compounds **1** and **2** are known of secolignans, a type of lignans. Lignans are phenylpropanoids that exhibit chemotherapeutic potential on various cancers including liver cancer cells (Li et al., 2007), colorectal, ovarian, lung, and breast cancer (Chau et al., 2015). Examples of lignans are podophyllotoxin and its semi-synthetic derivative, etoposide. Etoposide is currently used to treat small-cell lung and testicular cancer (National Cancer Institute drug dictionary). Secolignan peperomin E, a major component in *Peperomia dindygulensis*, is a well-known secolignan that shows anti-proliferation, cell cycle arrest, apoptosis inducing activity on prostate cancer cells (Li et al.,2019). It can also induce apoptosis and suppress the invasion of gastric cancer cells (Wang et al. 2016, Wang et al., 2018). Other new secolignans also have been isolated and studied for anti-proliferative activities on various cancer cells (Hu et al., 2011, Wu et al., 2006).

Compound **1** was first reported in a patent for 5^{α}-reductase inhibitory activity. It was isolated from *Urtica fissa* (Qin et al, 2018). Even though the patent claims to have isolated the *R*

configuration, which is **1**, it is not clear how they arrived at the conclusion since there was no further evidence besides NMR spectra data to support their claim. There were not any reports for**2**. Thus, this study is the first one to report two undescribed secolignans. Furthermore, these two enantiomers were isolated from the same plant species. Although uncommon, it is not rare for plants to have enantiomerically enriched mixtures or racemates. Lignans, for examples, can be isolated with different enantiomeric compositions. Lignans are biosynthetically derived from the cinnamate pathway. Within earlier stages of this pathway, there are dirigent proteins that are responsible for the enantiomeric diversity of compounds (Finefield et al., 2012). Therefore, this can explain the presence of enantiomeric mixtures of lignans.

This study shows that the anti-proliferative activity of *M.glauca* extract is most likely due to fraction 2 since it is the only fraction that exhibits growth inhibitory effect out of six fractions. In addition, data from this study have shown that fraction 2 only comprises **1** and **2;** therefore, any activity exhibited by fraction 2 is most likely due to these two compounds. Results from anti-proliferative assays show that **1** and **2** exhibit comparable growth inhibitory effects when compared with fraction 2. In conclusion, the anti-proliferative activity exhibited by *M. glauca* extract in HCT116 and HT29 cells is most likely due to the presence of **1** and **2**.

Chapter 4: Determine the mechanism of action of the anti-cancer effect

4.1 Materials and methods

4.1.1. Evaluation of apoptosis induction in colorectal cancer cells by *M. glauca* extract and its secondary metabolite/s

To determine whether the test samples can induce apoptosis in HCT-116 cells, cell apoptosis was quantitatively measured by using FACS (BD) (Vermes et al., 1995). Excitation was done using 15-mW, 488-nm argon-ion laser. Briefly, cells ($1x10^5$ cells/well) were seeded in a 12-well plate. Following 24 hr of incubation, cells were treated with DMSO (vehicle control), camptothecin (positive control), testing samples for 24 hr or 48 hr with one concentration above the GI_{50}, one concentration at/near GI_{50}, and one concentration below GI_{50}. For crude extract, the testing concentrations were 25 μg/mL, 12.5 μg/mL, and 6.25 μg/mL. For secolignan fraction 2, **1** and **2**, they were 10 μg/mL, 5 μg/mL, and 2.5 μg/mL. After the treatment of test samples, cells were collected and washed with cold 1x PBS twice and stained using FITC-AnnexinV/PI apoptosis detection kit in accordance with the manufacturer's protocol (BD Bio-Sciences). Detection of apoptotic cells was determined by the percentage of cells population that stained positive for FITC Annexin V alone and positive for both FITC Annexin V and propidium iodide. GraphPad Prism was used for statistical analysis. All experiments were performed using triplicate.

4.1.2 Determine the effect of 1 and 2 on the cell cycle in HCT116 cells

Propidium iodide (PI) staining buffer containing 50 μg/mL PI (Invitrogen, Cat# P1304MP), 10 μg/mL RNase A (Invitrogen, Cat# EN0531), and 0.1% BSA (Rockland, Cat#

BSA-50) was prepared freshly for each assay. Briefly, cells (15,000 cells/well) were seeded in a 96-well plate. Following 24 hr of incubation, **1** or **2** was added. After 24 hr of incubation, HCT116 cells were collected and washed with ice cold PBS. Subsequently, the cells were fixed with ice-cold 70% ethanol and incubated overnight at 4ºC. Cells were centrifuged at 3000g for 10 minutes to remove the ethanol and stained with 1 mL PI staining buffer at room temperature in dark for 1h. The distribution of the cell cycle was measured by flow cytometer (BD, FACSCalibur) and results were analyzed by Flowjo software.

4.1.3. Determine the effects of *M. glauca* in interfering with Wnt/β-catenin signaling pathway.

4.1.3a: Isolating and verifying plasmids.

Expression plasmids M50 Super 8x TOPFlash and M51 Super 8x FOPFlash (TOPFlash mutant) was a gift from Randall Moon (Addgene plasmid # 12456 and Addgene plasmid # 12457) (Veeman et al., 2003). Isolating these plasmids was performed using Qiagen Plasmid Maxi Kit (Cat No./ID: 12162). Plasmid DNA was sequenced for verification. Primer RVP3 was used (5'-CTA GCA AAA TAG GCT GTC CC-3'). Blast was used to compare the obtained sequence with the sequences from Addgene.

4.1.3b: Evaluation of *M.glauca* in interfering with the Wnt/β-catenin signaling pathway.

Briefly, 15,000 cells/well was seeded in 96-well plate. Following 24 hr of incubation, Lipofectamine 2000 was used for transiently transfecting the cells with luciferase reporter plasmids (0.3 μg TOPFlash or 0.3 μg FOPFlash). After six hr of transfection, medium was removed and cells were treated with testing samples or DMSO (vehicle control), or luteolin (25 μM, positive control) for 12 hr. Cells were lysed using the Luciferase Assay System (Promega) in accordance with the manufacturer's instructions. Light intensity was measured and luciferase

activities were normalized. Results were presented as relative luciferase activity. GraphPad Prism was used for statistical analysis.

4.1.4. Determine the effects of *M. glauca* on the expression levels of Wnt downstream target genes

Cells ($1x10^5$ cells/well) were seeded in a 12-well plate. After 24 hr of incubation, cells were treated with testing samples for an additional six hr. Total RNAs were extracted using NucleoSpin RNA Plus (Takara). RNAs were revered-transcribed using iScript Reverse Transcription Supermix for RT-qPCR (Bio-Rad). Real-time PCR was performed with a Real-Time PCR detection system (Bio-Rad) using iTaq Universal SYBR Green Supermix (Bio-Rad). The following sequences of primers were used. Quantification between treatments and DMSO control was normalized to the levels of GAPDH.

Table 4.1. Primers of the Wnt target genes.

Target Genes	Direction	Sequences
C-Myc	Forward	5'- CAC CAG CAG CGA CTC TGA-3'
	Reverse	5'- GAT CCA GAC TCT GAC CTT TTG-3'
CCND1	Forward	5'- GAA GAT CGT CGC CAC CTG-3'
	Reverse	5'- GAC CTC CTC CTC GCA CTT CT-3'
BIRC5	Forward	5'- CCG ACG TTG CCC CCT GC-3'
	Reverse	5'- TCG ATG GCA CGG CGC AC-3'

4.2. Results

M. glauca extract, fraction 2, compounds **1** and *2* were evaluated for apoptosis induction in HCT116 cells. Annexin V and propidium iodide staining showed that *M. glauca* crude extract induced apoptosis upon 24 hr incubation. There was a significant difference between 25 µg/mL treatment and DMSO control in early apoptosis. For cells treated with 25 µg/mL of *M. glauca*, 24.35% of total cells were early apoptotic cells. The early apoptotic cells population was decreased in cells treated with 12.5 µg/mL and 6.25 µg/mL crude extract (Figure 4.1). There is no significant difference between the lower concentration treatments and DMSO control.

Data also indicated that fraction 2 induces apoptosis in HCT116 cells. However, it takes 48 hr to see the apoptosis effect. Fraction 2 induces apoptosis in a concentration-dependent manner. Cells treated with 10 μg/mL of fraction 2 exhibited a high level of apoptotic cells (29.15%) as compared to DMSO (3.67%). When treated with 5 μg/mL, there were 14.71% of the total cells that undergo early apoptosis. Cells treated with 2.5 μg/mL have a lower percentage of early apoptotic cells (Figure 4.2). Consequently, upon 48 hr of incubation, fraction 2 shows concentration-dependent apoptosis-inducing activity in HCT116 cells.

Similar to fraction 2, **1** and **2** cause apoptosis in HCT116 cells upon 48 hr of incubation. Between the two compounds, **2** shows a more prominent apoptosis-inducing activity. Treatment with 10 μg/mL of **2** causes 27.38% of cells to undergo early apoptosis; whereas, 10 μg/mL of **1** induces 20.96% of cells to undergo early apoptosis. There are 15.19% or 9.87% of total cells population that undergo early apoptosis when treated with 5 μg/mL or 2.5 μg/mL of **2**, respectively (Figure 4.3). When treated with 5 μg/mL or 2.5 μg/mL of **1**, there is only 8.24% and 9.29% of cells that undergo apoptosis (Figure 4.4). There are significant differences between 10 μg/mL or 5 μg/mL treatments of **2** and DMSO control. These results indicate that **2** induces apoptosis in a concentration-dependent manner; the apoptosis-inducing activities of **2** and fraction 2 are comparable and they are both more prominent than that of **1**.

Compounds **1** and **2** also were evaluated for cell cycle arrest. The data collected by the flow cytometer revealed that the percentage of cells arrested in G2/M-phase significantly increased in groups treated with 5 μg/mL of **1** or 5 μg/mL of **2**, compared with the DMSO control group. However, this effect was not observed with a lower concentration of **1** and **2** (3.25 μM, 6.5 μM). The G2/M-phase arrest effect was more pronounced in 13 μM of **1** than 13 μM of

2 (figure 4.5). The results from the cell cycle and apoptosis analysis indicate that **1** and **2** induce apoptosis by arresting cells at G2/M-phase.

The Wnt signaling inhibitory activity of the crude extract, active fraction, and**1** and **2** were examined in HCT116 cells using reporter gene assay. TOPFlash contains wild-type TCF binding sites that are upstream of the luciferase open reading frame. FOPFlash contains the mutant binding sites and is used as a negative control. Plasmid DNAs were sequenced and verified. Results show that the crude extract significantly reduced the activity of the Wnt signal in a concentration-dependent manner. It suppresses the Wnt signaling pathway by 27, 48, and 85% at 6.25, 12.5, and 25 μg/mL, respectively; the active fraction also significantly inhibited the pathway by 50, 81, and 89% at 2.5, 5, and 10 μg/mL, respectively. Compounds **1** and **2** exhibited similar inhibitory activity of the Wnt signaling pathway. The results suggest that the active fraction showed a stronger inhibition as compared to the crude fraction, **1** and **2** (Figure 4.6). This is the first time that any secolignan was reported to have inhibitory activity against the Wnt signaling pathway in colorectal cancer cells.

To further confirm the suppression of the Wnt signaling pathway, three target genes *CMYC*, *CCND*1, and *BIRC5* of this pathway were analyzed. Results were normalized to GAPDH and expressed as relative mRNA levels. qRT-PCR analysis of these target genes shows the down regulation of their mRNA levels. Cells treated with *M. glauca* extract have reduced levels of mRNA expression for the three target genes. The mRNA levels of CMYC and CCND1 target genes were significantly reduced as compared to DMSO control. There was no significant reduction in mRNA levels of target gene BIRC5; however, there is a decreasing trend when cells treated with increasing concentration of extract. For fraction 2, similar trends were observed. There was a more prominent reduction of mRNA expressions of the three target genes. mRNA

expression of CMYC and CCND1 were more reduced than that of BIRC5. Fraction 2 decreases mRNA expression of the target genes in a concentration-dependent manner. Compounds **1** and **2** show a much stronger reduction of mRNA expressions of CMYC, CCND1, and BIRC5 as compared to *M. glauca* extract and fraction 2. Both compounds exhibited a similar reduction of mRNA levels.

4.3. Discussion

One of the hallmarks of cancer is the ability of cancer cells to evade apoptosis. As a result, cancer cells have minimal apoptotic events (Hanahan & Weinberg, 2000). It is the goal of cancer therapy to promote apoptosis of cancer cells. Therefore, it is essential to determine the effect of *M. glauca* and its metabolites on inducing apoptosis. Once apoptosis was determined, further investigations were performed to evaluate the effects of **1** and **2** on the cell cycle. As results indicated, both compounds cause a cell cycle arrest at the G2/M phase. Cells in the G2 phase undergo preparation before proceeding to mitosis. Therefore, this checkpoint is commonly targeted for cancer treatment. There have been more reports on lignans inducing apoptosis via cell cycle arrest at the G2/M phase in various cancer cells (Xin et al., 2013; Ho et al., 2019). Even though there is usually a correlation between G2/M phase arrest and anti-tubulin activities, there is increasing evidence of how the Wnt/β-catenin signaling pathway is enhanced in the G2 phase, especially in colorectal cancer. At the center of the Wnt signaling pathway is the β-catenin/TCF complex. The amount of this complex fluctuates with the cell cycle; it increases in the S phase and at its peak at the G2 phase. Besides , a study in HCT116 cells shows that inhibiting the β-catenin/TCF complex can delay cells to progress through the G2/M phase (Ding et al., 2014). Consequently, this demonstrates the important role of the Wnt signaling pathway in the cell cycle.

Our study is to determine the effect of *M.glauca* and its metabolites in interference with the Wnt/ β-catenin signaling pathway. Results demonstrate that *M. glauca*, the scalemic mixture, and the two enantiomers show suppression of the Wnt signaling pathway. Our results provide the first piece of evidence showing secolignans inhibit cell proliferation by suppressing Wnt/ β-catenin signaling pathway.

Relative quantification of mRNA levels of Wnt target genes shows a reduction of mRNA expression of CMYC, CCND1, and BIRC5 in colorectal cancer cells with treatment with *M. glauca*, the scalemic mixture, and the two compounds. These genes are responsible for cell proliferation and growth. Taken together, evidence from our study show that this suppression of the Wnt signaling pathway leads to reduced levels of target genes which are responsible for cell survival and growth, inhibiting cell proliferation. This suppression of Wnt signaling pathway also leads to cell cycle arrest at the G2/M phase, eventually causing cell apoptosis in colorectal cancer cells.

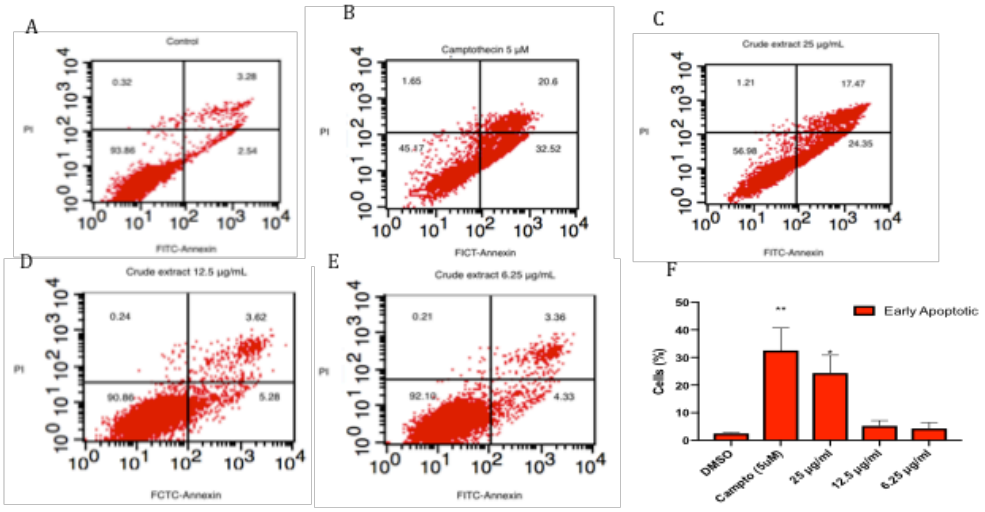

Figure 4.1. Cell apoptosis analyzed by flow cytometry with *M. glauca* treatment. *M. glauca* triggers apoptosis in HCT116 cells. Apoptotic cells were determined by flow cytometry using Annexin V and propidium iodide (PI) staining. Cells in the lower right quadrant FITC-Annexin V+/PI- are apoptotic cells, those in the lower left quadrant (FITC-Annexin V-/PI-) are normal, and those in the upper right quadrant (FITC-Annexin +/PI+) are late apoptotic cells. Cells were A) treated with 0.125% DMSO, B) treated with 5 µM camptothecin, or (C-E) treated with decreasing concentration of *M. glauca* crude extract. The histogram (F) represents the data from three independent experiments, expressed as mean ± S.D. Differences between groups vs. DMSO control were determined by means of a one-way analysis of variance followed by Dunnett's multiple comparison test. Differences were considered to be statistically significant for *p<9.95, **p<0.005.

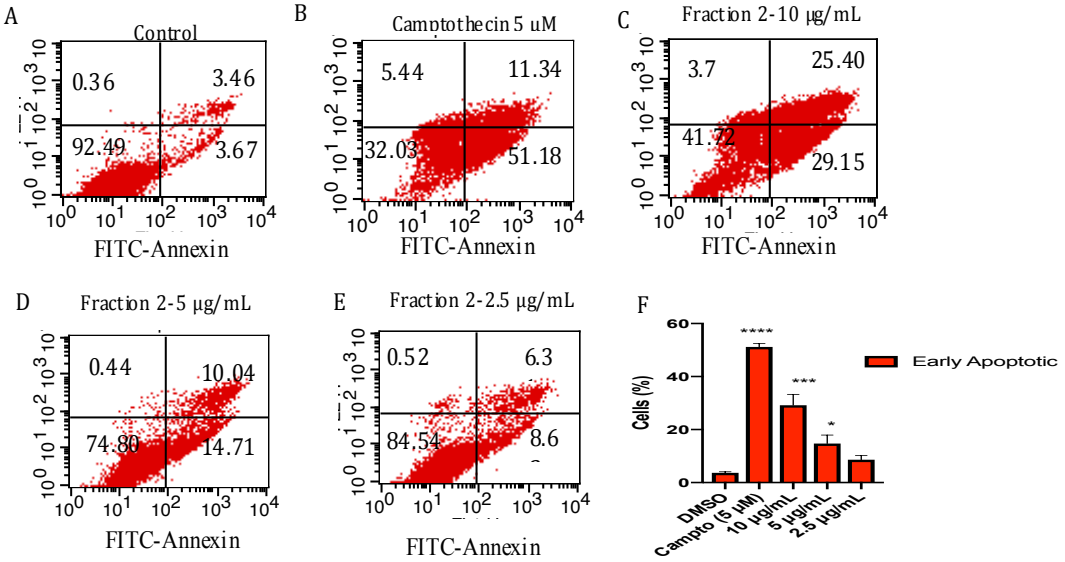

Figure. 4.2. Cell apoptosis analyzed by flow cytometry with the daughter fraction 2 treatment. Fraction 2 triggers apoptosis in HCT116 cells. Cells were A) treated with 0.125% DMSO, B) treated with 5 µM camptothecin, or (C-E) treated with decreasing concentrations of fraction 2. The histogram (F) represents the data from three independent experiments, expressed as mean ± S.D (n=3). Differences between treatment groups vs. DMSO control were determined by means of a one-way analysis of variance followed by Dunnett's multiple comparison test. Differences were considered to be statistically significant for * $p<0.05$, *** $p<0.001$, **** $p<0.0001$.

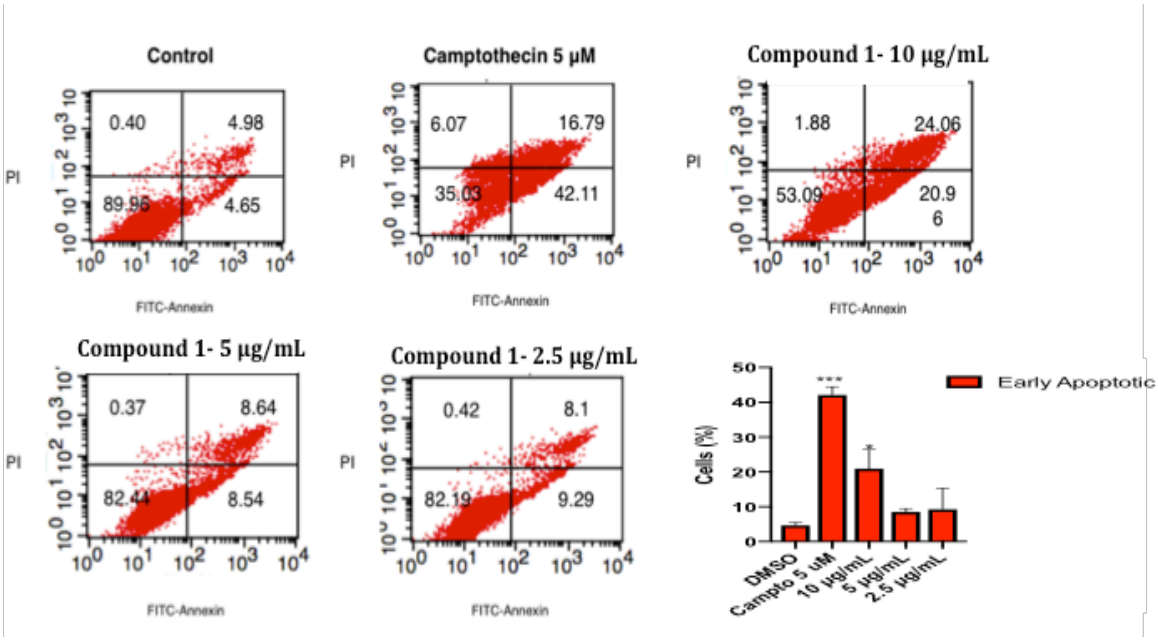

Figure. 4.3. Cell apoptosis analyzed by flow cytometry with **1** treatment**.**
Compound **1** triggers apoptosis in HCT116 cells. Cells were A) treated with 0.125% DMSO, B) treated with 5 µM camptothecin, or (C-E) treated with decreasing concentrations of **1**. The histogram (F) represents the data from three independent experiments, expressed as mean ± S.D (n=3). Differences between treatment groups vs. DMSO control were determined by means of a one-way analysis of variance followed by Dunnett's multiple comparison test. Differences were considered to be statistically significant for * $p<0.05$, ***$p<0.001$.

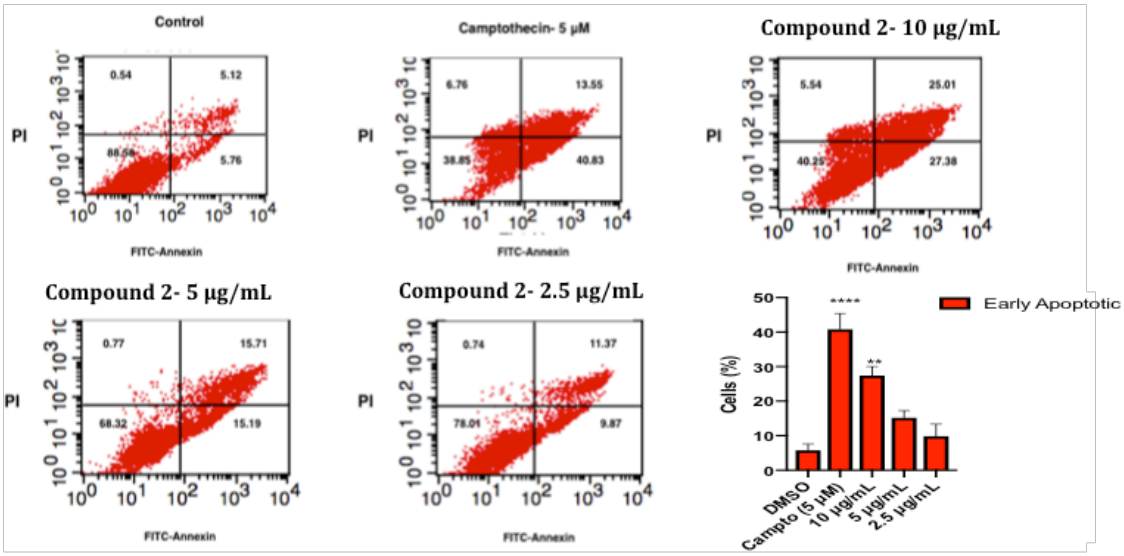

Figure 4.4. Cell apoptosis analyzed by flow cytometry with **2** treatment.
Compound **2** triggers apoptosis in HCT116 cells. Cells were A) treated with 0.125% DMSO, B) treated with 5 µM camptothecin, or (C-E) treated with decreasing concentrations of **2**. The histogram (F) represents the data from three independent experiments, expressed as mean ± S.D (n=3). Differences between treatment groups vs. DMSO control were determined by means of a one-way analysis of variance followed by Dunnett's multiple comparison test. Differences were considered to be statistically significant for ** $p<0.005$, ***$p<0.001$.

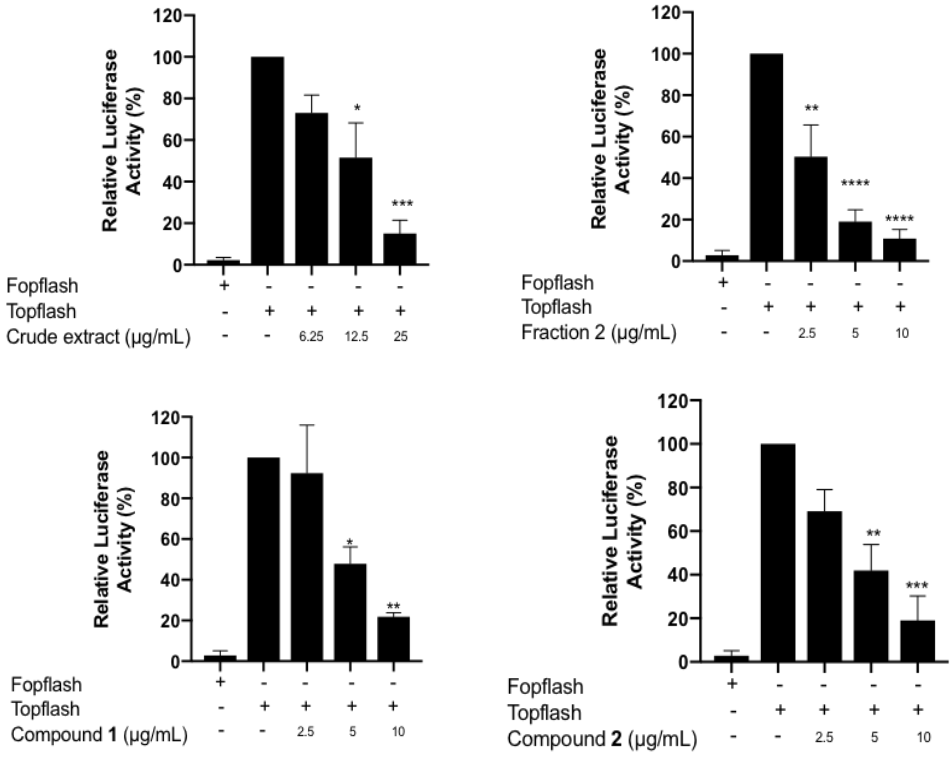

Figure 4.6. B-catenin/TCF transcriptional activity in HCT116 cells treated with *M. glauca*, fraction 2, **1,** or **2.**
Crude extract, active fraction, compounds 1 and 2 inhibits the activity of the Wnt signalling pathway in HCT116 cells. The data were expressed as mean ±S.D (n=3). Differences between treatment groups vs DMSO control were determined by means of a one-way analysis of variance followed by Dunnett's multiple comparison test. Differences were considered to be statistically significant for *p<0.05, ** p<0.005, ***p<0.0005, and ****p<0.0001

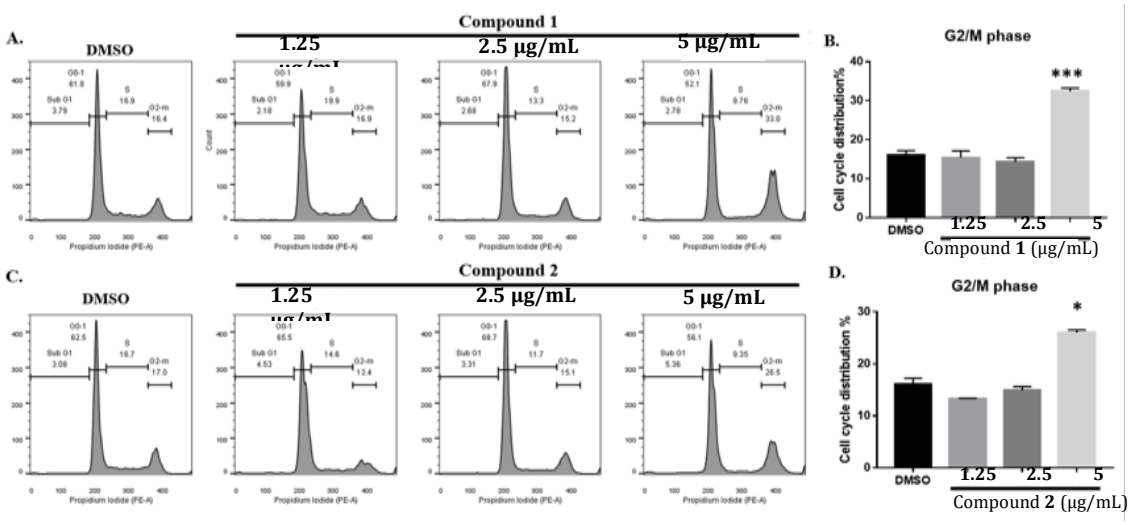

Figure 4.5. Cell cycle analysis of **1** and **2**.
Cells were treated 24 h with **(A)** DMSO only (final concentration 0.1%); 1.25 µM, 2.5 µM, and 5 µg/mL of **1**; **(C)** 1.25 µM, 2.5 µM, and 5 µg/mL of **2**. **(B & D)** Results are the mean ± SD of three separate experiments. Significant difference between each group and the DMSO control are shown as $p \leq 0.05$ (*); $p \leq 0.01$ (**) and $p \leq 0.001$ (***).

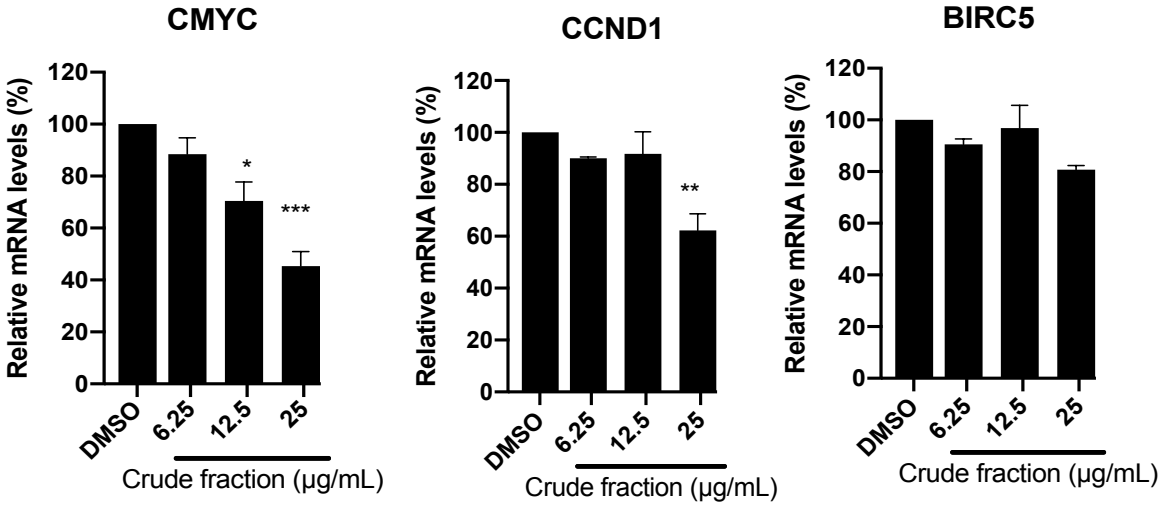

Figure 4.7. Expression levels of Wnt target genes measured by qRT-PCR in HCT116 cells that were treated with *M. glauca*.
Expression levels of *CMYC, CCND1,* and *BIRC5* were measured after 6 hr treatment of crude extract. Results were normalized to GAPDH mRNA. Data were from at least two independent experiments, expressed as mean ± S.D. Differences between treatment groups vs. DMSO control were determined by means of a one-way analysis of variance followed by Dunnett's multiple comparison test. Differences were considered to be statistically significant for *$p<0.05$, ** $p<0.005$, ***$p<0.001$.

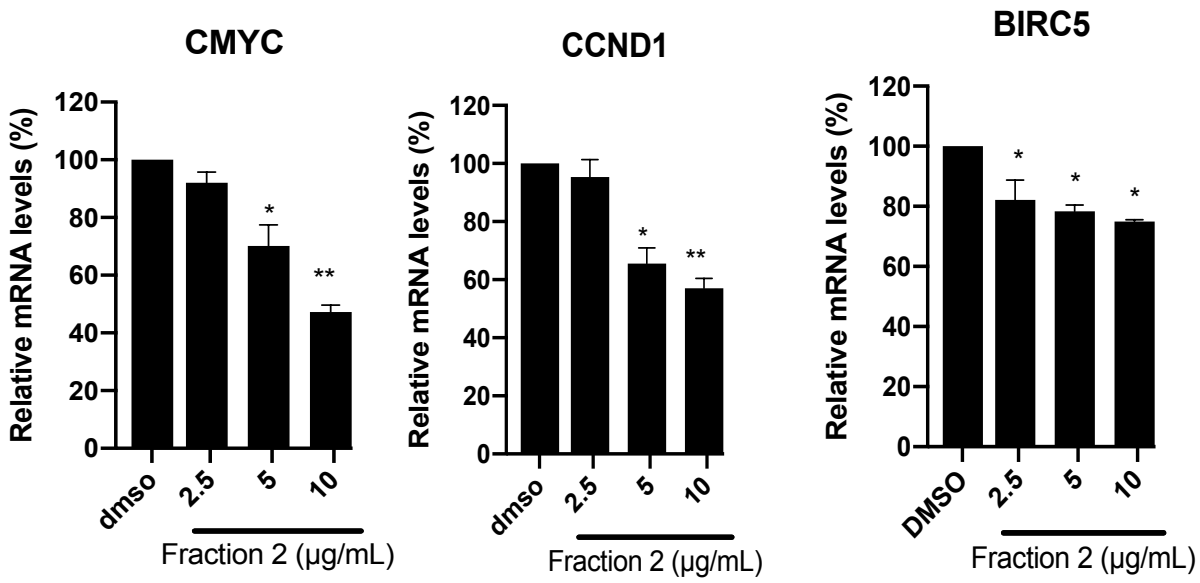

Figure 4.8. Expression levels of Wnt target genes measured by qRT-PCR in HCT116 cells that were treated with fraction 2.
Expression levels of *CMYC, CCND1,* and *BIRC5* were measured after 6 hr treatment of fraction 2. Results were normalized to GAPDH mRNA. Data were from at least two independent experiments, expressed as mean ± S.D. Differences between treatment groups vs. DMSO control were determined by means of a one-way analysis of variance followed by Dunnett's multiple comparison test. Differences were considered to be statistically significant for *$p<0.05$, ** $p<0.005$.

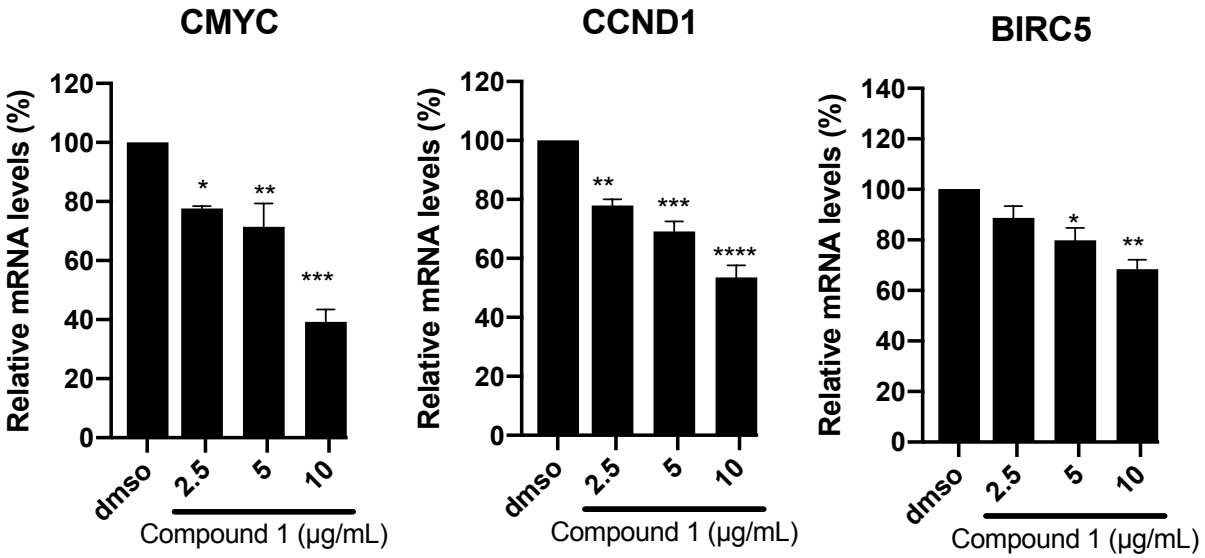

Figure 4.9. Expression levels of Wnt target genes measured by qRT-PCR in HCT116 cells that were treated with **1.**
Expression levels of *CMYC, CCND1,* and *BIRC5* were measured after 6 hr treatment of **1**. Results were normalized to GAPDH mRNA. Data were from at least two independent experiments, expressed as mean ± S.D. Differences between treatment groups vs. DMSO control were determined by means of a one-way analysis of variance followed by Dunnett's multiple comparison test. Differences were considered to be statistically significant for *p<0.05, ** p<0.005, ***p<0.0005, ****p<0.00005

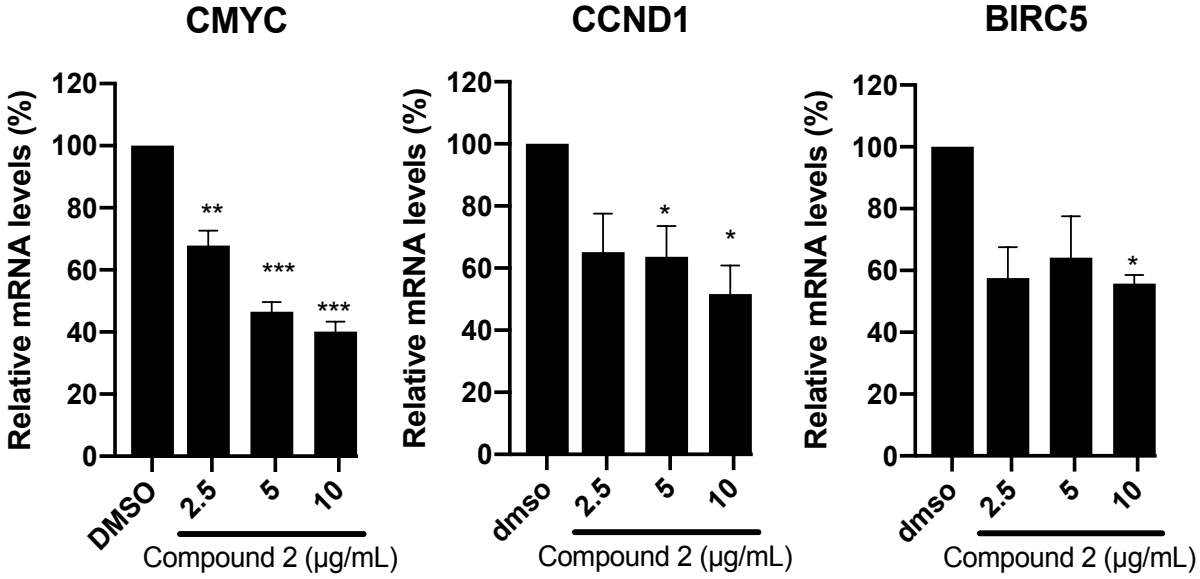

Figure 4.10. Expression levels of Wnt target genes measured by qRT-PCR in HCT116 cells that were treated with **2.**
Expression levels of *CMYC, CCND1,* and *BIRC5* were measured after 6 hr treatment of **2**. Results were normalized to GAPDH mRNA. Data were from at least two independent experiments, expressed as mean ± S.D. Differences between treatment groups vs. DMSO control were determined by means of a one-way analysis of variance followed by Dunnett's multiple comparison test. Differences were considered to be statistically significant for *$p<0.05$, ** $p<0.005$, ***$p<0.0005$.

Chapter 5: Evaluate drug combination *in-vitro*

5.1 Materials and methods

To evaluate the effects of **1** and **2** on the antiproliferative effect of irinotecan, combination studies were performed. The effect of **1** and **2**, when combined with irinotecan, were evaluated on HCT116 and HT29 cells. Briefly, cells (5000 cells/well) were seeded in a 96-well plate. After 24 hr of incubation, cells were either treated with 5 µg/mL, 2.5 µg/mL, and 1.25 µg/mL of **1** or**2** in combination with irinotecan (20 µg/mL, 10 µg/mL, 5µg/mL, 2.5 µg/mL, and 1.25 µg/mL). Cells were further incubated for 48 hr and cell viability was assayed using WST-8 dye as described earlier. Combination index (CI) was calculated by using the following formula

$$\mathrm{CI} = \frac{C_{A,X}}{IC_{X,A}} + \frac{C_{B,X}}{IC_{X,B}}$$

where $C_{a,x}$ and $C_{B,x}$ are concentrations of test samples A and B to achieve certain effects when used in combination. $IC_{X,A}$ and $IC_{X,B}$ are the concentration of single test samples needed to achieve the same effect. CI<1 indicates synergism; CI=1 indicates addition; CI>1 indicates antagonism (Chou T.C., 2006).

5.2 Results and Discussion

The concentration-response curve shows that when the cells treated with irinotecan in combination with 5 µg/mL of **1**, the response curve shifted to the left, indicating a stronger response. When combined with 1.25 or 2.5 µg/mL of **1**, the responses were not as strong. The curves were shifted to the right of the irinotecan-single treatment curve (Figure 5.1). The isobologram shows IC_{30}, IC_{50}, and IC_{70} values of irinotecan and **1**, as well as the concentration of

irinotecan and **1** when combined to achieve the same effects. For isobologram, when the data lies on the straight line that connects the two IC values, it indicates an additive effect. When the data lies below this line, then it is synergism; when the data lies above the line, then it is antagonism. As depicted from the isobologram, most of the combinations with **1** resulted in slight antagonisms, with only two combinations resulted in synergism at inhibiting 50% and 70% cell growth (Figure 5.2). When combined with 1.25 or 2.5 μg/mL of **2**, the concentration-response curves shifted to the right of the irinotecan-single treatment curve; however, when combined with 5 μg/mL of **2**, the effects were too efficacious as the curve shifted downward. As a result, combination with this concentration does not have any CI_{50}, CI_{30}, or CI_{70} values (Figure 5.3). For HT29 cells, irinotecan in combination with **1** does show strong effects on HT 29 cells when combining with 1.25 μg/mL. This combination shows the synergism effect at inhibiting 70% and 50%. Because of this synergism effect, in combination, **1** and irinotecan would have to require a lower concentration or amount whereas, in a single test, irinotecan, and **1** would need more amount to achieve the same effect of inhibiting 70% or 50% of cell growth (Figure 5.5 and 5.6). When combined with 2.5 or 5 μg/mL of**1**, there is also a synergism effect at GI_{70} (Figure 5.5). The combination of irinotecan with **2** shows weak responses toward inhibiting cell proliferation. There is one combination where it shows synergism. That combination is with 2.5 μg/mL to inhibit 70% of cell growth in HT29 cells (Figure 5.7 and 5.8). Table 5.1 shows the CI values of all the combinations to inhibit 30%, 50%, and 70% cell growth.

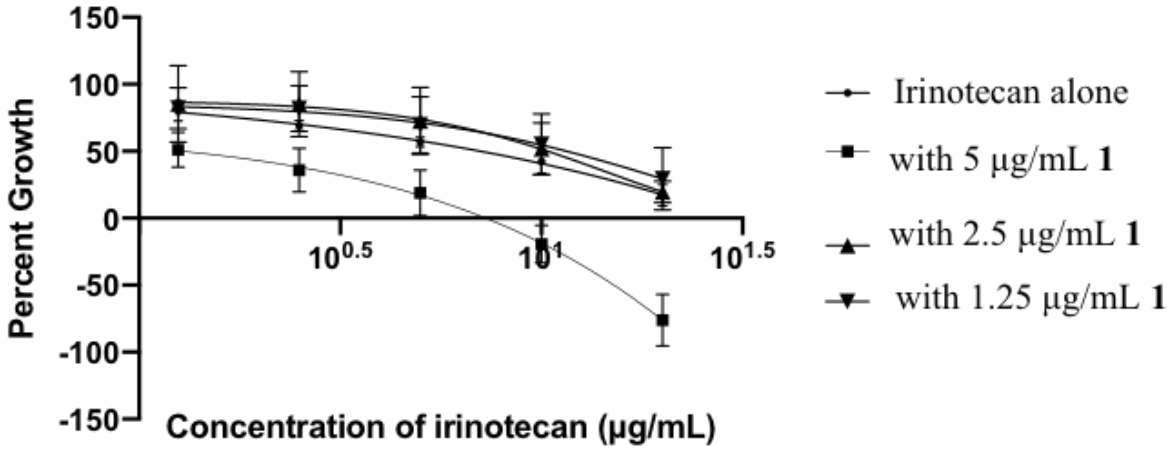

Figure 5.1. Concentration-response curve of irinotecan in combinationa with **1** in HCT116 cells.

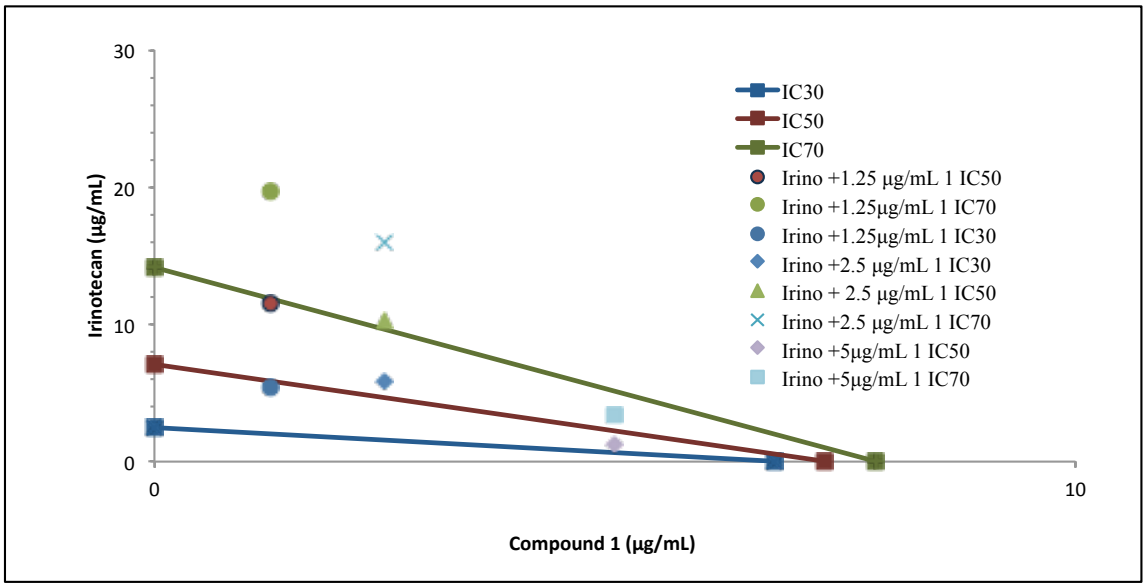

Figure 5.2. Isobologrram representation of irinotecan in combination with **1** in HCT116 cells.

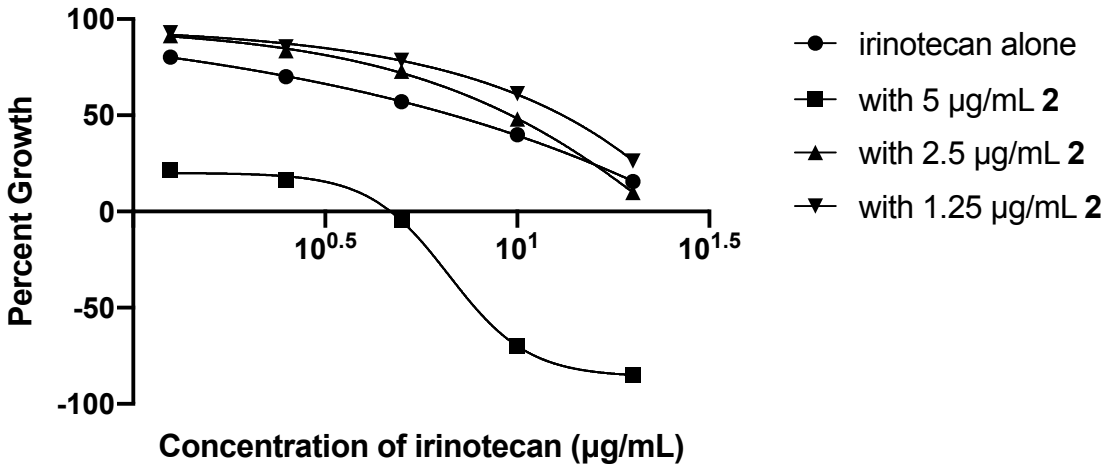

Figure 5.3. Concentration-response curve of irinotecan in combination with **2** in HCT116 cells

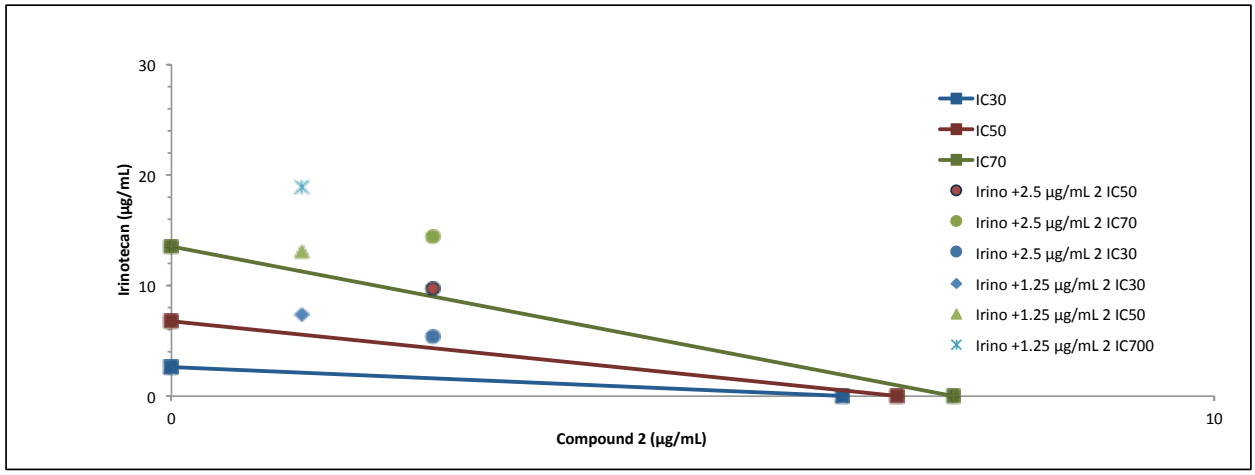

Figure 5.4. Isobologrram representation of irinotecan in combination with **2** in HCT116 cells.

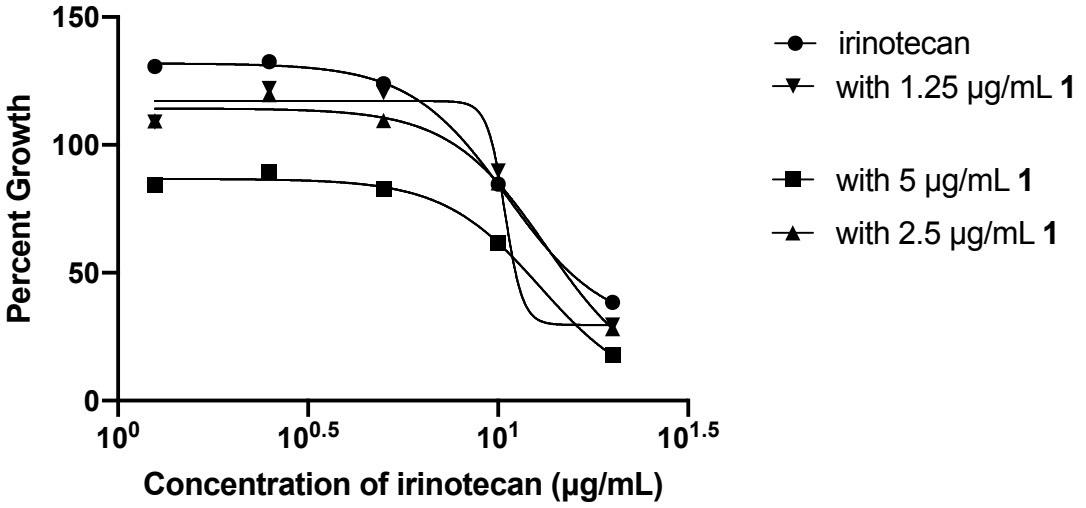

Figure 5.5. Concentration-response curves of irinotecan in combinations with **1** in HT29 cells

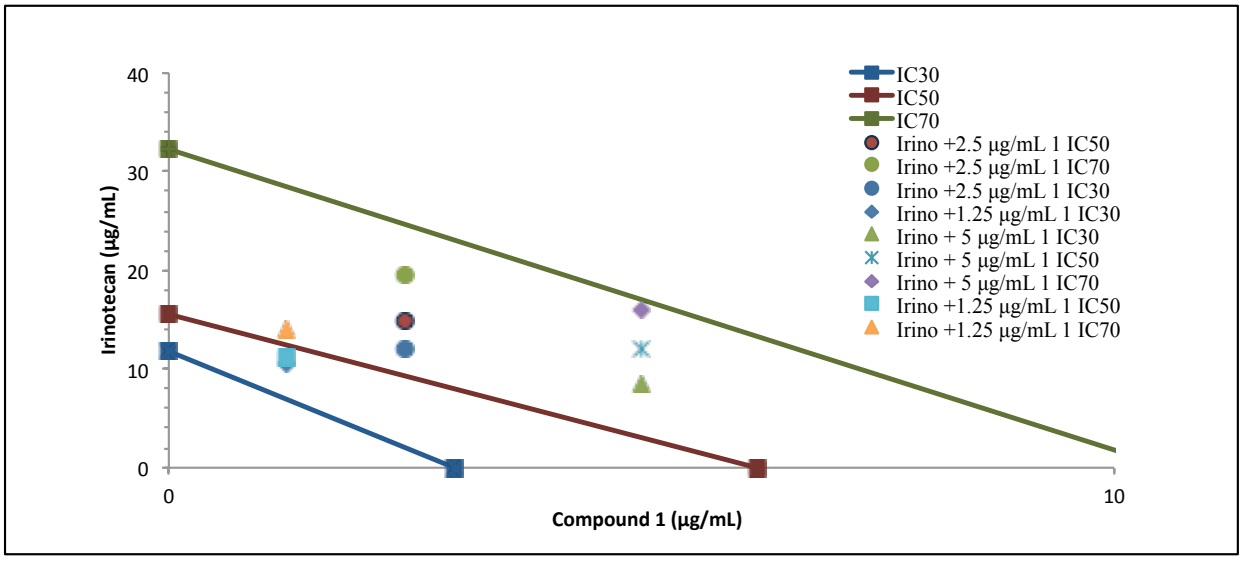

Figure 5.6. Isobologrram representation of irinotecan in combinations with **1** in HT29 cells.

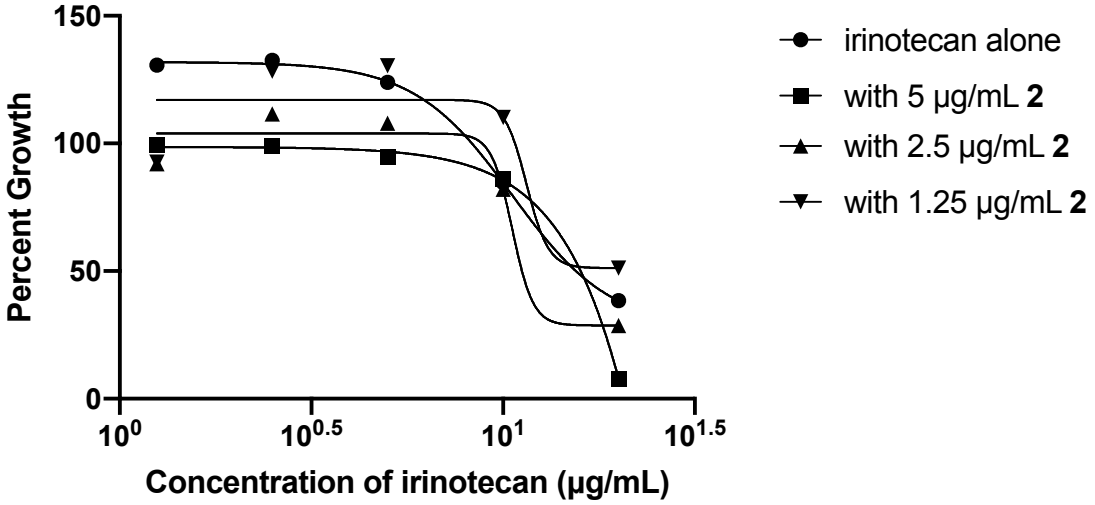

Figure 5.7. Concentration-response curve for irinotecan in combinations with **2** in HT29 cells.

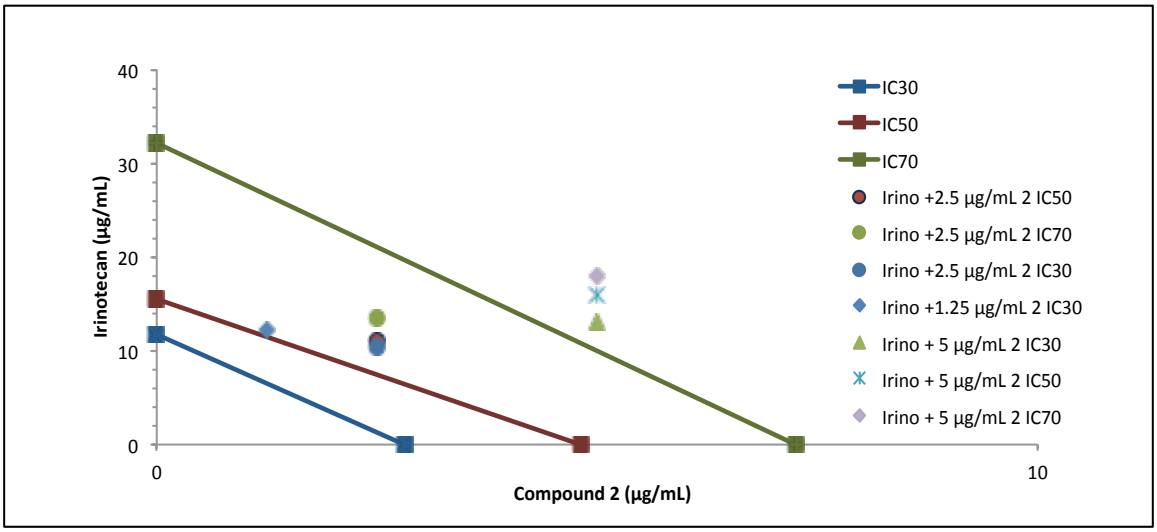

Figure 5.8. Isobologrram representation of irinotecan in combinations with **2** in HT29 cells.

Table 5.1. Combination indices of all combinations

		CI30	CI50	CI70	CI30	CI50	CI70	CI30	CI50	CI70
	Cell lines	irino + 1.25 µg/mL			irino+ 2.5 µg/mL			irino + 5 µg/mL		
Compound 1	HCT116	2.32	1.81	1.54	2.70	1.81	1.44	ND	0.87	0.88
	HT29	1.30	0.92	0.55	1.85	1.37	0.84	2.38	1.57	0.97
Compound 2	HCT116	2.50	1.78	1.40	3.08	2.11	1.57	ND	ND	ND
	HT29	1.44	ND	ND	1.77	1.24	0.77	2.90	2.07	1.25

ND: Not determined

In summary, interests have recently shifted back to natural sources for drug discovery and plant-based discovery can provide potential advantages giving their biodiversity and abundance. This dissertation focuses on drug discovery from natural sources and bio-evaluation of the promising hits. *M. glauca*, a plant species belonging to the Annonaceae family, was selected based on its anti-proliferative activity on colorectal cancer cells. Further, more advanced studies were carried out to evaluate the effect of the extract and two of its secolignans on apoptosis and cell cycle as well as wnt signaling pathway and its downstream target genes. This study focuses on CRC as it is a global concern. Its incidence is rising even among the younger individuals. Epidemiological evidence suggests that a sedentary lifestyle, consumptions of red meat and alcohol, and smoking increase the risks of developing this cancer. There is a strong correlation between high incidence and developing countries; thus, this disease is a marker for the economic growth index. Based on the current trends, this cancer is expected to claim more than two million new cases in 2030 (Arnold et al., 2017).

Our goals were to discover or identify natural products that would be effective against the proliferation of colorectal cancer we have successfully carried out our goals for this study. We

have selected potential plant extracts from a collection of plant species for further evaluations based on their anti-proliferative effects on colorectal cancer cells. New secolignans were identified and were evaluated to determine their effects on apoptosis, cell cycle, and suppression of the Wnt pathway. Our results indicate that the scalemicc mixture is most likely responsible for the growth inhibitory effect of the crude extract. Fractionation of the crude extract yielded six fractions with only the scalemic mixture exhibiting anti-proliferative activity on HCT116 and HT29 cells. Further resolution of this mixture successfully separated the two enantiomers. Further bio-evaluations of the two enantiomers suggest their roles in suppressing the Wnt pathway, leading to the growth inhibitory effects, and apoptosis via arresting cells at the G2/M phase. Together, our findings demonstrate the potential for therapeutic use of these secolignans.

Bibliography

American Cancer Society, Colorectal cancer facts and figures, 2019.

Annan, K., Dickson, R., Sarpong, K., Asare, C., Amponsah, K., Woode, E. (2013). Antipyretic activity of *Polyalthia longifolia* Benth. & Hook. F. var. pendula (Annonaceae), on lipopolysaccharide-induced fever in rats. J Med Biomed Sci, 2, 8–12.

Arnold, M., Sierra, M. S., Laversanne, M., Soerjomataram, I., Jemal, A., & Bray, F. (2017). Global patterns and trends in colorectal cancer incidence and mortality. Gut, 66(4), 683–691.

Atanasov, A.G., Waltenberger, B., Pferschy-Wenzig, E.M., et al. (2015). Discovery and resupply of pharmacologically active plant-derived natural products: A review. Biotechnol Adv, 33, 8:1582–1614.

Bagnardi, V., Rota, M., Botteri, E., Tramacere, I., Islami, F., Fedirko, V., et al. (2013). Light alcohol drinking and cancer: a meta-analysis. Ann Oncol, 24(2), 301–308.

Bagnardi, V., Rota, M., Botteri, E., Tramacere, I., Islami, F., Fedirko, V., et al. (2015). Alcohol consumption and site-specific cancer risk: a comprehensive dose–response meta-analysis. Br J Cancer, 112(3), 580–593.

Boyd, M.R., and Paull, K.D (1995). Some practical considerations and applications of the national cancer institute in vitro anticancer drug discovery screen. Drug Dev Res, 34: 91–109.

Butterworth, A. S., Higgins, J. P. T., & Pharoah, P. (2006). Relative and absolute risk of colorectal cancer for individuals with a family history: A meta-analysis. Eur J Cancer, 42(2), 216–227.

Cheng, X., Xu, X., Chen, D., Zhao, F., Wang, W. (2019). Therapeutic potential of targeting the Wnt/β-Catenin signaling pathway in colorectal cancer. Biomed Pharmacother, 110: 473–481.

Chokchaisiri, R., Chaichompoo, W., Chalermglin, R., Suksamrarn, A. (2015). Potent antiplasmodial alkaloids and flavonoids from *Dasymaschalon acuminatum*. Rec Nat Prod, 9, 243.

Cochrane, C.B., Nair, P.K.R., Melnick, S.J., Resek, A.P., Ramachandran, C. (2008). Anticancer fffects of *Annona glabra* plant extracts in human leukemia cell lines. Anticancer res, 28: 965–71.

Cross, A. J., Ferrucci, L. M., Risch, A., Graubard, B. I., Ward, M. H., Park, Y., Sinha, R. (2010). A large prospective study of meat consumption and colorectal cancer risk: an investigation of potential mechanisms underlying this association. Cancer Res, 70(6), 2406–2414.

Devkota, S., Wang, Y., Musch, M. W., Leone, V., Fehlner-Peach, H., Nadimpalli, A., Antonopoulos, D.A., Chang, E. B. (2012). Dietary-fat-induced taurocholic acid promotes pathobiont expansion and colitis in Il10−/− mice. Nature, 487(7405), 104–108.

Edwards, B. K., Ward, E., Kohler, B. A., Eheman, C., Zauber, A. G., Anderson, R. N., et al. (2010). Annual report to the nation on the status of cancer, 1975-2006, featuring colorectal cancer trends and impact of interventions (risk factors, screening, and treatment) to reduce future rates. Cancer, 116(3), 544–573.

Emons, G., Spitzner, M., Reineke, S., Möller, J., Auslander, N., Kramer, F., et al. (2017). Chemoradiotherapy resistance in colorectal cancer cells is mediated by Wnt/β-catenin signaling. Mol Cancer Res, 15(11), 1481–1490.

Fearon, E. R., & Vogelstein, B. (1990). A genetic model for colorectal tumorigenesis. Cell, 61(5), 759–767.

Ferlay, J., Colombet, M., & Bray, F. (2018). Cancer incidence in five continents, CI5plus: IARC CancerBase No. 9 [Internet]. Lyon, France: International Agency for Research on Cancer. Available from: http://ci5.iarc.fr

Finefield, J. M., Sherman, D. H., Kreitman, M., & Williams, R. M. (2012). Enantiomeric Natural Products: Occurrence and Biogenesis. Angew Chem, 51(20), 4802–4836.

Gavert N., Conacci-Sorrell. M., Gast D, Schneider A, Altevogt P, Brabletz T, Ben-Ze'ev A. (2005). L1, a novel target of beta-catenin signaling, transforms cells and is expressed at the invasive front of colon cancers. J Cell Biol, 168:633–642.

Gavert, N., Sheffer, M., Raveh, S., Spaderna, S., Shtutman, M., Brabletz, T., et al. (2007). Expression of L1-CAM and ADAM10 in human colon cancer cells induces metastasis. Cancer Res, 67(16), 7703–7712.

Gonsalves, F. C., Klein, K., Carson, B. B., Katz, S., Ekas, L. A., Evans, S., et al. (2011). An RNAi-based chemical genetic screen identifies three small-molecule inhibitors of the Wnt/wingless signalling pathway. PNAS, 108(15), 5954–5963.

Hannan, L. M., Jacobs, E. J., & Thun, M. J. (2009). The association between cigarette smoking and risk of colorectal cancer in a large prospective cohort from the United States. Cancer Epidem Bioma, 18(12), 3362–3367.

Hu, Q.-F., Mu, H.-X., Huang, H.-T., Lv, H.-Y., Li, S.-L., Tu, P.-F., & Li, G.-P. (2011). Secolignans, neolignans and phenylpropanoids from *Daphne feddei* and their biological activities. Chem Pharm Bull, 59(11), 1421–1424.

Kinzler, K. W., & Vogelstein, B. (1996). Lessons from hereditary colorectal cancer. Cell, 87(2), 159-170.

Krishnamurthy, N., & Kurzrock, R. (2018). Targeting the Wnt/beta-catenin pathway in cancer: update on effectors and inhibitors. Cancer Treat Rev, 62, 50–60.

Leufkens, A. M., Van Duijnhoven, F. J. B., Siersema, P. D., Boshuizen, H. C., Vrieling, A., Agudo, A., et al. (2011). Cigarette smoking and colorectal cancer risk in the European

prospective investigation into cancer and nutrition study. Clin GastroEnterol Hepatol, 9(2), 137–144.

Li, N., Wu, J.-L., Hasegawa, T., Sakai, J.-I., Bai, L.-M., Wang, L.-Y., Ando, M. (2007). Bioactive Lignans fromPeperomia duclouxii. J Nat Prod, 70(4), 544–548.

Li, Y., Pan, J., & Gou, M. (2019). The anti-proliferation, cycle arrest and apoptotic inducing activity of Peperomin E on prostate cancer PC-3 cell line. Molecules, 24(8), 1472.

Liu, J., Pan, S., Hsieh, M. H., Ng, N., Sun, F., Wang, T., et al. (2013). Targeting Wnt-driven cancer through the inhibition of Porcupine by LGK974. PNAS, 110(50), 20224–20229.

Lukas, Kevin, Simon, J., Darjus, Johan, Clevers, H., & Scott. (2015). Apc restoration promotes cellular differentiation and reestablishes crypt homeostasis in colorectal cancer. Cell, 161(7), 1539–1552.

Lutgens, M. W. M. D., Van Oijen, M. G. H., Van Der Heijden, G. J. M. G., Vleggaar, F. P., Siersema, P. D., & Oldenburg, B. (2013). Declining risk of colorectal cancer in inflammatory bowel disease. Inflamm Bowel Dis, 19(4), 789–799.

Ma, Y., Yang, Y., Wang, F., Zhang, P., Shi, C., Zou, Y., & Qin, H. (2013). Obesity and risk of colorectal cancer: a systematic review of prospective studies. PLoS ONE, 8(1), e53916.

Malebo, H. M., Wenzler, T., Cal, M., Swaleh, S. M., Omolo, M. O., Hassanali, A., et al. (2013). Anti-protozoal activity of aporphine and protoberberine alkaloids from *Annickia kummeriae* (Engl. & Diels) Setten & Maas (Annonaceae). BMC Complement. Altern Med, 13, 48.

Martin-Orozco, E., Sanchez-Fernandez, A., Ortiz-Parra, I., & Ayala-San Nicolas, M. (2019). WNT signaling in tumors: the way to evade drugs and immunity. Front Immunol, 10(2854).

Martinez, M. E., Jacobs, E. T., Ashbeck, E. L., Sinha, R., Lance, P., Alberts, D. S., & Thompson, P. A. (2007). Meat intake, preparation methods, mutagens and colorectal adenoma recurrence. Carcinogenesis, 28(9), 2019–2027.

Minh, C.V., Nhiem, N.X., Yen, H.T. et al. (2015). Chemical constituents of *Trichosanthes kirilowii* and their cytotoxic activities. Arch Pharm Res, 38:1443–1448.

Muzny, D. M., Bainbridge M.N., Chang, K., et al. Cancer Genome Atlas Network (2012). Comprehensive molecular characterization of human colon and rectal cancer. Nature, 487:330–337.

NCI Drug Dictionary. https://www.cancer.gov/publications/dictionaries/cancer-drug/def/etoposide?redirect=true

Newman, D.J., Cragg, G.M. (2014). Natural products as sources of new drugs from 1981 to 2014. J. Nat. Prod, 79, 3: 629–661.

Patel, S. G., & Ahnen, D. J. (2012). Familial colon cancer syndromes: an update of a rapidly evolving field. Curr Gastroenterol Rep, 14(5), 428–438.

Patridge, E., Gareiss, P., Kinch, M.S., Hoyer, D. (2016). An analysis of FDA-approved drugs: natural products and their derivatives. Drug Discov. Today, 21, 2: 204–207.

Rayanil, K.O., Sutassanawichanna, W., Suntornwat, O., Tuntiwachwuttikul, P. (2016). A new dihydrobenzofuran lignan and potential α-glucosidase inhibitory activity of isolated compounds from *Mitrephora teysmannii*. Nat Prod Res, 30: 2675–2681.

Robbins, A. S., Siegel, R. L., & Jemal, A. (2012). Racial disparities in stage-specific colorectal cancer mortality rates from 1985 to 2008. J Clin Oncol, 30(4), 401–405.

Sargent, D., Sobrero, A., Grothey, A., O'Connell, M. J., Buyse, M., Andre, T., et al. (2009). Evidence for cure by adjuvant therapy in colon cancer: observations based on individual patient data from 20,898 patients on 18 randomized trials. J Clin Oncol, 27(6), 872–877.

Scannell, J.W., Blanckley, A., Boldon, H., Warrington, B. (2012). Diagnosing the decline in pharmaceutical R&D efficiency. Nat Rev Drug Discov, 11:191–200.

Shah, M. A., Renfro, L. A., Allegra, C. J., André, T., De Gramont, A., Schmoll, H.-J., et al. (2016). Impact of patient factors on recurrence risk and time dependency of oxaliplatin benefit in patients with colon cancer: analysis from dodern-era adjuvant studies in the adjuvant colon cancer end points (ACCENT) Database. J Clin Oncol, 34(8), 843–853.

Shang-Tse Ho, C.-C. L., Yu-Tang Tung, and Jyh-Horng Wu (2019). Molecular mechanisms underlying Yatein-induced cell-cycle arrest and microtubule destabilization in human lung adenocarcinoma cells. Cancer, 11(1384).

Smith, D. C., Rosen, L. S., Chugh, R., Goldman, J. W., Xu, L., Kapoun, A., et al. (2013). First-in-human evaluation of the human monoclonal antibody vantictumab (OMP-18R5; anti-Frizzled) targeting the WNT pathway in a phase I study for patients with advanced solid tumors. J Clin Oncol, 31(15_suppl), 2540–2540.

Soladoye, M.O., Amusa, M.A., Raji-Esan, S.O., Chukwuma, E.C., Taiwo, A.A. (2010). Ethnobotanical survey of anti-cancer plants in Ogun State, Nigeria. Ann Biol Res, 1, 4: 261–273.

Stewart, B. W. and Wild, C. P. edit. (2014). World cancer report 2014. Lyon, France: International Agency for Research on Cancer. 392–393.

Stewart, S. L., Wike, J. M., Kato, I., Lewis, D. R., & Michaud, F. (2006). A population-based study of colorectal cancer histology in the United States, 1998–2001. Cancer, 107(S5), 1128–1141.

Surveillance, Epidemiology, and End Results (SEER) Program (www.seer.cancer.gov) SEER*Stat Database: Incidence – SEER 18 regs research data with delay-adjustment, malignant Only, Nov 2015 Sub (2000-2013) - Linked To County Attributes – Total U.S., 1969-2014 Counties, National Cancer Institute, DCCPS, Surveillance Research Program, Surveillance Systems Branch, released April 2016.

Torre, L. A., Sauer, A. M. G., Chen, M. S., Kagawa-Singer, M., Jemal, A., & Siegel, R. L. (2016). Cancer statistics for Asian Americans, Native Hawaiians, and Pacific Islanders, 2016: converging incidence in males and females. CA- Cancer J Clin, 66(3), 182–202.

Tsilidis, K. K., Kasimis, J. C., Lopez, D. S., Ntzani, E. E., & Ioannidis, J. P. A. (2015). Type 2 diabetes and cancer: umbrella review of meta-analyses of observational studies. BMJ, 350:7607–7607.

Veeman, M.T., Slusarski, D.C., Kaykas. A., Louie. S.H., Moon, R.T. (2003). Zebrafish prickle, a modulator of noncanonical Wnt/Fz signaling, regulates gastrulation movements. Curr Biol, 13(8), 680–5.

Vermes, I., Haanen, C., Steffens-Nakken, H., & Reutellingsperger, C. (1995). A novel assay for apoptosis Flow cytometric detection of phosphatidylserine expression on early apoptotic cells using fluorescein labelled Annexin V. J Immuno Methods, 184(1), 39–51.

Verpoorte, R. (2000). Pharmacognosy in the new millennium: leadfinding and biotechnology. J Pharm Pharmacol, 52: 253–262.

Wang, N., Khankari, N. K., Cai, H., Li, H.-L., Yang, G., Gao, Y.-T., et al. (2017). Prediagnosis body mass index and waist-hip circumference ratio in association with colorectal cancer survival. Int J Cancer, 140(2), 292–301.

Wang, X.-z., Cheng, Y., Wu, H., Li, N., Liu, R., Yang, X.-l., et al. (2016). The natural secolignan peperomin E induces apoptosis of human gastric carcinoma cells via the mitochondrial and PI3K/Akt signaling pathways in vitro and in vivo. Phytomedicine, 23(8), 818–827.

Watt, J.M., Breyer-Brandwijk, M.G. (1962). The medicinal and poisonous plants of southern and Eastern Africa; being an account of their medicinal and other uses, chemical composition, pharmacological effects and toxicology in man and animal. E. & S. Livingstone Edinburgh, p56–58.

Wolin, K. Y., Yan, Y., & Colditz, G. A. (2011). Physical activity and risk of colon adenoma: a meta-analysis. Br J Cancer, 104(5), 882–885.

Wolin, K. Y., Yan, Y., Colditz, G. A., & Lee, I. M. (2009). Physical activity and colon cancer prevention: a meta-analysis. Br J Cancer, 100(4), 611–616.

Wu, J.-L., et al. (2006). Bioactive Secolignans from Peperomia dindygulensis. J. Nat Prod, 69(5), 790–794.

Xin, H., Kong, Y., Wang, Y., Zhou, Y., Zhu, Y., Li, D., & Tan, W. (2013). Lignans extracted from Vitex negundo possess cytotoxic activity by G2/M phase cell cycle arrest and apoptosis induction. Phytomedicine, 20(7), 640–647.

Xin, Z., Gu, J.-L., Gao, M., Bian, Y., Liang, J.-Y., Wen, H.-M., & Wu, H. (2018). Peperomin E induces promoter hypomethylation of metastatic-suppressor genes and attenuates metastasis in poorly differentiated gastric cancer. Cell Physiol Biochem, 50(6), 2341–2364.

Yoo, J.-H., Lee, H. J., Kang, K., Jho, E. H., Kim, C. Y., Baturen, D.,et al. (2010). Lignans inhibit cell growth via regulation of Wnt/β-catenin signaling. Food Chem Toxicol, 48(8-9), 2247–2252.

Zhan, T., Rindtorff, N., & Boutros, M. (2017). Wnt signaling in cancer. Oncogene, 36(11), 1461–1473.

Appendices

STATEMENT OF CONTRIBUTIONS

Dr. Zulfiqar Ali contributed towards the isolation and structure elucidation of **1** and **2**. Dr. Bharathi Avula contributed towards the UHPLC-MS analysis of the crude extract. Dr. Frank Fronczek contributed towards analysis of the crystal structures for X-ray crystallography data. John Trott contributed towards screening of *M. glauca* crude extract on SK-Mel, KB, BT-549, and SK-OV-3 cells. Yusheng Li contributed towards analysis of cell cycle. Dr. Amar Chittiboyina guided on how to grow crystals and isolation of **1** and **2.** The whole project was performed under scientific guidance from Dr. Ikhlas Khan and Dr. Shabana Khan.

My personal contributions towards this dissertation include initial screening of 85 extracts, fractionation and isolation of **1** and **2,** acquisition of NMR spectra, acquisition of specific rotation, and growing crystal structures. I was also responsible for sample preparation, data acquisition, and data analysis to evaluate the anti-proliferative activities, cell apoptosis, inhibitory activities on the Wnt signalling pathway and its target genes, and drug-isolated compounds combination effects on colorectal cancer cells. In addition, I was responsible for maintaining cell cultures. I was partially involved in the sample preparation for cell cycle analysis.

Thanh-Thanh (Claire) V. Tran

Appendix I: NMR spectra

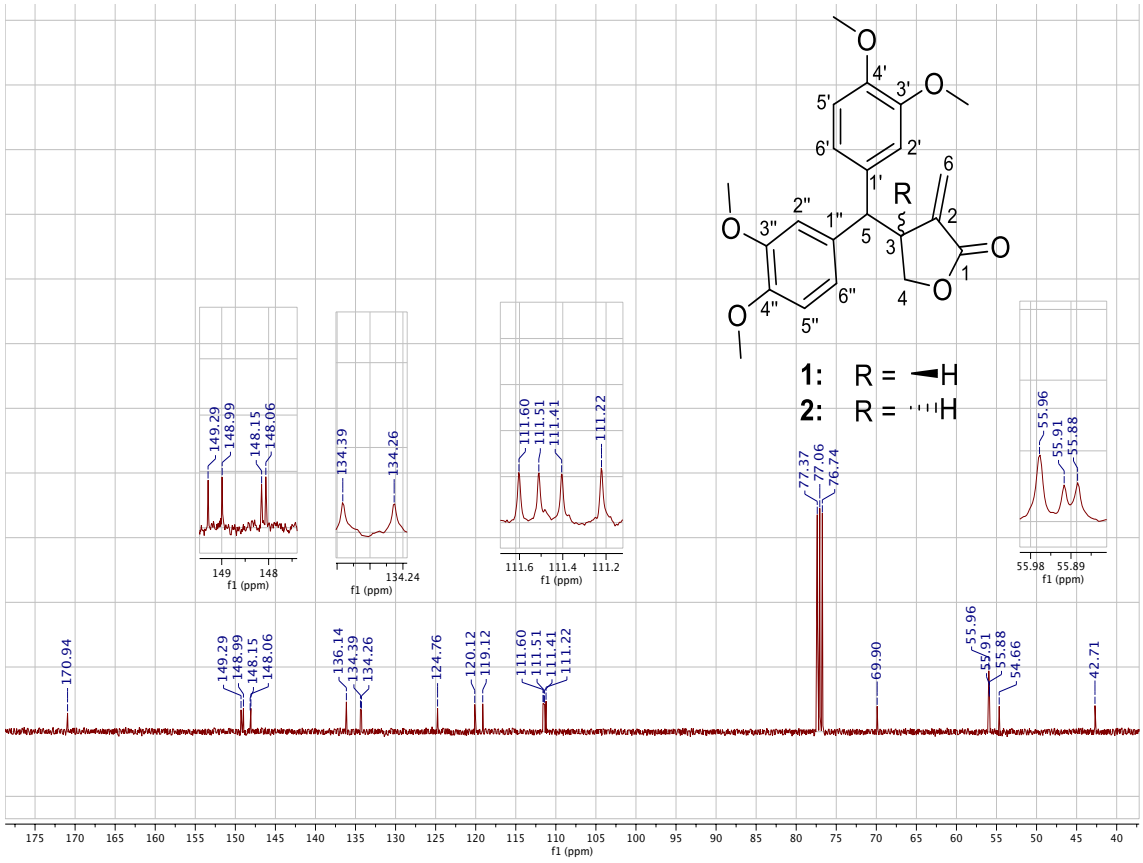

Figure 3.6. ^{13}C NMR spectrum of the daughter fraction 2 which is a scalemic mixture, comprised of**1** and **2**

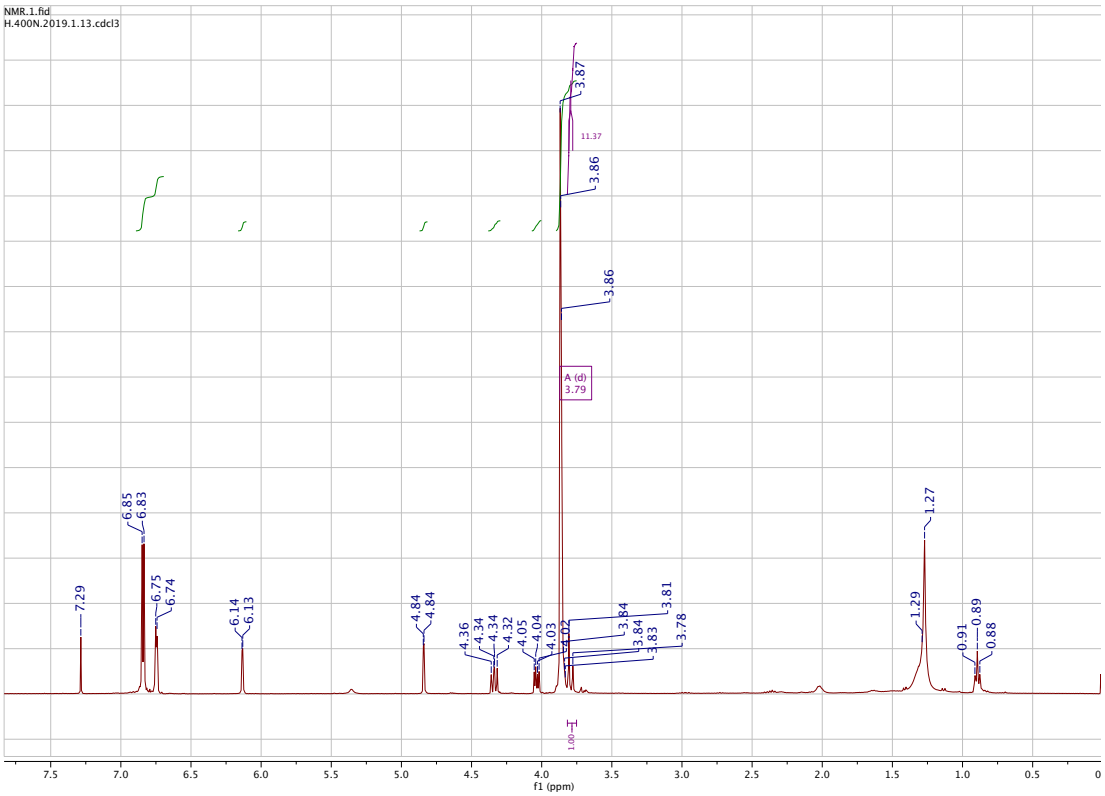

Figure 3.7. ^{1}H NMR spectrum of the daughterfraction 2

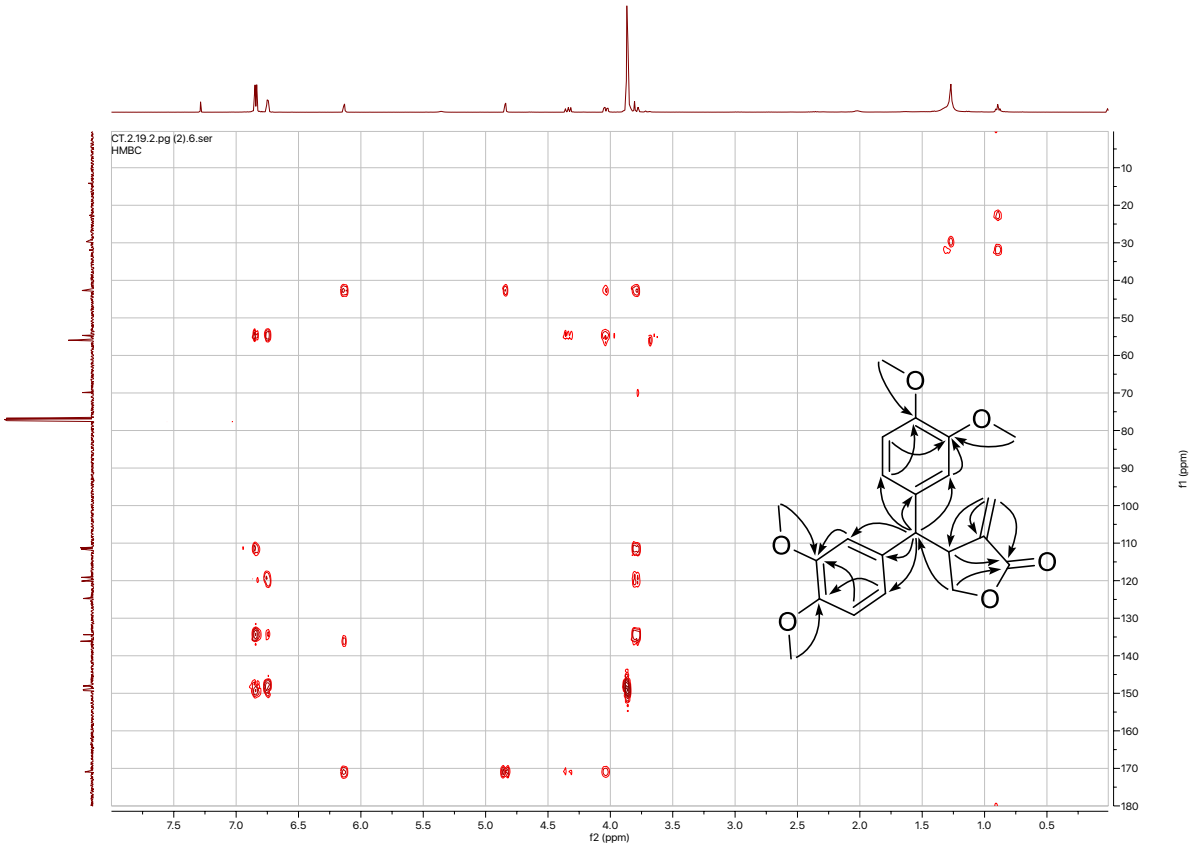

Figure 3.8. HMBC NMR spectrum of the daughter fraction 2

Appendix II: UHPLC-MS spectra for the composition of *M. glauca* crude extract.

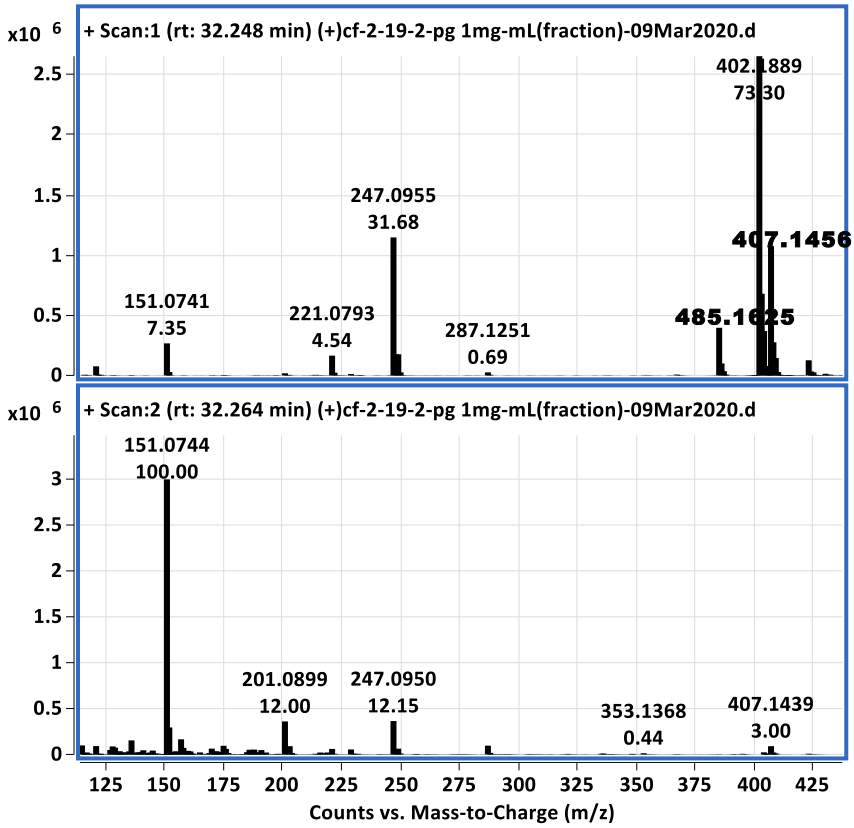

Figure 3.9. MS and MS/MS spectra for daughter fraction 2 (comprised of **1** and **2**).

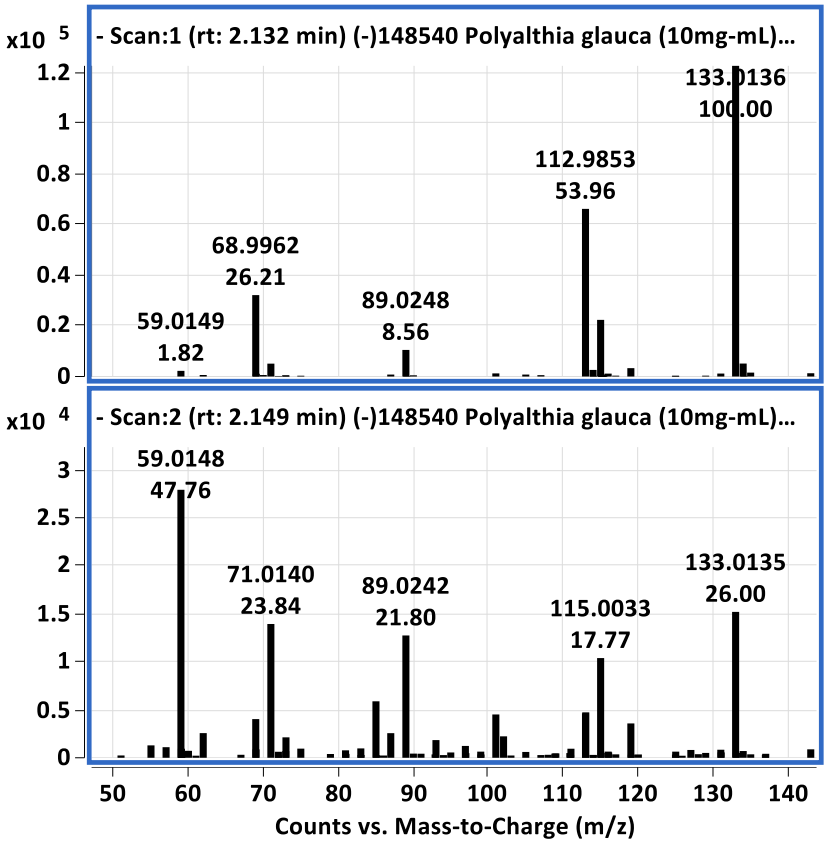

Figure 3.13. MS and MS/MS spectra for malic acid

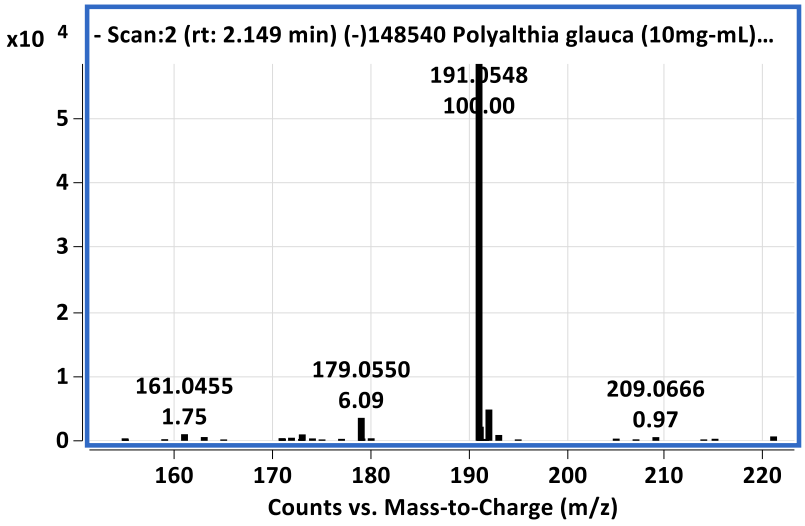

Figure 3.14. MS/MS spectrum for quinic acid

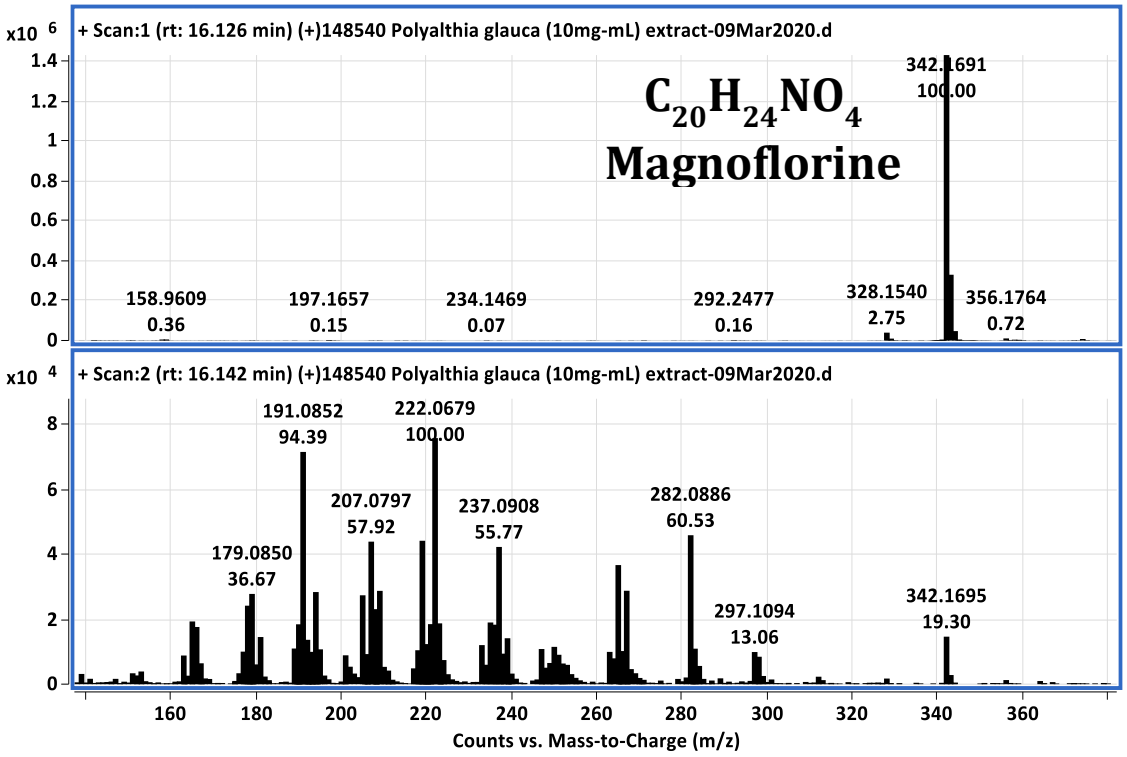

Figure 3.15. MS and MS/MS spectra for magnoflorine

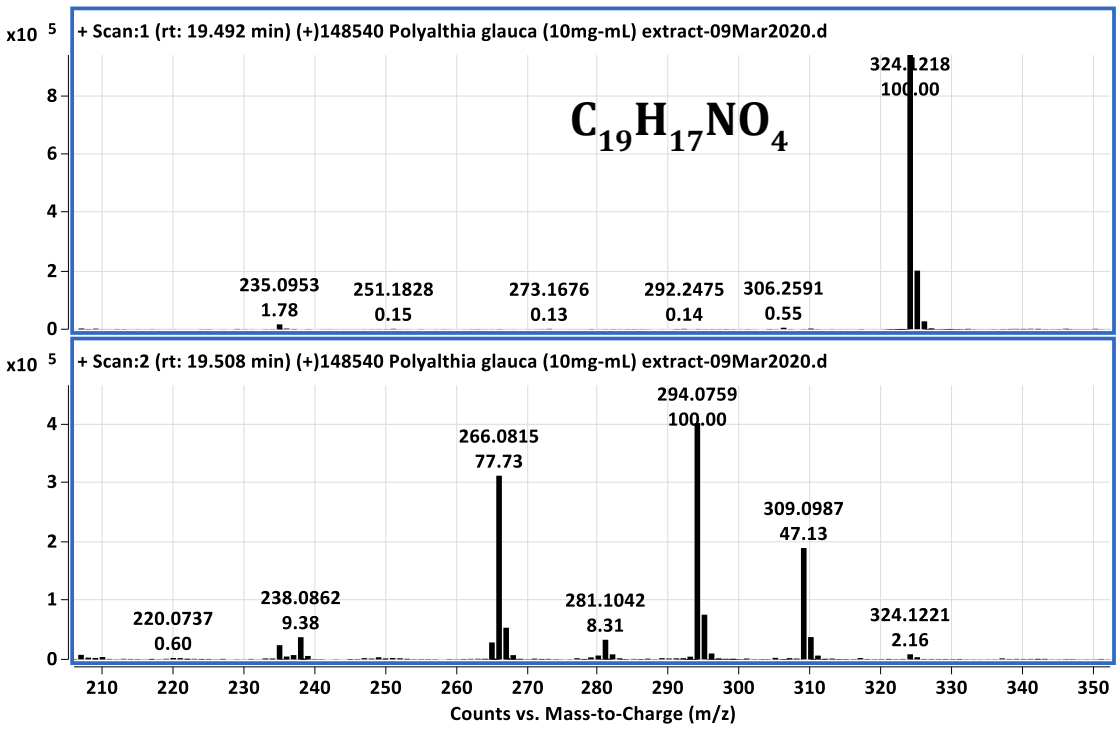

Figure 3.16. MS and MS/MS spectra for the unknown compound with molecular formula

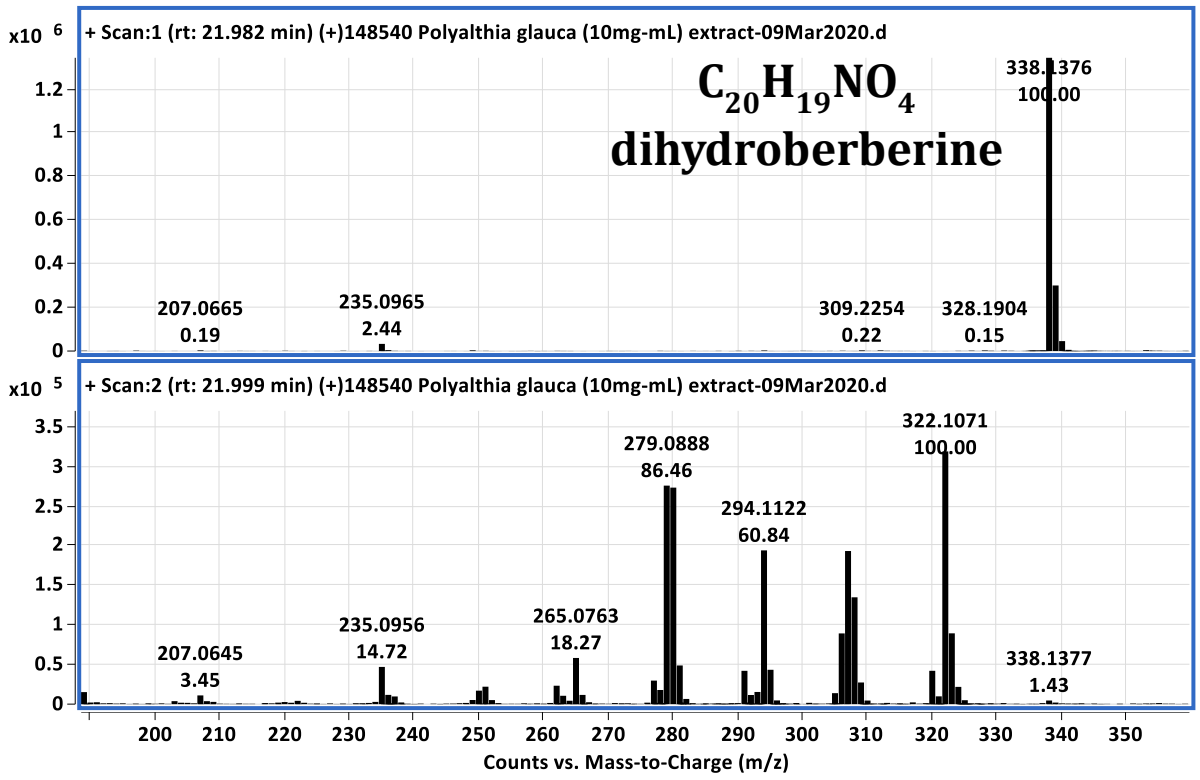

Figure 3. 17. MS and MS/MS spectra for dihydroberberine

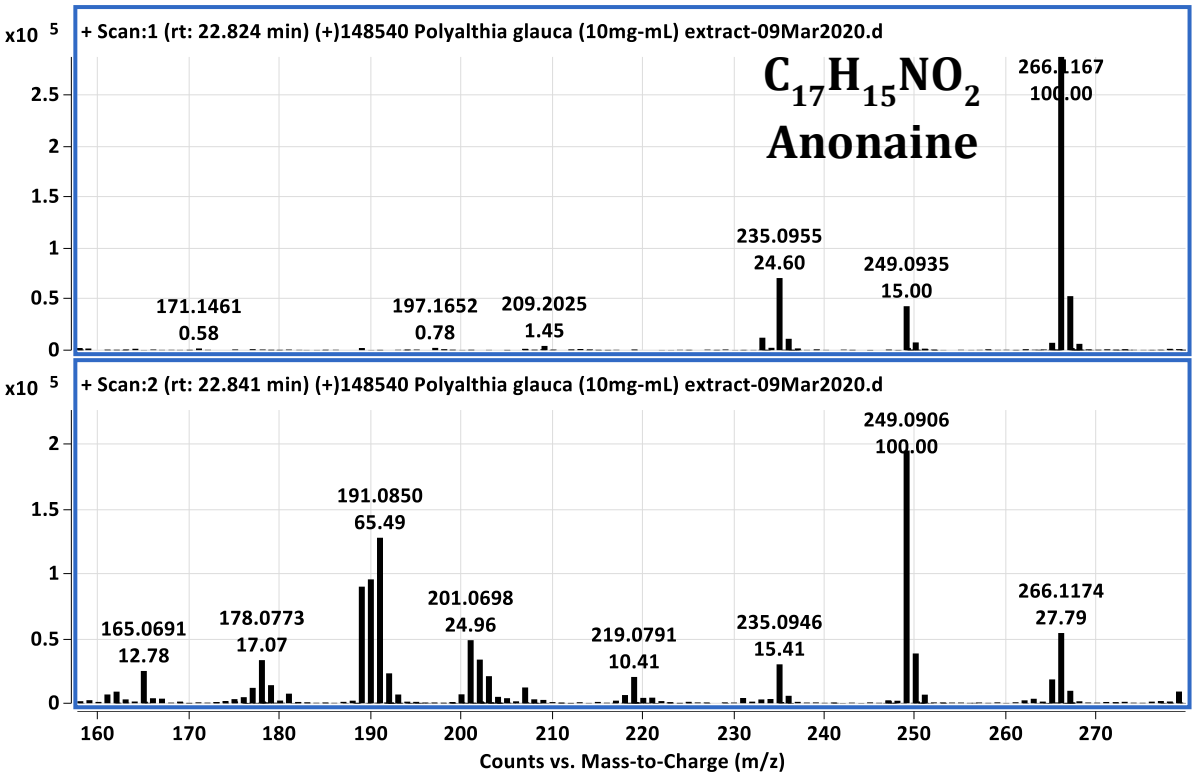

Figure 3.18. MS and MS/MS spectra for anonaine

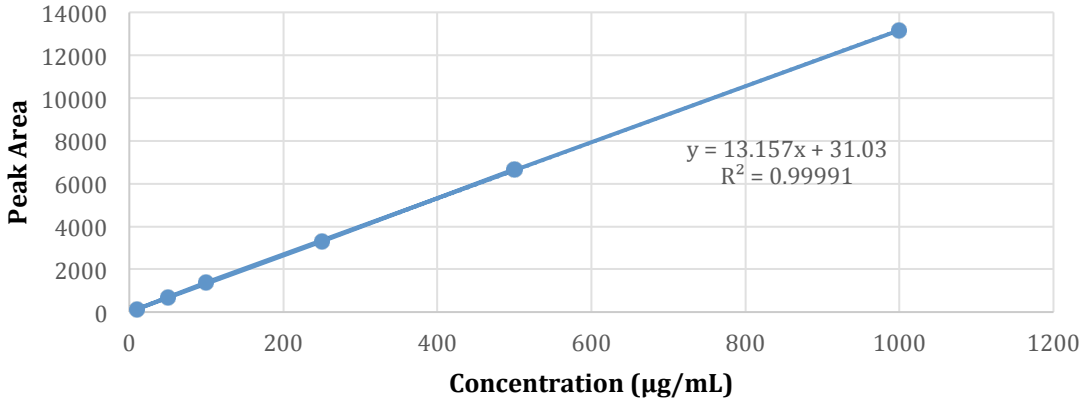

Figure 3.19. Calibration curve for relative quantification for the daughter fraction 2 (comprised of **1** and **2**)

Appendix III: X-ray crystallography supplemental data

supporting information

Title

Computing details

Data collection: Bruker *APEX3*; cell refinement: Bruker *SAINT*; data reduction: Bruker *SAINT*; program(s) used to solve structure: *SHELXS97* (Sheldrick, 2008); program(s) used to refine structure: *SHELXL2014*/7 (Sheldrick, 2014).

(CTran1)

Crystal data

$C_{22}H_{24}O_6$
$M_r = 384.41$
Triclinic, $P\overline{1}$
$a = 10.9220\ (4)$ Å
$b = 11.4265\ (5)$ Å
$c = 16.7548\ (6)$ Å
$\alpha = 71.022\ (2)°$
$\beta = 84.137\ (2)°$
$\gamma = 77.425\ (2)°$
$V = 1928.80\ (13)$ Å^3
$Z = 4$
$F(000) = 816$
$D_x = 1.324$ Mg m^{-3}
Cu $K\alpha$ radiation, $\lambda = 1.54184$ Å
Cell parameters from 9943 reflections
$\theta = 4.2–68.1°$
$\mu = 0.79$ mm^{-1}
$T = 90$ K
Plate, colourless
0.38 × 0.33 × 0.06 mm

Data collection

Bruker Kappa APEX-II DUO diffractometer
Radiation source: IμS microfocus
QUAZAR multilayer optics monochromator
φ and ω scans
Absorption correction: multi-scan *SADABS* (Sheldrick, 2004)
$T_{min} = 0.828$, $T_{max} = 0.954$
42528 measured reflections
11874 independent reflections
10800 reflections with $I > 2\sigma(I)$
$R_{int} = 0.037$
$\theta_{max} = 69.0°$, $\theta_{min} = 2.8°$
$h = -12\rightarrow13$
$k = -13\rightarrow13$
$l = -20\rightarrow17$

Refinement

Refinement on F^2
Least-squares matrix: full
$R[F^2 > 2\sigma(F^2)] = 0.059$
$wR(F^2) = 0.161$
$S = 1.04$
11874 reflections
1054 parameters
36 restraints
Hydrogen site location: inferred from neighbouring sites
H-atom parameters constrained
$w = 1/[\sigma^2(F_o^2) + (0.0837P)^2 + 1.5248P]$ where $P = (F_o^2 + 2F_c^2)/3$
$(\Delta/\sigma)_{max} = 0.001$
$\Delta\rho_{max} = 0.76$ e Å^{-3}
$\Delta\rho_{min} = -0.35$ e Å^{-3}
Absolute structure: Refined as an inversion twin.
Absolute structure parameter: 0.3 (3)

Special details

Geometry. All e.s.d.'s (except the e.s.d. in the dihedral angle between two l.s. planes) are estimated using the full covariance matrix. The cell e.s.d.'s are taken into account individually in the estimation of e.s.d.'s in distances, angles and torsion angles; correlations between e.s.d.'s in cell parameters are only used when they are defined by crystal symmetry. An approximate (isotropic) treatment of cell e.s.d.'s is used for estimating e.s.d.'s involving l.s. planes.
Refinement. Refined as a 2-component inversion twin.

Fractional atomic coordinates and isotropic or equivalent isotropic displacement parameters (Å²)

	x	*y*	*z*	U_{iso}*/U_{eq}	Occ. (<1)
O1	−0.1543 (5)	1.1560 (5)	0.4196 (3)	0.0566 (13)	
O2	−0.2197 (6)	1.0005 (6)	0.5212 (3)	0.0709 (15)	
O3	0.1297 (4)	1.2293 (4)	0.0063 (2)	0.0350 (9)	
O4	0.2970 (4)	1.3347 (4)	0.0334 (2)	0.0359 (9)	
O5	0.3824 (4)	0.6374 (4)	0.4459 (3)	0.0390 (9)	
O6	0.3111 (4)	0.5025 (4)	0.3692 (3)	0.0432 (10)	
C1	−0.1802 (6)	1.0387 (7)	0.4502 (4)	0.0441 (15)	
C2	−0.1424 (6)	0.9713 (7)	0.3883 (4)	0.0483 (17)	
C3	−0.0762 (6)	1.0514 (8)	0.3132 (4)	0.0561 (17)	
H3	−0.1063	1.0526	0.2585	0.067*	
C4	−0.1229 (7)	1.1809 (9)	0.3298 (4)	0.062 (2)	
H4A	−0.0564	1.2317	0.3129	0.074*	
H4B	−0.1977	1.2287	0.2964	0.074*	
C5	−0.1747 (7)	0.8675 (7)	0.3926 (5)	0.0513 (17)	
H5A	−0.2267	0.8295	0.4385	0.062*	
H5B	−0.1465	0.8289	0.3499	0.062*	
C6	0.0692 (6)	1.0173 (7)	0.3162 (4)	0.0488 (15)	
H6	0.0917	1.0323	0.3679	0.059*	
C7	0.1287 (6)	1.1080 (6)	0.2404 (4)	0.0444 (15)	
C8	0.0953 (6)	1.1260 (6)	0.1573 (4)	0.0366 (13)	
H8	0.0332	1.0854	0.1483	0.044*	
C9	0.1526 (5)	1.2019 (5)	0.0898 (3)	0.0296 (12)	
C10	0.2454 (5)	1.2612 (5)	0.1034 (4)	0.0323 (12)	
C11	0.2743 (6)	1.2427 (6)	0.1860 (4)	0.0383 (13)	
H11	0.3366	1.2821	0.1963	0.046*	
C12	0.2137 (5)	1.1676 (6)	0.2539 (4)	0.0391 (13)	
H12	0.2324	1.1584	0.3100	0.047*	
C13	0.0436 (6)	1.1643 (7)	−0.0122 (4)	0.0434 (15)	
H13A	0.0722	1.0731	0.0129	0.065*	
H13B	0.0395	1.1851	−0.0735	0.065*	
H13C	−0.0398	1.1903	0.0114	0.065*	
C14	0.3911 (6)	1.3960 (6)	0.0448 (4)	0.0419 (14)	
H14A	0.3557	1.4521	0.0784	0.063*	
H14B	0.4210	1.4454	−0.0104	0.063*	
H14C	0.4614	1.3325	0.0743	0.063*	
C15	0.1275 (5)	0.8778 (6)	0.3245 (3)	0.0373 (14)	
C16	0.2276 (5)	0.8216 (6)	0.3791 (3)	0.0338 (12)	
H16	0.2562	0.8700	0.4073	0.041*	
C17	0.2852 (5)	0.6974 (6)	0.3926 (3)	0.0329 (12)	
C18	0.2476 (5)	0.6237 (6)	0.3503 (4)	0.0363 (13)	
C19	0.1482 (7)	0.6820 (8)	0.2952 (4)	0.0474 (16)	
H19	0.1199	0.6355	0.2653	0.057*	
C20	0.0900 (6)	0.8087 (7)	0.2836 (4)	0.0497 (17)	
H20	0.0226	0.8464	0.2461	0.060*	
C21	0.4211 (6)	0.7047 (6)	0.4941 (4)	0.0466 (15)	
H21A	0.4455	0.7820	0.4559	0.070*	
H21B	0.4928	0.6516	0.5278	0.070*	
H21C	0.3516	0.7267	0.5318	0.070*	
C22	0.2761 (8)	0.4252 (8)	0.3257 (5)	0.0553 (18)	

H22A	0.1874	0.4204	0.3383	0.083*	
H22B	0.3278	0.3401	0.3445	0.083*	
H22C	0.2894	0.4625	0.2647	0.083*	
O7	0.2905 (5)	0.8677 (5)	0.0967 (3)	0.0551 (12)	
O8	0.2706 (5)	0.6825 (5)	0.0896 (3)	0.0532 (12)	
O9	0.5637 (5)	1.1608 (5)	0.3117 (3)	0.0523 (12)	
O10	0.6675 (4)	1.2990 (4)	0.1798 (3)	0.0402 (10)	
O11	0.9892 (5)	0.4996 (5)	0.2052 (3)	0.0596 (14)	
O12	0.9677 (5)	0.4231 (5)	0.3645 (3)	0.0638 (15)	
C23	0.3262 (6)	0.7396 (6)	0.1157 (4)	0.0389 (14)	
C24	0.4399 (6)	0.6948 (7)	0.1675 (5)	0.0481 (16)	
C26	0.3750 (7)	0.9175 (7)	0.1311 (5)	0.0523 (17)	
H26A	0.3271	0.9724	0.1634	0.063*	0.727 (7)
H26B	0.4239	0.9685	0.0850	0.063*	0.727 (7)
H26C	0.3402	0.9308	0.1851	0.063*	0.273 (7)
H26D	0.3901	0.9989	0.0912	0.063*	0.273 (7)
C27	0.4952 (7)	0.5787 (7)	0.1943 (5)	0.0527 (17)	
H27A	0.4637	0.5161	0.1813	0.063*	
H27B	0.5676	0.5553	0.2272	0.063*	
C25	0.4655 (7)	0.8039 (8)	0.1906 (5)	0.0349 (17)	0.727 (7)
H25	0.4424	0.7950	0.2513	0.042*	0.727 (7)
C28	0.6025 (6)	0.8215 (7)	0.1700 (5)	0.0269 (14)	0.727 (7)
H28	0.6262	0.8208	0.1109	0.032*	0.727 (7)
C25A	0.5078 (14)	0.8089 (15)	0.1464 (12)	0.0349 (17)	0.273 (7)
H25A	0.5654	0.8176	0.0954	0.042*	0.273 (7)
C28A	0.5667 (13)	0.8169 (13)	0.2234 (10)	0.0269 (14)	0.273 (7)
H28A	0.5117	0.8119	0.2755	0.032*	0.273 (7)
C29	0.6151 (6)	0.9484 (6)	0.1784 (5)	0.0517 (18)	
C30	0.5776 (6)	0.9917 (6)	0.2470 (5)	0.0495 (18)	
H30	0.5381	0.9408	0.2949	0.059*	
C31	0.5967 (6)	1.1095 (6)	0.2472 (4)	0.0395 (14)	
C32	0.6545 (5)	1.1841 (5)	0.1766 (4)	0.0335 (13)	
C33	0.6901 (6)	1.1398 (6)	0.1099 (4)	0.0428 (15)	
H33	0.7296	1.1900	0.0618	0.051*	
C34	0.6706 (7)	1.0229 (7)	0.1096 (5)	0.0514 (17)	
H34	0.6960	0.9954	0.0616	0.062*	
C35	0.5056 (7)	1.0876 (9)	0.3864 (5)	0.070 (2)	
H35A	0.4287	1.0695	0.3716	0.105*	
H35B	0.4848	1.1351	0.4269	0.105*	
H35C	0.5636	1.0081	0.4118	0.105*	
C36	0.7438 (6)	1.3668 (6)	0.1170 (4)	0.0445 (15)	
H36A	0.8305	1.3192	0.1216	0.067*	
H36B	0.7410	1.4490	0.1244	0.067*	
H36C	0.7134	1.3793	0.0612	0.067*	
C37	0.6928 (6)	0.7138 (6)	0.2323 (5)	0.0439 (15)	
C38	0.7974 (5)	0.6585 (6)	0.1924 (4)	0.0397 (15)	
H38	0.8078	0.6880	0.1326	0.048*	
C39	0.8844 (6)	0.5624 (6)	0.2389 (4)	0.0419 (15)	
C40	0.8735 (6)	0.5178 (6)	0.3260 (4)	0.0391 (14)	
C41	0.7689 (7)	0.5716 (7)	0.3662 (5)	0.0528 (18)	
H41	0.7590	0.5428	0.4260	0.063*	
C42	0.6784 (7)	0.6688 (7)	0.3176 (6)	0.060 (2)	

H42	0.6058	0.7037	0.3449	0.072*
C43	1.0113 (8)	0.5422 (8)	0.1161 (5)	0.064 (2)
H43A	0.9439	0.5281	0.0880	0.096*
H43B	1.0920	0.4952	0.1014	0.096*
H43C	1.0132	0.6324	0.0976	0.096*
C44	0.9651 (13)	0.3792 (12)	0.4544 (6)	0.116 (5)
H44A	0.9651	0.4495	0.4758	0.175*
H44B	1.0394	0.3132	0.4739	0.175*
H44C	0.8892	0.3446	0.4754	0.175*
O13	0.7012 (4)	0.1987 (4)	0.8982 (3)	0.0436 (10)
O14	0.7149 (5)	0.3836 (5)	0.9089 (3)	0.0549 (12)
O15	0.0074 (4)	0.5656 (4)	0.8001 (3)	0.0497 (12)
O16	0.0230 (4)	0.6391 (5)	0.6388 (3)	0.0529 (13)
O17	0.4383 (4)	−0.0991 (4)	0.6884 (3)	0.0433 (10)
O18	0.3270 (4)	−0.2377 (4)	0.8152 (3)	0.0419 (10)
C45	0.6611 (6)	0.3226 (6)	0.8816 (4)	0.0382 (14)
C46	0.5514 (6)	0.3677 (6)	0.8266 (4)	0.0383 (13)
C47	0.5274 (6)	0.2558 (6)	0.8069 (4)	0.0433 (14)
H47	0.5493	0.2648	0.7461	0.052*
C48	0.6207 (6)	0.1446 (6)	0.8628 (5)	0.0520 (18)
H48A	0.5749	0.0891	0.9084	0.062*
H48B	0.6711	0.0939	0.8286	0.062*
C49	0.4966 (6)	0.4892 (6)	0.8013 (4)	0.0430 (15)
H49A	0.5277	0.5485	0.8184	0.052*
H49B	0.4264	0.5167	0.7660	0.052*
C50	0.3907 (5)	0.2370 (6)	0.8267 (4)	0.0375 (13)
H50	0.3714	0.2370	0.8863	0.045*
C51	0.2960 (6)	0.3458 (6)	0.7728 (4)	0.0347 (13)
C52	0.1967 (5)	0.4031 (5)	0.8112 (4)	0.0321 (12)
H52	0.1883	0.3745	0.8711	0.039*
C53	0.1065 (5)	0.5024 (5)	0.7657 (4)	0.0324 (12)
C54	0.1181 (6)	0.5434 (6)	0.6769 (4)	0.0401 (14)
C55	0.2185 (7)	0.4875 (6)	0.6370 (4)	0.0432 (16)
H55	0.2278	0.5157	0.5772	0.052*
C56	0.3074 (6)	0.3883 (6)	0.6855 (4)	0.0444 (15)
H56	0.3769	0.3495	0.6579	0.053*
C57	−0.0154 (6)	0.5211 (7)	0.8891 (4)	0.0502 (17)
H57A	−0.0384	0.4381	0.9047	0.075*
H57B	−0.0841	0.5805	0.9057	0.075*
H57C	0.0607	0.5141	0.9180	0.075*
C58	0.0267 (9)	0.6849 (10)	0.5522 (5)	0.078 (3)
H58A	0.1066	0.7121	0.5323	0.117*
H58B	−0.0428	0.7569	0.5333	0.117*
H58C	0.0189	0.6184	0.5291	0.117*
C59	0.3743 (5)	0.1079 (5)	0.8247 (4)	0.0361 (13)
C60	0.4186 (5)	0.0663 (6)	0.7536 (4)	0.0386 (14)
H60	0.4608	0.1174	0.7074	0.046*
C61	0.3998 (5)	−0.0486 (6)	0.7518 (4)	0.0344 (13)
C62	0.3378 (5)	−0.1226 (5)	0.8201 (4)	0.0360 (13)
C63	0.2941 (6)	−0.0817 (6)	0.8903 (4)	0.0402 (14)
H63	0.2512	−0.1318	0.9366	0.048*
C64	0.3152 (5)	0.0336 (6)	0.8902 (4)	0.0387 (13)

H64	0.2871	0.0614	0.9377	0.046*	
C65	0.5001 (7)	−0.0247 (7)	0.6169 (4)	0.0447 (15)	
H65A	0.4437	0.0561	0.5917	0.067*	
H65B	0.5227	−0.0698	0.5751	0.067*	
H65C	0.5762	−0.0092	0.6347	0.067*	
C66	0.2478 (7)	−0.3074 (6)	0.8794 (5)	0.0472 (16)	
H66A	0.2864	−0.3338	0.9344	0.071*	
H66B	0.2383	−0.3821	0.8658	0.071*	
H66C	0.1652	−0.2535	0.8815	0.071*	
O21	0.6187 (4)	0.4134 (4)	0.5630 (3)	0.0432 (10)	
O22	0.6839 (4)	0.5589 (4)	0.6328 (3)	0.0402 (10)	
O23	0.8621 (4)	−0.1676 (4)	1.0006 (3)	0.0425 (10)	
O24	0.6975 (4)	−0.2686 (4)	0.9633 (2)	0.0349 (9)	
O19	1.159 (8)	−0.098 (4)	0.587 (3)	0.0487 (18)	0.462 (5)
O20	1.2180 (11)	0.0573 (16)	0.4811 (8)	0.069 (2)	0.462 (5)
C67	1.198 (3)	0.011 (3)	0.5596 (12)	0.037 (3)	0.462 (5)
C68	1.141 (5)	0.089 (3)	0.614 (3)	0.054 (7)	0.462 (5)
C69	1.0757 (9)	0.0064 (10)	0.6869 (7)	0.0244 (13)	0.462 (5)
H69	1.1029	0.0095	0.7412	0.029*	0.462 (5)
C70	1.1301 (18)	−0.1304 (15)	0.6771 (12)	0.040 (3)	0.462 (5)
H70A	1.2062	−0.1730	0.7103	0.048*	0.462 (5)
H70B	1.0666	−0.1847	0.6944	0.048*	0.462 (5)
C72	0.9319 (9)	0.0400 (9)	0.6842 (6)	0.0199 (13)	0.462 (5)
H72	0.9031	0.0118	0.6399	0.024*	0.462 (5)
O19A	1.164 (7)	−0.111 (3)	0.580 (3)	0.0487 (18)	0.538 (5)
O20A	1.2805 (8)	0.0098 (12)	0.4915 (6)	0.069 (2)	0.538 (5)
C67A	1.188 (2)	0.004 (2)	0.5417 (10)	0.037 (3)	0.538 (5)
C68A	1.137 (4)	0.087 (3)	0.594 (2)	0.054 (7)	0.538 (5)
C69A	1.0251 (7)	0.0307 (7)	0.6369 (5)	0.0244 (13)	0.538 (5)
H69A	0.9560	0.0548	0.5963	0.029*	0.538 (5)
C70A	1.0885 (14)	−0.1163 (12)	0.6563 (10)	0.040 (3)	0.538 (5)
H70C	1.1404	−0.1480	0.7069	0.048*	0.538 (5)
H70D	1.0249	−0.1691	0.6633	0.048*	0.538 (5)
C72A	0.9770 (7)	0.0672 (7)	0.7168 (4)	0.0199 (13)	0.538 (5)
H72A	1.0494	0.0602	0.7512	0.024*	0.538 (5)
C71	1.1779 (6)	0.1889 (7)	0.5991 (5)	0.057 (2)	
H71A	1.2391	0.2107	0.5553	0.068*	
H71B	1.1451	0.2439	0.6315	0.068*	
C73	0.8701 (11)	0.1782 (10)	0.6729 (7)	0.024 (2)*	0.462 (5)
C74	0.7708 (10)	0.2331 (10)	0.6180 (7)	0.0221 (15)*	0.462 (5)
H74	0.7467	0.1855	0.5872	0.027*	0.462 (5)
C75	0.7066 (12)	0.3555 (10)	0.6075 (8)	0.0241 (16)*	0.462 (5)
C76	0.7458 (12)	0.4298 (12)	0.6473 (8)	0.0241 (15)*	0.462 (5)
C77	0.8434 (16)	0.3770 (13)	0.7020 (13)	0.025 (2)	0.462 (5)
H77	0.8692	0.4268	0.7305	0.030*	0.462 (5)
C78	0.9054 (14)	0.2507 (13)	0.7165 (10)	0.029 (2)	0.462 (5)
H78	0.9708	0.2149	0.7557	0.035*	0.462 (5)
C73A	0.8988 (9)	0.2022 (9)	0.6934 (7)	0.025 (2)*	0.538 (5)
C74A	0.7965 (8)	0.2372 (8)	0.6415 (6)	0.0221 (15)*	0.538 (5)
H74A	0.7744	0.1777	0.6197	0.027*	0.538 (5)
C75A	0.7256 (10)	0.3622 (9)	0.6215 (7)	0.0241 (16)*	0.538 (5)
C76A	0.7601 (10)	0.4441 (10)	0.6578 (7)	0.0241 (15)*	0.538 (5)

C77A	0.8584 (13)	0.4080 (11)	0.7100 (10)	0.025 (2)	0.538 (5)
H77A	0.8788	0.4656	0.7341	0.030*	0.538 (5)
C78A	0.9288 (11)	0.2862 (11)	0.7275 (8)	0.029 (2)	0.538 (5)
H78A	0.9982	0.2608	0.7634	0.035*	0.538 (5)
C79	0.5828 (7)	0.3413 (8)	0.5165 (5)	0.059 (2)	
H79A	0.6558	0.3110	0.4844	0.088*	
H79B	0.5169	0.3946	0.4776	0.088*	
H79C	0.5510	0.2691	0.5559	0.088*	
C80	0.7137 (7)	0.6384 (8)	0.6763 (5)	0.0590 (19)	
H80A	0.7238	0.5909	0.7364	0.088*	
H80B	0.6456	0.7122	0.6700	0.088*	
H80C	0.7920	0.6662	0.6522	0.088*	
C81	0.8919 (8)	−0.0346 (7)	0.7684 (5)	0.066 (2)	
C82	0.9116 (6)	−0.0604 (6)	0.8541 (5)	0.0502 (17)	
H82	0.9708	−0.0230	0.8701	0.060*	
C83	0.8462 (6)	−0.1398 (5)	0.9163 (4)	0.0351 (13)	
C84	0.7575 (5)	−0.1949 (5)	0.8952 (3)	0.0305 (12)	
C85	0.7354 (7)	−0.1708 (7)	0.8111 (4)	0.0518 (18)	
H85	0.6761	−0.2077	0.7948	0.062*	
C86	0.8036 (9)	−0.0897 (8)	0.7503 (4)	0.083 (4)	
H86	0.7871	−0.0721	0.6925	0.099*	
C87	0.9459 (7)	−0.1076 (8)	1.0245 (6)	0.064 (2)	
H87A	1.0304	−0.1320	1.0017	0.096*	
H87B	0.9474	−0.1333	1.0863	0.096*	
H87C	0.9182	−0.0159	1.0023	0.096*	
C88	0.6041 (6)	−0.3252 (6)	0.9443 (5)	0.0469 (16)	
H88A	0.5384	−0.2590	0.9117	0.070*	
H88B	0.5671	−0.3741	0.9971	0.070*	
H88C	0.6429	−0.3812	0.9113	0.070*	

Atomic displacement parameters (Å²)

	U^{11}	U^{22}	U^{33}	U^{12}	U^{13}	U^{23}
O1	0.061 (3)	0.054 (3)	0.051 (3)	−0.011 (2)	0.005 (2)	−0.014 (2)
O2	0.096 (4)	0.081 (3)	0.038 (3)	−0.055 (3)	0.007 (2)	0.000 (2)
O3	0.040 (2)	0.039 (2)	0.033 (2)	−0.0217 (18)	0.0021 (17)	−0.0130 (17)
O4	0.041 (2)	0.034 (2)	0.039 (2)	−0.0151 (18)	−0.0035 (18)	−0.0137 (17)
O5	0.035 (2)	0.035 (2)	0.044 (2)	−0.0022 (16)	−0.0064 (17)	−0.0096 (18)
O6	0.041 (2)	0.038 (2)	0.052 (3)	−0.0066 (19)	0.002 (2)	−0.019 (2)
C1	0.036 (3)	0.054 (4)	0.043 (4)	−0.012 (3)	0.005 (3)	−0.016 (3)
C2	0.032 (3)	0.051 (4)	0.050 (4)	−0.012 (3)	0.006 (3)	0.001 (3)
C3	0.036 (3)	0.076 (5)	0.039 (3)	0.002 (3)	0.006 (3)	−0.005 (3)
C4	0.042 (4)	0.102 (6)	0.045 (4)	−0.005 (4)	0.017 (3)	−0.039 (4)
C5	0.045 (4)	0.051 (4)	0.057 (4)	0.004 (3)	−0.004 (3)	−0.025 (3)
C6	0.040 (3)	0.053 (4)	0.039 (3)	0.005 (3)	−0.001 (3)	−0.004 (3)
C7	0.041 (3)	0.041 (3)	0.030 (3)	0.016 (3)	0.008 (2)	0.000 (2)
C8	0.031 (3)	0.031 (3)	0.043 (3)	−0.002 (2)	0.006 (2)	−0.010 (2)
C9	0.032 (3)	0.027 (3)	0.028 (3)	0.000 (2)	−0.003 (2)	−0.010 (2)
C10	0.034 (3)	0.028 (3)	0.035 (3)	0.004 (2)	−0.003 (2)	−0.015 (2)
C11	0.038 (3)	0.042 (3)	0.034 (3)	0.004 (2)	−0.005 (2)	−0.017 (3)
C12	0.035 (3)	0.045 (3)	0.037 (3)	0.009 (2)	−0.011 (2)	−0.020 (3)
C13	0.045 (3)	0.057 (4)	0.046 (3)	−0.030 (3)	0.006 (3)	−0.030 (3)

C14	0.036 (3)	0.043 (3)	0.050 (4)	−0.010 (3)	−0.007 (3)	−0.015 (3)
C15	0.033 (3)	0.046 (3)	0.022 (2)	−0.005 (2)	0.010 (2)	−0.002 (2)
C16	0.026 (2)	0.041 (3)	0.025 (3)	−0.006 (2)	0.0106 (19)	−0.002 (2)
C17	0.027 (3)	0.041 (3)	0.027 (3)	−0.010 (2)	0.008 (2)	−0.005 (2)
C18	0.031 (3)	0.045 (3)	0.029 (3)	−0.007 (2)	0.009 (2)	−0.010 (2)
C19	0.048 (4)	0.072 (5)	0.025 (3)	−0.020 (3)	0.005 (3)	−0.015 (3)
C20	0.031 (3)	0.070 (4)	0.027 (3)	−0.001 (3)	−0.001 (2)	0.006 (3)
C21	0.039 (3)	0.044 (3)	0.056 (4)	−0.004 (3)	−0.009 (3)	−0.015 (3)
C22	0.056 (4)	0.053 (4)	0.070 (5)	−0.017 (3)	0.007 (4)	−0.034 (4)
O7	0.057 (3)	0.050 (3)	0.063 (3)	−0.012 (2)	−0.009 (2)	−0.021 (2)
O8	0.055 (3)	0.065 (3)	0.054 (3)	−0.029 (2)	0.006 (2)	−0.030 (2)
O9	0.052 (3)	0.053 (3)	0.041 (3)	−0.007 (2)	0.007 (2)	−0.006 (2)
O10	0.042 (2)	0.036 (2)	0.040 (2)	−0.0062 (19)	0.0079 (19)	−0.0119 (19)
O11	0.044 (3)	0.061 (3)	0.060 (3)	−0.003 (2)	0.008 (2)	−0.007 (3)
O12	0.054 (3)	0.061 (3)	0.053 (3)	−0.016 (2)	−0.012 (2)	0.021 (2)
C23	0.043 (3)	0.046 (4)	0.032 (3)	−0.019 (3)	0.014 (2)	−0.015 (3)
C24	0.039 (3)	0.043 (4)	0.064 (4)	−0.011 (3)	0.009 (3)	−0.020 (3)
C26	0.042 (4)	0.043 (4)	0.077 (5)	−0.001 (3)	−0.006 (3)	−0.029 (4)
C27	0.039 (3)	0.048 (4)	0.074 (5)	−0.011 (3)	0.010 (3)	−0.025 (4)
C25	0.023 (4)	0.044 (4)	0.042 (5)	−0.007 (3)	0.012 (3)	−0.022 (4)
C28	0.022 (3)	0.033 (4)	0.026 (4)	−0.005 (3)	0.010 (3)	−0.013 (3)
C25A	0.023 (4)	0.044 (4)	0.042 (5)	−0.007 (3)	0.012 (3)	−0.022 (4)
C28A	0.022 (3)	0.033 (4)	0.026 (4)	−0.005 (3)	0.010 (3)	−0.013 (3)
C29	0.028 (3)	0.039 (4)	0.090 (5)	0.000 (3)	−0.016 (3)	−0.024 (4)
C30	0.026 (3)	0.036 (3)	0.071 (5)	−0.008 (3)	−0.011 (3)	0.008 (3)
C31	0.033 (3)	0.036 (3)	0.042 (3)	0.000 (3)	−0.005 (3)	−0.006 (3)
C32	0.028 (3)	0.029 (3)	0.038 (3)	0.001 (2)	0.000 (2)	−0.008 (2)
C33	0.030 (3)	0.049 (4)	0.048 (4)	−0.004 (3)	0.008 (3)	−0.020 (3)
C34	0.041 (3)	0.048 (4)	0.069 (5)	0.002 (3)	−0.003 (3)	−0.028 (4)
C35	0.043 (4)	0.088 (6)	0.048 (4)	0.001 (4)	0.007 (3)	0.008 (4)
C36	0.047 (4)	0.034 (3)	0.056 (4)	−0.014 (3)	0.006 (3)	−0.017 (3)
C37	0.036 (3)	0.029 (3)	0.068 (5)	−0.008 (3)	−0.004 (3)	−0.014 (3)
C38	0.035 (3)	0.033 (3)	0.046 (4)	−0.020 (3)	−0.013 (3)	0.006 (3)
C39	0.031 (3)	0.043 (4)	0.049 (4)	−0.012 (3)	0.001 (3)	−0.009 (3)
C40	0.045 (3)	0.031 (3)	0.038 (3)	−0.018 (3)	−0.006 (3)	0.002 (3)
C41	0.068 (5)	0.056 (4)	0.043 (4)	−0.032 (4)	0.011 (3)	−0.018 (3)
C42	0.043 (4)	0.039 (4)	0.105 (7)	−0.006 (3)	0.006 (4)	−0.036 (4)
C43	0.060 (5)	0.069 (5)	0.054 (5)	−0.010 (4)	0.010 (4)	−0.012 (4)
C44	0.138 (10)	0.110 (9)	0.052 (5)	−0.025 (8)	−0.026 (6)	0.049 (6)
O13	0.038 (2)	0.042 (2)	0.048 (3)	−0.0075 (19)	−0.0009 (19)	−0.010 (2)
O14	0.069 (3)	0.060 (3)	0.041 (3)	−0.022 (3)	0.001 (2)	−0.018 (2)
O15	0.034 (2)	0.047 (3)	0.046 (3)	0.004 (2)	0.0085 (19)	0.005 (2)
O16	0.040 (2)	0.049 (3)	0.049 (3)	−0.016 (2)	−0.012 (2)	0.019 (2)
O17	0.047 (2)	0.044 (2)	0.040 (2)	−0.012 (2)	0.0123 (19)	−0.0157 (19)
O18	0.048 (2)	0.024 (2)	0.055 (3)	−0.0096 (18)	0.014 (2)	−0.0158 (19)
C45	0.033 (3)	0.047 (4)	0.042 (3)	−0.013 (3)	0.007 (3)	−0.023 (3)
C46	0.042 (3)	0.040 (3)	0.039 (3)	−0.017 (3)	0.009 (3)	−0.018 (3)
C47	0.042 (3)	0.043 (3)	0.048 (4)	−0.010 (3)	0.007 (3)	−0.019 (3)
C48	0.031 (3)	0.040 (4)	0.090 (5)	−0.010 (3)	−0.004 (3)	−0.024 (4)
C49	0.038 (3)	0.035 (3)	0.058 (4)	−0.009 (3)	0.005 (3)	−0.017 (3)
C50	0.033 (3)	0.034 (3)	0.042 (3)	−0.005 (2)	0.006 (2)	−0.011 (2)
C51	0.041 (3)	0.034 (3)	0.034 (3)	−0.015 (3)	−0.004 (2)	−0.011 (2)

C52	0.029 (3)	0.031 (3)	0.037 (3)	−0.008 (2)	0.002 (2)	−0.011 (2)
C53	0.026 (3)	0.030 (3)	0.035 (3)	−0.012 (2)	0.002 (2)	0.002 (2)
C54	0.032 (3)	0.036 (3)	0.048 (4)	−0.017 (3)	−0.005 (3)	0.001 (3)
C55	0.060 (4)	0.039 (3)	0.034 (3)	−0.026 (3)	0.002 (3)	−0.009 (3)
C56	0.049 (4)	0.040 (3)	0.051 (4)	−0.013 (3)	0.012 (3)	−0.026 (3)
C57	0.038 (3)	0.050 (4)	0.048 (4)	−0.004 (3)	0.018 (3)	−0.005 (3)
C58	0.072 (5)	0.103 (7)	0.049 (5)	−0.023 (5)	−0.017 (4)	−0.001 (4)
C59	0.031 (3)	0.032 (3)	0.049 (4)	0.004 (2)	−0.004 (3)	−0.023 (3)
C60	0.029 (3)	0.039 (3)	0.043 (3)	−0.008 (2)	0.001 (2)	−0.007 (3)
C61	0.025 (3)	0.036 (3)	0.040 (3)	0.000 (2)	0.005 (2)	−0.014 (3)
C62	0.028 (3)	0.031 (3)	0.050 (4)	−0.004 (2)	0.005 (3)	−0.016 (3)
C63	0.035 (3)	0.030 (3)	0.053 (4)	−0.002 (2)	0.005 (3)	−0.016 (3)
C64	0.030 (3)	0.036 (3)	0.051 (4)	−0.004 (2)	0.008 (3)	−0.019 (3)
C65	0.049 (4)	0.049 (4)	0.037 (3)	−0.014 (3)	0.012 (3)	−0.015 (3)
C66	0.045 (4)	0.036 (4)	0.053 (4)	−0.010 (3)	0.009 (3)	−0.006 (3)
O21	0.034 (2)	0.042 (2)	0.057 (3)	−0.0078 (18)	0.0043 (19)	−0.023 (2)
O22	0.043 (2)	0.032 (2)	0.043 (2)	−0.0047 (18)	−0.0013 (19)	−0.0107 (18)
O23	0.051 (3)	0.047 (3)	0.040 (2)	−0.029 (2)	0.0045 (19)	−0.019 (2)
O24	0.042 (2)	0.033 (2)	0.032 (2)	−0.0160 (17)	−0.0037 (17)	−0.0067 (16)
O19	0.048 (5)	0.048 (5)	0.048 (6)	−0.007 (7)	0.009 (4)	−0.017 (3)
O20	0.029 (5)	0.142 (9)	0.063 (4)	−0.018 (5)	0.017 (4)	−0.071 (5)
C67	0.063 (6)	0.054 (4)	0.007 (7)	−0.043 (4)	−0.010 (7)	−0.004 (5)
C68	0.041 (4)	0.039 (4)	0.084 (18)	0.007 (3)	−0.003 (10)	−0.031 (6)
C69	0.023 (3)	0.025 (3)	0.025 (4)	−0.005 (2)	−0.001 (2)	−0.008 (3)
C70	0.050 (9)	0.035 (4)	0.037 (8)	−0.022 (5)	0.013 (6)	−0.011 (5)
C72	0.020 (3)	0.023 (3)	0.019 (3)	−0.002 (2)	−0.001 (2)	−0.011 (2)
O19A	0.048 (5)	0.048 (5)	0.048 (6)	−0.007 (7)	0.009 (4)	−0.017 (3)
O20A	0.029 (5)	0.142 (9)	0.063 (4)	−0.018 (5)	0.017 (4)	−0.071 (5)
C67A	0.063 (6)	0.054 (4)	0.007 (7)	−0.043 (4)	−0.010 (7)	−0.004 (5)
C68A	0.041 (4)	0.039 (4)	0.084 (18)	0.007 (3)	−0.003 (10)	−0.031 (6)
C69A	0.023 (3)	0.025 (3)	0.025 (4)	−0.005 (2)	−0.001 (2)	−0.008 (3)
C70A	0.050 (9)	0.035 (4)	0.037 (8)	−0.022 (5)	0.013 (6)	−0.011 (5)
C72A	0.020 (3)	0.023 (3)	0.019 (3)	−0.002 (2)	−0.001 (2)	−0.011 (2)
C71	0.036 (3)	0.046 (4)	0.073 (5)	−0.009 (3)	0.006 (3)	0.001 (3)
C77	0.027 (4)	0.034 (6)	0.026 (4)	−0.018 (4)	0.001 (3)	−0.018 (4)
C78	0.031 (5)	0.038 (6)	0.021 (4)	−0.006 (4)	−0.004 (3)	−0.013 (4)
C77A	0.027 (4)	0.034 (6)	0.026 (4)	−0.018 (4)	0.001 (3)	−0.018 (4)
C78A	0.031 (5)	0.038 (6)	0.021 (4)	−0.006 (4)	−0.004 (3)	−0.013 (4)
C79	0.053 (4)	0.069 (5)	0.075 (5)	−0.030 (4)	0.021 (4)	−0.045 (4)
C80	0.050 (4)	0.055 (4)	0.083 (5)	−0.021 (3)	0.001 (4)	−0.030 (4)
C81	0.055 (4)	0.038 (3)	0.062 (5)	0.022 (3)	0.038 (4)	0.010 (3)
C82	0.041 (3)	0.024 (3)	0.069 (4)	0.002 (2)	0.027 (3)	−0.006 (3)
C83	0.036 (3)	0.023 (3)	0.041 (3)	−0.006 (2)	0.013 (2)	−0.008 (2)
C84	0.034 (3)	0.025 (3)	0.026 (3)	0.000 (2)	0.001 (2)	−0.003 (2)
C85	0.056 (4)	0.049 (4)	0.037 (4)	0.018 (3)	−0.009 (3)	−0.010 (3)
C86	0.097 (7)	0.072 (6)	0.022 (3)	0.051 (5)	0.017 (4)	0.014 (3)
C87	0.048 (4)	0.074 (5)	0.096 (6)	−0.035 (4)	0.009 (4)	−0.048 (5)
C88	0.046 (4)	0.036 (3)	0.068 (4)	−0.011 (3)	−0.018 (3)	−0.021 (3)

Geometric parameters (Å, º)

O1—C1	1.353 (9)	O17—C65	1.427 (8)
O1—C4	1.456 (8)	O18—C62	1.374 (7)
O2—C1	1.197 (8)	O18—C66	1.446 (8)
O3—C9	1.368 (7)	C45—C46	1.482 (9)
O3—C13	1.429 (6)	C46—C49	1.332 (9)
O4—C10	1.352 (7)	C46—C47	1.500 (9)
O4—C14	1.422 (7)	C47—C50	1.542 (8)
O5—C17	1.369 (7)	C47—C48	1.545 (9)
O5—C21	1.428 (8)	C47—H47	1.0000
O6—C18	1.357 (8)	C48—H48A	0.9900
O6—C22	1.442 (8)	C48—H48B	0.9900
C1—C2	1.459 (11)	C49—H49A	0.9500
C2—C5	1.287 (10)	C49—H49B	0.9500
C2—C3	1.516 (10)	C50—C51	1.527 (8)
C3—C6	1.552 (9)	C50—C59	1.536 (8)
C3—C4	1.561 (12)	C50—H50	1.0000
C3—H3	1.0000	C51—C52	1.358 (9)
C4—H4A	0.9900	C51—C56	1.384 (9)
C4—H4B	0.9900	C52—C53	1.394 (8)
C5—H5A	0.9500	C52—H52	0.9500
C5—H5B	0.9500	C53—C54	1.408 (9)
C6—C7	1.542 (9)	C54—C55	1.371 (10)
C6—C15	1.548 (9)	C55—C56	1.404 (10)
C6—H6	1.0000	C55—H55	0.9500
C7—C12	1.339 (10)	C56—H56	0.9500
C7—C8	1.413 (9)	C57—H57A	0.9800
C8—C9	1.371 (8)	C57—H57B	0.9800
C8—H8	0.9500	C57—H57C	0.9800
C9—C10	1.409 (8)	C58—H58A	0.9800
C10—C11	1.390 (8)	C58—H58B	0.9800
C11—C12	1.388 (9)	C58—H58C	0.9800
C11—H11	0.9500	C59—C64	1.352 (9)
C12—H12	0.9500	C59—C60	1.425 (9)
C13—H13A	0.9800	C60—C61	1.381 (9)
C13—H13B	0.9800	C60—H60	0.9500
C13—H13C	0.9800	C61—C62	1.395 (9)
C14—H14A	0.9800	C62—C63	1.406 (9)
C14—H14B	0.9800	C63—C64	1.385 (9)
C14—H14C	0.9800	C63—H63	0.9500
C15—C20	1.346 (10)	C64—H64	0.9500
C15—C16	1.400 (8)	C65—H65A	0.9800
C16—C17	1.375 (8)	C65—H65B	0.9800
C16—H16	0.9500	C65—H65C	0.9800
C17—C18	1.406 (8)	C66—H66A	0.9800
C18—C19	1.402 (9)	C66—H66B	0.9800
C19—C20	1.407 (11)	C66—H66C	0.9800
C19—H19	0.9500	O21—C75	1.209 (12)
C20—H20	0.9500	O21—C79	1.435 (8)
C21—H21A	0.9800	O21—C75A	1.492 (10)
C21—H21B	0.9800	O22—C76A	1.352 (11)
C21—H21C	0.9800	O22—C76	1.435 (13)

C22—H22A	0.9800	O22—C80	1.439 (8)
C22—H22B	0.9800	O23—C83	1.364 (8)
C22—H22C	0.9800	O23—C87	1.412 (7)
O7—C23	1.367 (8)	O24—C84	1.380 (7)
O7—C26	1.434 (8)	O24—C88	1.431 (7)
O8—C23	1.184 (8)	O19—C67	1.33 (2)
O9—C31	1.372 (8)	O19—C70	1.45 (3)
O9—C35	1.434 (9)	O20—C67	1.264 (19)
O10—C32	1.369 (7)	C67—C68	1.483 (18)
O10—C36	1.405 (8)	C68—C71	1.23 (2)
O11—C39	1.385 (9)	C68—C69	1.50 (2)
O11—C43	1.425 (9)	C69—C72	1.535 (13)
O12—C40	1.357 (8)	C69—C70	1.602 (16)
O12—C44	1.423 (11)	C69—H69	1.0000
C23—C24	1.487 (10)	C70—H70A	0.9900
C24—C27	1.283 (10)	C70—H70B	0.9900
C24—C25	1.507 (10)	C72—C81	1.472 (12)
C24—C25A	1.563 (17)	C72—C73	1.534 (15)
C26—C25	1.567 (11)	C72—H72	1.0000
C26—C25A	1.672 (17)	O19A—C67A	1.330 (16)
C26—H26A	0.9900	O19A—C70A	1.44 (2)
C26—H26B	0.9900	O20A—C67A	1.247 (18)
C26—H26C	0.9900	C67A—C68A	1.480 (16)
C26—H26D	0.9900	C68A—C71	1.36 (2)
C27—H27A	0.9500	C68A—C69A	1.51 (2)
C27—H27B	0.9500	C69A—C72A	1.538 (10)
C25—C28	1.542 (10)	C69A—C70A	1.609 (13)
C25—H25	1.0000	C69A—H69A	1.0000
C28—C29	1.538 (10)	C70A—H70C	0.9900
C28—C37	1.558 (9)	C70A—H70D	0.9900
C28—H28	1.0000	C72A—C73A	1.538 (11)
C25A—C28A	1.536 (19)	C72A—C81	1.619 (11)
C25A—H25A	1.0000	C72A—H72A	1.0000
C28A—C37	1.590 (15)	C71—H71A	0.9500
C28A—C29	1.623 (15)	C71—H71B	0.9500
C28A—H28A	1.0000	C73—C74	1.396 (15)
C29—C34	1.366 (11)	C73—C78	1.400 (16)
C29—C30	1.384 (11)	C74—C75	1.385 (14)
C30—C31	1.407 (10)	C74—H74	0.9500
C30—H30	0.9500	C75—C76	1.390 (14)
C31—C32	1.396 (9)	C76—C77	1.379 (15)
C32—C33	1.361 (9)	C77—C78	1.407 (17)
C33—C34	1.399 (10)	C77—H77	0.9500
C33—H33	0.9500	C78—H78	0.9500
C34—H34	0.9500	C73A—C78A	1.373 (13)
C35—H35A	0.9800	C73A—C74A	1.394 (13)
C35—H35B	0.9800	C74A—C75A	1.419 (12)
C35—H35C	0.9800	C74A—H74A	0.9500
C36—H36A	0.9800	C75A—C76A	1.400 (12)
C36—H36B	0.9800	C76A—C77A	1.361 (13)
C36—H36C	0.9800	C77A—C78A	1.389 (15)
C37—C42	1.358 (11)	C77A—H77A	0.9500

C37—C38	1.399 (10)	C78A—H78A	0.9500
C38—C39	1.362 (9)	C79—H79A	0.9800
C38—H38	0.9500	C79—H79B	0.9800
C39—C40	1.383 (9)	C79—H79C	0.9800
C40—C41	1.394 (11)	C80—H80A	0.9800
C41—C42	1.404 (11)	C80—H80B	0.9800
C41—H41	0.9500	C80—H80C	0.9800
C42—H42	0.9500	C81—C86	1.366 (14)
C43—H43A	0.9800	C81—C82	1.398 (12)
C43—H43B	0.9800	C82—C83	1.391 (9)
C43—H43C	0.9800	C82—H82	0.9500
C44—H44A	0.9800	C83—C84	1.394 (8)
C44—H44B	0.9800	C84—C85	1.380 (8)
C44—H44C	0.9800	C85—C86	1.408 (13)
O13—C45	1.331 (8)	C85—H85	0.9500
O13—C48	1.446 (8)	C86—H86	0.9500
O14—C45	1.217 (8)	C87—H87A	0.9800
O15—C53	1.352 (8)	C87—H87B	0.9800
O15—C57	1.425 (8)	C87—H87C	0.9800
O16—C54	1.367 (8)	C88—H88A	0.9800
O16—C58	1.374 (9)	C88—H88B	0.9800
O17—C61	1.357 (7)	C88—H88C	0.9800
C1—O1—C4	107.8 (6)	C46—C47—C48	103.1 (5)
C9—O3—C13	116.1 (5)	C50—C47—C48	111.8 (5)
C10—O4—C14	117.6 (5)	C46—C47—H47	109.5
C17—O5—C21	118.3 (5)	C50—C47—H47	109.5
C18—O6—C22	116.8 (5)	C48—C47—H47	109.5
O2—C1—O1	120.5 (6)	O13—C48—C47	106.9 (5)
O2—C1—C2	128.9 (7)	O13—C48—H48A	110.3
O1—C1—C2	110.4 (6)	C47—C48—H48A	110.3
C5—C2—C1	124.6 (7)	O13—C48—H48B	110.3
C5—C2—C3	125.4 (8)	C47—C48—H48B	110.3
C1—C2—C3	109.4 (7)	H48A—C48—H48B	108.6
C2—C3—C6	114.0 (6)	C46—C49—H49A	120.0
C2—C3—C4	98.0 (6)	C46—C49—H49B	120.0
C6—C3—C4	109.0 (7)	H49A—C49—H49B	120.0
C2—C3—H3	111.7	C51—C50—C59	112.4 (5)
C6—C3—H3	111.7	C51—C50—C47	113.0 (5)
C4—C3—H3	111.7	C59—C50—C47	112.5 (5)
O1—C4—C3	108.0 (6)	C51—C50—H50	106.1
O1—C4—H4A	110.1	C59—C50—H50	106.1
C3—C4—H4A	110.1	C47—C50—H50	106.1
O1—C4—H4B	110.1	C52—C51—C56	118.4 (6)
C3—C4—H4B	110.1	C52—C51—C50	119.3 (5)
H4A—C4—H4B	108.4	C56—C51—C50	122.3 (6)
C2—C5—H5A	120.0	C51—C52—C53	122.1 (5)
C2—C5—H5B	120.0	C51—C52—H52	118.9
H5A—C5—H5B	120.0	C53—C52—H52	118.9
C7—C6—C15	111.3 (5)	O15—C53—C52	125.1 (5)
C7—C6—C3	110.6 (5)	O15—C53—C54	116.0 (5)
C15—C6—C3	115.1 (6)	C52—C53—C54	118.9 (5)

C7—C6—H6	106.4	O16—C54—C55	126.3 (6)
C15—C6—H6	106.4	O16—C54—C53	113.8 (6)
C3—C6—H6	106.4	C55—C54—C53	119.8 (6)
C12—C7—C8	120.5 (6)	C54—C55—C56	119.3 (6)
C12—C7—C6	119.5 (6)	C54—C55—H55	120.3
C8—C7—C6	120.0 (6)	C56—C55—H55	120.3
C9—C8—C7	120.0 (6)	C51—C56—C55	121.4 (6)
C9—C8—H8	120.0	C51—C56—H56	119.3
C7—C8—H8	120.0	C55—C56—H56	119.3
O3—C9—C8	126.9 (5)	O15—C57—H57A	109.5
O3—C9—C10	113.3 (5)	O15—C57—H57B	109.5
C8—C9—C10	119.8 (5)	H57A—C57—H57B	109.5
O4—C10—C11	125.4 (5)	O15—C57—H57C	109.5
O4—C10—C9	116.1 (5)	H57A—C57—H57C	109.5
C11—C10—C9	118.4 (6)	H57B—C57—H57C	109.5
C12—C11—C10	121.1 (6)	O16—C58—H58A	109.5
C12—C11—H11	119.5	O16—C58—H58B	109.5
C10—C11—H11	119.5	H58A—C58—H58B	109.5
C7—C12—C11	120.1 (5)	O16—C58—H58C	109.5
C7—C12—H12	120.0	H58A—C58—H58C	109.5
C11—C12—H12	120.0	H58B—C58—H58C	109.5
O3—C13—H13A	109.5	C64—C59—C60	119.4 (6)
O3—C13—H13B	109.5	C64—C59—C50	120.0 (5)
H13A—C13—H13B	109.5	C60—C59—C50	120.6 (6)
O3—C13—H13C	109.5	C61—C60—C59	119.8 (6)
H13A—C13—H13C	109.5	C61—C60—H60	120.1
H13B—C13—H13C	109.5	C59—C60—H60	120.1
O4—C14—H14A	109.5	O17—C61—C60	125.5 (5)
O4—C14—H14B	109.5	O17—C61—C62	115.1 (5)
H14A—C14—H14B	109.5	C60—C61—C62	119.4 (5)
O4—C14—H14C	109.5	O18—C62—C61	116.0 (5)
H14A—C14—H14C	109.5	O18—C62—C63	123.1 (5)
H14B—C14—H14C	109.5	C61—C62—C63	120.8 (5)
C20—C15—C16	118.7 (6)	C64—C63—C62	118.2 (6)
C20—C15—C6	125.3 (6)	C64—C63—H63	120.9
C16—C15—C6	116.1 (6)	C62—C63—H63	120.9
C17—C16—C15	121.1 (6)	C59—C64—C63	122.3 (6)
C17—C16—H16	119.4	C59—C64—H64	118.9
C15—C16—H16	119.4	C63—C64—H64	118.9
O5—C17—C16	123.5 (5)	O17—C65—H65A	109.5
O5—C17—C18	115.4 (5)	O17—C65—H65B	109.5
C16—C17—C18	121.1 (5)	H65A—C65—H65B	109.5
O6—C18—C19	127.4 (6)	O17—C65—H65C	109.5
O6—C18—C17	115.6 (5)	H65A—C65—H65C	109.5
C19—C18—C17	117.1 (6)	H65B—C65—H65C	109.5
C18—C19—C20	120.5 (7)	O18—C66—H66A	109.5
C18—C19—H19	119.7	O18—C66—H66B	109.5
C20—C19—H19	119.7	H66A—C66—H66B	109.5
C15—C20—C19	121.6 (6)	O18—C66—H66C	109.5
C15—C20—H20	119.2	H66A—C66—H66C	109.5
C19—C20—H20	119.2	H66B—C66—H66C	109.5
O5—C21—H21A	109.5	C75—O21—C79	112.6 (7)

O5—C21—H21B	109.5	C79—O21—C75A	122.3 (6)
H21A—C21—H21B	109.5	C76A—O22—C80	109.7 (6)
O5—C21—H21C	109.5	C76—O22—C80	123.3 (6)
H21A—C21—H21C	109.5	C83—O23—C87	117.2 (5)
H21B—C21—H21C	109.5	C84—O24—C88	116.4 (5)
O6—C22—H22A	109.5	C67—O19—C70	110 (3)
O6—C22—H22B	109.5	O20—C67—O19	118 (3)
H22A—C22—H22B	109.5	O20—C67—C68	122 (3)
O6—C22—H22C	109.5	O19—C67—C68	109.4 (15)
H22A—C22—H22C	109.5	C71—C68—C67	115.5 (16)
H22B—C22—H22C	109.5	C71—C68—C69	136 (3)
C23—O7—C26	110.8 (5)	C67—C68—C69	106.5 (14)
C31—O9—C35	117.4 (6)	C68—C69—C72	114 (3)
C32—O10—C36	117.7 (5)	C68—C69—C70	101.8 (12)
C39—O11—C43	117.9 (6)	C72—C69—C70	111.9 (10)
C40—O12—C44	117.8 (8)	C68—C69—H69	109.6
O8—C23—O7	120.5 (6)	C72—C69—H69	109.6
O8—C23—C24	129.9 (7)	C70—C69—H69	109.6
O7—C23—C24	109.6 (5)	O19—C70—C69	101.3 (16)
C27—C24—C23	123.6 (7)	O19—C70—H70A	111.5
C27—C24—C25	127.5 (7)	C69—C70—H70A	111.5
C23—C24—C25	108.5 (6)	O19—C70—H70B	111.5
C27—C24—C25A	124.3 (8)	C69—C70—H70B	111.5
C23—C24—C25A	106.6 (8)	H70A—C70—H70B	109.3
O7—C26—C25	108.3 (6)	C81—C72—C73	106.9 (8)
O7—C26—C25A	105.4 (7)	C81—C72—C69	103.2 (8)
O7—C26—H26A	110.0	C73—C72—C69	116.9 (9)
C25—C26—H26A	110.0	C81—C72—H72	109.8
O7—C26—H26B	110.0	C73—C72—H72	109.8
C25—C26—H26B	110.0	C69—C72—H72	109.8
H26A—C26—H26B	108.4	C67A—O19A—C70A	111.7 (15)
O7—C26—H26C	110.7	O20A—C67A—O19A	115 (3)
C25A—C26—H26C	110.7	O20A—C67A—C68A	128.2 (16)
O7—C26—H26D	110.7	O19A—C67A—C68A	110.0 (13)
C25A—C26—H26D	110.7	C71—C68A—C67A	129.3 (16)
H26C—C26—H26D	108.8	C71—C68A—C69A	130.3 (14)
C24—C27—H27A	120.0	C67A—C68A—C69A	100.4 (15)
C24—C27—H27B	120.0	C68A—C69A—C72A	112.9 (12)
H27A—C27—H27B	120.0	C68A—C69A—C70A	98.7 (14)
C24—C25—C28	112.5 (6)	C72A—C69A—C70A	113.5 (8)
C24—C25—C26	101.2 (6)	C68A—C69A—H69A	110.4
C28—C25—C26	109.9 (6)	C72A—C69A—H69A	110.4
C24—C25—H25	111.0	C70A—C69A—H69A	110.4
C28—C25—H25	111.0	O19A—C70A—C69A	99.9 (16)
C26—C25—H25	111.0	O19A—C70A—H70C	111.8
C29—C28—C25	109.5 (6)	C69A—C70A—H70C	111.8
C29—C28—C37	108.5 (5)	O19A—C70A—H70D	111.8
C25—C28—C37	110.5 (6)	C69A—C70A—H70D	111.8
C29—C28—H28	109.4	H70C—C70A—H70D	109.5
C25—C28—H28	109.4	C73A—C72A—C69A	110.8 (7)
C37—C28—H28	109.4	C73A—C72A—C81	111.0 (6)
C28A—C25A—C24	113.3 (13)	C69A—C72A—C81	105.1 (6)

C28A—C25A—C26	105.9 (11)	C73A—C72A—H72A	110.0
C24—C25A—C26	94.4 (9)	C69A—C72A—H72A	110.0
C28A—C25A—H25A	113.8	C81—C72A—H72A	110.0
C24—C25A—H25A	113.8	C68—C71—H71A	120.0
C26—C25A—H25A	113.8	C68—C71—H71B	120.0
C25A—C28A—C37	102.6 (11)	H71A—C71—H71B	120.0
C25A—C28A—C29	98.2 (11)	C74—C73—C78	118.5 (10)
C37—C28A—C29	102.9 (8)	C74—C73—C72	118.0 (11)
C25A—C28A—H28A	116.8	C78—C73—C72	123.5 (10)
C37—C28A—H28A	116.8	C75—C74—C73	121.3 (11)
C29—C28A—H28A	116.8	C75—C74—H74	119.3
C34—C29—C30	118.8 (6)	C73—C74—H74	119.3
C34—C29—C28	114.1 (7)	O21—C75—C74	127.9 (10)
C30—C29—C28	127.0 (7)	O21—C75—C76	111.7 (9)
C34—C29—C28A	148.2 (9)	C74—C75—C76	120.3 (11)
C30—C29—C28A	93.0 (8)	C77—C76—C75	119.1 (11)
C29—C30—C31	121.3 (6)	C77—C76—O22	120.5 (10)
C29—C30—H30	119.3	C75—C76—O22	120.4 (9)
C31—C30—H30	119.3	C76—C77—C78	121.1 (12)
O9—C31—C32	114.8 (6)	C76—C77—H77	119.4
O9—C31—C30	126.0 (6)	C78—C77—H77	119.4
C32—C31—C30	119.2 (6)	C73—C78—C77	119.6 (11)
C33—C32—O10	125.2 (6)	C73—C78—H78	120.2
C33—C32—C31	118.4 (6)	C77—C78—H78	120.2
O10—C32—C31	116.4 (5)	C78A—C73A—C74A	120.7 (9)
C32—C33—C34	122.4 (7)	C78A—C73A—C72A	118.6 (9)
C32—C33—H33	118.8	C74A—C73A—C72A	120.7 (10)
C34—C33—H33	118.8	C73A—C74A—C75A	119.4 (9)
C29—C34—C33	119.8 (7)	C73A—C74A—H74A	120.3
C29—C34—H34	120.1	C75A—C74A—H74A	120.3
C33—C34—H34	120.1	C76A—C75A—C74A	117.6 (8)
O9—C35—H35A	109.5	C76A—C75A—O21	117.7 (8)
O9—C35—H35B	109.5	C74A—C75A—O21	124.7 (8)
H35A—C35—H35B	109.5	O22—C76A—C77A	127.1 (9)
O9—C35—H35C	109.5	O22—C76A—C75A	110.5 (8)
H35A—C35—H35C	109.5	C77A—C76A—C75A	122.4 (9)
H35B—C35—H35C	109.5	C76A—C77A—C78A	119.4 (9)
O10—C36—H36A	109.5	C76A—C77A—H77A	120.3
O10—C36—H36B	109.5	C78A—C77A—H77A	120.3
H36A—C36—H36B	109.5	C73A—C78A—C77A	120.4 (9)
O10—C36—H36C	109.5	C73A—C78A—H78A	119.8
H36A—C36—H36C	109.5	C77A—C78A—H78A	119.8
H36B—C36—H36C	109.5	O21—C79—H79A	109.5
C42—C37—C38	119.1 (6)	O21—C79—H79B	109.5
C42—C37—C28	127.3 (6)	H79A—C79—H79B	109.5
C38—C37—C28	113.6 (6)	O21—C79—H79C	109.5
C42—C37—C28A	93.0 (8)	H79A—C79—H79C	109.5
C38—C37—C28A	147.9 (8)	H79B—C79—H79C	109.5
C39—C38—C37	120.2 (6)	O22—C80—H80A	109.5
C39—C38—H38	119.9	O22—C80—H80B	109.5
C37—C38—H38	119.9	H80A—C80—H80B	109.5
C38—C39—C40	121.7 (6)	O22—C80—H80C	109.5

C38—C39—O11	124.6 (6)	H80A—C80—H80C	109.5
C40—C39—O11	113.8 (6)	H80B—C80—H80C	109.5
O12—C40—C39	115.6 (6)	C86—C81—C82	116.1 (6)
O12—C40—C41	126.0 (6)	C86—C81—C72	102.6 (8)
C39—C40—C41	118.4 (6)	C82—C81—C72	141.3 (9)
C40—C41—C42	119.5 (7)	C86—C81—C72A	137.0 (8)
C40—C41—H41	120.2	C82—C81—C72A	106.6 (8)
C42—C41—H41	120.2	C83—C82—C81	121.2 (7)
C37—C42—C41	121.1 (7)	C83—C82—H82	119.4
C37—C42—H42	119.5	C81—C82—H82	119.4
C41—C42—H42	119.5	O23—C83—C82	123.3 (6)
O11—C43—H43A	109.5	O23—C83—C84	115.7 (5)
O11—C43—H43B	109.5	C82—C83—C84	121.0 (6)
H43A—C43—H43B	109.5	O24—C84—C85	126.1 (6)
O11—C43—H43C	109.5	O24—C84—C83	114.6 (5)
H43A—C43—H43C	109.5	C85—C84—C83	119.2 (6)
H43B—C43—H43C	109.5	C84—C85—C86	117.9 (8)
O12—C44—H44A	109.5	C84—C85—H85	121.1
O12—C44—H44B	109.5	C86—C85—H85	121.1
H44A—C44—H44B	109.5	C81—C86—C85	124.7 (7)
O12—C44—H44C	109.5	C81—C86—H86	117.7
H44A—C44—H44C	109.5	C85—C86—H86	117.7
H44B—C44—H44C	109.5	O23—C87—H87A	109.5
C45—O13—C48	111.4 (5)	O23—C87—H87B	109.5
C53—O15—C57	118.4 (5)	H87A—C87—H87B	109.5
C54—O16—C58	117.8 (7)	O23—C87—H87C	109.5
C61—O17—C65	116.6 (5)	H87A—C87—H87C	109.5
C62—O18—C66	116.4 (5)	H87B—C87—H87C	109.5
O14—C45—O13	120.7 (6)	O24—C88—H88A	109.5
O14—C45—C46	128.6 (6)	O24—C88—H88B	109.5
O13—C45—C46	110.7 (5)	H88A—C88—H88B	109.5
C49—C46—C45	121.0 (6)	O24—C88—H88C	109.5
C49—C46—C47	131.8 (6)	H88A—C88—H88C	109.5
C45—C46—C47	107.2 (5)	H88B—C88—H88C	109.5
C46—C47—C50	113.2 (5)		

C4—O1—C1—O2	−173.2 (7)	C45—O13—C48—C47	8.1 (7)
C4—O1—C1—C2	11.9 (7)	C46—C47—C48—O13	−8.6 (7)
O2—C1—C2—C5	18.6 (12)	C50—C47—C48—O13	−130.5 (6)
O1—C1—C2—C5	−167.1 (7)	C46—C47—C50—C51	63.8 (7)
O2—C1—C2—C3	−169.4 (7)	C48—C47—C50—C51	179.7 (5)
O1—C1—C2—C3	4.9 (8)	C46—C47—C50—C59	−167.6 (5)
C5—C2—C3—C6	−90.7 (9)	C48—C47—C50—C59	−51.7 (7)
C1—C2—C3—C6	97.4 (8)	C59—C50—C51—C52	103.9 (6)
C5—C2—C3—C4	154.2 (7)	C47—C50—C51—C52	−127.4 (6)
C1—C2—C3—C4	−17.7 (7)	C59—C50—C51—C56	−75.8 (7)
C1—O1—C4—C3	−23.9 (7)	C47—C50—C51—C56	52.9 (8)
C2—C3—C4—O1	24.6 (7)	C56—C51—C52—C53	0.1 (8)
C6—C3—C4—O1	−94.3 (7)	C50—C51—C52—C53	−179.6 (5)
C2—C3—C6—C7	−176.7 (7)	C57—O15—C53—C52	−6.4 (9)
C4—C3—C6—C7	−68.3 (7)	C57—O15—C53—C54	174.5 (5)
C2—C3—C6—C15	56.1 (9)	C51—C52—C53—O15	−178.2 (5)

C4—C3—C6—C15	164.5 (6)	C51—C52—C53—C54	0.9 (8)
C15—C6—C7—C12	−103.0 (7)	C58—O16—C54—C55	0.1 (9)
C3—C6—C7—C12	127.8 (7)	C58—O16—C54—C53	−179.9 (6)
C15—C6—C7—C8	75.8 (7)	O15—C53—C54—O16	−2.4 (7)
C3—C6—C7—C8	−53.4 (8)	C52—C53—C54—O16	178.5 (5)
C12—C7—C8—C9	1.9 (9)	O15—C53—C54—C55	177.6 (5)
C6—C7—C8—C9	−176.9 (5)	C52—C53—C54—C55	−1.5 (8)
C13—O3—C9—C8	−4.9 (8)	O16—C54—C55—C56	−178.9 (5)
C13—O3—C9—C10	175.2 (5)	C53—C54—C55—C56	1.1 (9)
C7—C8—C9—O3	−179.4 (6)	C52—C51—C56—C55	−0.5 (9)
C7—C8—C9—C10	0.5 (8)	C50—C51—C56—C55	179.2 (5)
C14—O4—C10—C11	1.7 (8)	C54—C55—C56—C51	−0.1 (9)
C14—O4—C10—C9	180.0 (5)	C51—C50—C59—C64	−101.6 (6)
O3—C9—C10—O4	0.0 (7)	C47—C50—C59—C64	129.5 (6)
C8—C9—C10—O4	−179.9 (5)	C51—C50—C59—C60	77.1 (7)
O3—C9—C10—C11	178.4 (5)	C47—C50—C59—C60	−51.8 (7)
C8—C9—C10—C11	−1.5 (8)	C64—C59—C60—C61	0.5 (9)
O4—C10—C11—C12	178.4 (5)	C50—C59—C60—C61	−178.2 (5)
C9—C10—C11—C12	0.1 (8)	C65—O17—C61—C60	−1.9 (9)
C8—C7—C12—C11	−3.2 (9)	C65—O17—C61—C62	178.8 (5)
C6—C7—C12—C11	175.6 (5)	C59—C60—C61—O17	−179.3 (5)
C10—C11—C12—C7	2.2 (9)	C59—C60—C61—C62	−0.1 (8)
C7—C6—C15—C20	−85.7 (8)	C66—O18—C62—C61	−171.5 (5)
C3—C6—C15—C20	41.1 (9)	C66—O18—C62—C63	10.8 (8)
C7—C6—C15—C16	93.9 (6)	O17—C61—C62—O18	1.7 (8)
C3—C6—C15—C16	−139.3 (6)	C60—C61—C62—O18	−177.6 (5)
C20—C15—C16—C17	−1.5 (8)	O17—C61—C62—C63	179.4 (5)
C6—C15—C16—C17	178.9 (5)	C60—C61—C62—C63	0.1 (9)
C21—O5—C17—C16	4.0 (8)	O18—C62—C63—C64	177.0 (6)
C21—O5—C17—C18	−176.8 (5)	C61—C62—C63—C64	−0.5 (9)
C15—C16—C17—O5	−179.3 (5)	C60—C59—C64—C63	−1.0 (9)
C15—C16—C17—C18	1.7 (8)	C50—C59—C64—C63	177.7 (6)
C22—O6—C18—C19	2.3 (9)	C62—C63—C64—C59	1.0 (9)
C22—O6—C18—C17	−178.9 (5)	C70—O19—C67—O20	−174 (4)
O5—C17—C18—O6	1.1 (7)	C70—O19—C67—C68	−28 (8)
C16—C17—C18—O6	−179.7 (5)	O20—C67—C68—C71	−41 (7)
O5—C17—C18—C19	180.0 (5)	O19—C67—C68—C71	174 (6)
C16—C17—C18—C19	−0.8 (8)	O20—C67—C68—C69	153 (3)
O6—C18—C19—C20	178.7 (6)	O19—C67—C68—C69	8 (7)
C17—C18—C19—C20	−0.1 (9)	C71—C68—C69—C72	90 (7)
C16—C15—C20—C19	0.6 (9)	C67—C68—C69—C72	−108 (4)
C6—C15—C20—C19	−179.8 (6)	C71—C68—C69—C70	−150 (7)
C18—C19—C20—C15	0.2 (10)	C67—C68—C69—C70	12 (5)
C26—O7—C23—O8	−176.9 (6)	C67—O19—C70—C69	35 (7)
C26—O7—C23—C24	1.1 (7)	C68—C69—C70—O19	−27 (5)
O8—C23—C24—C27	−1.8 (12)	C72—C69—C70—O19	95 (4)
O7—C23—C24—C27	−179.5 (7)	C68—C69—C72—C81	−168.9 (15)
O8—C23—C24—C25	−174.7 (7)	C70—C69—C72—C81	76.3 (12)
O7—C23—C24—C25	7.6 (7)	C68—C69—C72—C73	−51.9 (17)
O8—C23—C24—C25A	152.7 (9)	C70—C69—C72—C73	−166.7 (11)
O7—C23—C24—C25A	−25.0 (9)	C70A—O19A—C67A—O20A	159 (4)
C23—O7—C26—C25	−9.0 (8)	C70A—O19A—C67A—C68A	5 (7)

C23—O7—C26—C25A	21.4 (10)	O20A—C67A—C68A—C71	1 (8)
C27—C24—C25—C28	58.3 (11)	O19A—C67A—C68A—C71	151 (6)
C23—C24—C25—C28	−129.1 (6)	O20A—C67A—C68A—C69A	179 (2)
C27—C24—C25—C26	175.5 (8)	O19A—C67A—C68A—C69A	−31 (6)
C23—C24—C25—C26	−11.9 (7)	C71—C68A—C69A—C72A	−21 (6)
O7—C26—C25—C24	12.6 (7)	C67A—C68A—C69A—C72A	161 (2)
O7—C26—C25—C28	131.7 (6)	C71—C68A—C69A—C70A	−141 (5)
C24—C25—C28—C29	168.8 (7)	C67A—C68A—C69A—C70A	41 (3)
C26—C25—C28—C29	57.0 (8)	C67A—O19A—C70A—C69A	22 (6)
C24—C25—C28—C37	−71.7 (8)	C68A—C69A—C70A—O19A	−39 (4)
C26—C25—C28—C37	176.5 (6)	C72A—C69A—C70A—O19A	−158 (3)
C27—C24—C25A—C28A	−63.0 (16)	C68A—C69A—C72A—C73A	78 (2)
C23—C24—C25A—C28A	142.7 (10)	C70A—C69A—C72A—C73A	−170.7 (8)
C27—C24—C25A—C26	−172.5 (8)	C68A—C69A—C72A—C81	−162 (2)
C23—C24—C25A—C26	33.2 (10)	C70A—C69A—C72A—C81	−50.7 (9)
O7—C26—C25A—C28A	−148.6 (10)	C81—C72—C73—C74	−107.1 (11)
O7—C26—C25A—C24	−32.8 (11)	C69—C72—C73—C74	138.0 (10)
C24—C25A—C28A—C37	79.1 (13)	C81—C72—C73—C78	70.9 (15)
C26—C25A—C28A—C37	−178.8 (9)	C69—C72—C73—C78	−44.0 (16)
C24—C25A—C28A—C29	−175.7 (10)	C78—C73—C74—C75	−1.1 (18)
C26—C25A—C28A—C29	−73.5 (11)	C72—C73—C74—C75	177.0 (11)
C25—C28—C29—C34	−128.3 (7)	C79—O21—C75—C74	−0.9 (17)
C37—C28—C29—C34	111.0 (7)	C79—O21—C75—C76	175.7 (10)
C25—C28—C29—C30	52.1 (9)	C73—C74—C75—O21	−179.1 (12)
C37—C28—C29—C30	−68.6 (8)	C73—C74—C75—C76	4.5 (19)
C25A—C28A—C29—C34	−41.8 (17)	O21—C75—C76—C77	178.4 (15)
C37—C28A—C29—C34	63.2 (16)	C74—C75—C76—C77	−5 (2)
C25A—C28A—C29—C30	138.4 (9)	O21—C75—C76—O22	−0.4 (18)
C37—C28A—C29—C30	−116.6 (8)	C74—C75—C76—O22	176.5 (11)
C34—C29—C30—C31	−0.6 (9)	C80—O22—C76—C77	−3.3 (19)
C28—C29—C30—C31	178.9 (6)	C80—O22—C76—C75	175.5 (10)
C28A—C29—C30—C31	179.2 (7)	C75—C76—C77—C78	2 (3)
C35—O9—C31—C32	−179.1 (5)	O22—C76—C77—C78	−179.7 (15)
C35—O9—C31—C30	0.8 (9)	C74—C73—C78—C77	−2 (2)
C29—C30—C31—O9	−179.7 (6)	C72—C73—C78—C77	179.9 (14)
C29—C30—C31—C32	0.1 (9)	C76—C77—C78—C73	2 (3)
C36—O10—C32—C33	−12.7 (8)	C69A—C72A—C73A—C78A	−127.8 (10)
C36—O10—C32—C31	169.2 (5)	C81—C72A—C73A—C78A	115.8 (11)
O9—C31—C32—C33	180.0 (5)	C69A—C72A—C73A—C74A	54.7 (10)
C30—C31—C32—C33	0.1 (8)	C81—C72A—C73A—C74A	−61.6 (11)
O9—C31—C32—O10	−1.8 (7)	C78A—C73A—C74A—C75A	2.3 (16)
C30—C31—C32—O10	178.4 (5)	C72A—C73A—C74A—C75A	179.6 (9)
O10—C32—C33—C34	−177.9 (6)	C73A—C74A—C75A—C76A	−2.2 (16)
C31—C32—C33—C34	0.1 (9)	C73A—C74A—C75A—O21	176.5 (9)
C30—C29—C34—C33	0.9 (9)	C79—O21—C75A—C76A	174.3 (9)
C28—C29—C34—C33	−178.7 (6)	C79—O21—C75A—C74A	−4.4 (14)
C28A—C29—C34—C33	−178.9 (12)	C80—O22—C76A—C77A	−5.6 (17)
C32—C33—C34—C29	−0.7 (10)	C80—O22—C76A—C75A	175.1 (9)
C29—C28—C37—C42	73.7 (8)	C74A—C75A—C76A—O22	−179.9 (9)
C25—C28—C37—C42	−46.3 (9)	O21—C75A—C76A—O22	1.3 (14)
C29—C28—C37—C38	−107.9 (6)	C74A—C75A—C76A—C77A	1 (2)
C25—C28—C37—C38	132.0 (6)	O21—C75A—C76A—C77A	−178.1 (12)

C25A—C28A—C37—C42	−137.4 (10)	O22—C76A—C77A—C78A	−178.5 (12)
C29—C28A—C37—C42	121.0 (8)	C75A—C76A—C77A—C78A	1 (2)
C25A—C28A—C37—C38	41.9 (18)	C74A—C73A—C78A—C77A	−0.8 (19)
C29—C28A—C37—C38	−59.7 (16)	C72A—C73A—C78A—C77A	−178.2 (12)
C42—C37—C38—C39	−1.1 (9)	C76A—C77A—C78A—C73A	−1 (2)
C28—C37—C38—C39	−179.6 (5)	C73—C72—C81—C86	103.9 (9)
C28A—C37—C38—C39	179.6 (12)	C69—C72—C81—C86	−132.3 (7)
C37—C38—C39—C40	−0.8 (9)	C73—C72—C81—C82	−73.1 (13)
C37—C38—C39—O11	178.4 (6)	C69—C72—C81—C82	50.7 (13)
C43—O11—C39—C38	3.2 (10)	C73A—C72A—C81—C86	76.7 (11)
C43—O11—C39—C40	−177.6 (6)	C69A—C72A—C81—C86	−43.1 (11)
C44—O12—C40—C39	176.1 (8)	C73A—C72A—C81—C82	−96.8 (8)
C44—O12—C40—C41	−4.3 (10)	C69A—C72A—C81—C82	143.4 (6)
C38—C39—C40—O12	−179.0 (6)	C86—C81—C82—C83	1.3 (9)
O11—C39—C40—O12	1.7 (8)	C72—C81—C82—C83	178.0 (9)
C38—C39—C40—C41	1.4 (9)	C72A—C81—C82—C83	176.4 (5)
O11—C39—C40—C41	−177.9 (6)	C87—O23—C83—C82	2.6 (9)
O12—C40—C41—C42	−179.6 (6)	C87—O23—C83—C84	−176.4 (6)
C39—C40—C41—C42	0.0 (9)	C81—C82—C83—O23	−179.9 (6)
C38—C37—C42—C41	2.5 (9)	C81—C82—C83—C84	−0.9 (9)
C28—C37—C42—C41	−179.2 (6)	C88—O24—C84—C85	0.2 (8)
C28A—C37—C42—C41	−177.9 (8)	C88—O24—C84—C83	179.0 (5)
C40—C41—C42—C37	−2.0 (10)	O23—C83—C84—O24	0.7 (7)
C48—O13—C45—O14	177.6 (6)	C82—C83—C84—O24	−178.3 (5)
C48—O13—C45—C46	−4.1 (7)	O23—C83—C84—C85	179.6 (5)
O14—C45—C46—C49	−1.2 (10)	C82—C83—C84—C85	0.6 (8)
O13—C45—C46—C49	−179.3 (6)	O24—C84—C85—C86	178.1 (6)
O14—C45—C46—C47	176.4 (7)	C83—C84—C85—C86	−0.6 (9)
O13—C45—C46—C47	−1.8 (7)	C82—C81—C86—C85	−1.4 (10)
C49—C46—C47—C50	−55.6 (9)	C72—C81—C86—C85	−179.3 (7)
C45—C46—C47—C50	127.3 (6)	C72A—C81—C86—C85	−174.5 (7)
C49—C46—C47—C48	−176.5 (7)	C84—C85—C86—C81	1.1 (11)
C45—C46—C47—C48	6.3 (6)		

VITA

Education:

Doctor of Philosophy in Pharmaceutical Sciences, Department of BioMolecular Sciences, Division of Pharmacognosy, School of pharmacy, the University of Mississippi, USA. 2020

Master of Arts in Biomedical Sciences, Midwestern University, USA. 2015

Bachelor of Science in Biology, Emory University, USA. 2014

Skills

- Molecular biological assays-based evaluation of natural products on signaling pathways
- Bioactivity-guided fractionation
- Mammalian cell culture

Research Experience:

University of Mississippi **Graduate Research Assistant**

Department of BioMolecular Sciences August 2015–May 2020

National Center for Natural Products Research

Faser Hall PO Box 1848, School of Pharmacy, University, MS 38677

Advisor: Ikhlas Khan, Ph.D.

- Develop protocols to screen natural products for anti-proliferative activity against colorectal cancer cells in high throughput 96-well plate assays
- Evaluate apoptosis and detect caspase activity in colorectal cancer cells by flow cytometry and Western blots
- Utilize molecular biological assays to assess the effects of natural products on the Wnt or

Nrf-2/ARE signaling pathway in colorectal cancer cells

- Perform extraction, fractionation, and isolation of lignans from plant species using chromatography techniques

Emory University

Whitehead Biomedical Research Building — **Undergraduate Researcher**

Department of Human Genetics — January 2013–December 2013

615 Michael St., Atlanta, GA 30322

Advisor: Judith Fridovich-Keil, Ph.D.

- Isolated DNA from saliva and/or blood samples for conducting polymerase chain reaction
- Analyzed DNA sequences to find novel mutations causing galactosemia
- Identified de novo mutations leading to galactosemia.

Emory Eye Center — **Summer Undergraduate Research Scholar**

Ophthalmology Research — June 2012–August 2012

1365 Clifton Rd B, Atlanta, GA 30322

Advisor: Jeffrey Boatright, Ph.D.

- Exposed rodents to whole-body exercise using treadmills
- Anesthetized rodents to perform optic nerve crush to study the effect of exercise on retinal degeneration

- Maintained a proper housing environment for rodents in accordance with the Institutional Animal Care and Use Committee

Publications:

- **Tran, T.C.,** Khan, S., Ali, Z., Fronczek, F., Chittiboyina, A., Khan, I.A. Purification of Scalemic Mixture of Undescribed Secolignans from the Barks of *Maasia glauca* and Their Inhibitory Activity on the Wnt Signaling Pathway in Colorectal Cancer. In progress.
- **Tran, T.C**., Liu, Y., Zwick, M.E., Ramachandran, D., Cutler, D.J., Huang, X., Berry, G.T., & Fridovich-Keil, J.L. (2014). A De Novo Variant in Galactose-1-P Uridylyltransferase (GALT) Leading to Classic Galactosemia. *Journal of Inherited Metabolic Disease Reports*, 19:1–6.
- Hoeksema, J.D., Roy, M., Łaska, G., Sienkiewicz, A., Horning, A., Abbott, M.J., **Tran, C.**, & Mattox, J. (2018). *Pulsatilla Patens* (Ranunculaceae), a Perennial Herb, is Ectomycorrhizal in Northeastern Poland and Likely Shares Ectomycorrhizal Fungi with *Pinus sylvestris*. *Acta Societatis Botanicorum Poloniae,* 87(1):1–3.

Conferences

- **Tran, C.**, Khan, S.I., Ali, Z., Khan, I.A. (2019, April 8–11). Annonaceae Family: A Venture into the Unknowns. Poster presented at the 19th Annual Oxford International Conference on the Science of Botanicals, Oxford, MS.

- **Tran, C**., Khan, S.I., Ali, Z., Khan, I.A. (2019, March 26). Bio-Guided Fractionation of Plant Extracts from the Annonaceae Family. Poster presented at the 9th Annual Graduate Research Symposium, University, MS.
- **Tran, C.**, Khan, S.I., Khan, I.A. (2018, July 21–25). Screening of Anti-Proliferative Activity of a Collection of Plant Extracts Belonging to Annonaceae Family and Their Activity Toward NRF-2/ARE Pathway. Poster presented at the 59th Annual The American Society of Pharmacognosy Meeting, Lexington, KY.
- **Tran, C.**, Khan, S.I., Khan, I.A. (2018, April 9–12). Screening of Anti-Proliferative Activity of a Collection of Plant Extracts Belonging to Annonaceae Family and Their Activity Toward NRF-2/ARE Pathway. Poster presented at the 18th Annual Oxford International Conference on the Science of Botanicals, Oxford, MS.